SYNTHESIS, STRUCTURE AND PROPERTY STUDIES OF POLYOLEFINS PREPARED USING LATE TRANSITION METAL CATALYSTS

A THESIS

SUBMITTED TO THE

UNIVERSITY OF PUNE

FOR THE DEGREE OF

DOCTOR OF PHILOSOPHY

IN

CHEMISTRY

BY

U. SUBRAMANYAM

POLYMER SCIENCE AND ENGINEERING DIVISION
NATIONAL CHEMICAL LABORATORY
PUNE 411 008
INDIA

May 2006

CERTIFACATE BY RESEARCH GUIDE

Certified that the work incorporated in the thesis entitled: "**Synthesis, structure and property studies of polyolefins prepared using late transition metal catalysts**", submitted by Mr. U. Subramanyam, for the Degree of **Doctor of Philosophy**, was carried out by the candidate, under my supervision at Polymer Science and Engineering Division, National Chemical Laboratory, Pune 411 008, India. Such material as has been obtained from other sources has been duly acknowledged in the thesis.

Dr. S. Sivaram
(Research Guide)

DECLARATION BY RESEARCH SCHOLAR

I hereby declare that the thesis entitled: "**Synthesis, structure and property studies of polyolefins prepared using late transition metal catalysts**", submitted for the Degree of **Doctor of Philosophy** to the University of Pune, has been carried out by me at Polymer Science and Engineering Division, National Chemical Laboratory, Pune 411 008, Inida, under the supervision of Dr. S. Sivaram. The work is original and has not been submitted in part or fully by me for any other degree of diploma to this or any other University.

Mr. U. Subramanyam

(Research Scholar)

Dedicated to My Teacher,

Late Prof. A. Kameswara Rao

Acknowledgement

It is my great pleasure to acknowledge my research supervisor Padma Shri Dr. Swaminathan Sivaram, Director, National Chemical Laboratory, who introduced my to a fascinating realm of chemistry. His invaluable guidance, constant inspiration, unending support and constructive criticism helped me a lot to focus my views in proper perspective. His tirelss enthusiasm has always been a source of inspiration for me. My deepest personal regards are due for him forever. I express my sincerest gratitude to Dr. (Smt.) Rama Sivaram.

I wish to express my sincere gratitude to Dr. P.R. Rajamohanan, Head of NMR facility, for his help and cooperation in understanding the studies of microstructure analysis by NMR techniques.

I am thankful to all my lab-mates, Drs. Rajesh Kumar, Yanjarappa, Saptarshi Ray and Mr. Rajesh for their extensive help and cooperation through the entire period of my research at NCL. I convey my sincerest thanks to Dr. T.P. Mohandas, Shri D.H. Gholap, Mrs. Dhoble, Drs. D. Baskaran, U. Natarajan, (Mr & Mrs) Idage, C. Ramesh, J.P. Jog, C.V. Avadhani and Mr. Menon for their helpful attitude at all times of need. I am also thankful to all members of Polymer Chemistry Division, NCL, for maintaining a warm and friendly atmosphere.

My special thanks to NMR facility, liquid nitrogen plant, elemental analysis facility, stores & purchase section, engineering services, staff of administrative office.

I wish to thank Mr. Shaikh, Mrs. Gracy and Ms. Khare for their help in office matters.

I also take this golden opportunity to convey my earnest respect to my teachers, Late Shri Alfred Vijayam, Shri. Venkateswarlu, Late Shri Jamalaiah, Shri. Vasantha Reddy, Shri Ramanujam, Shri. Venkata Subbaiah, who inspired me to achieve higher education in my life. I wish to thank my professors Late, Prof. A. Kameswara Rao, Drs. K. Chowdoji Rao, M. C. S. Subha, A.Varda Rajulu, S.Venkata Naidu and K. Mohanraju of Sri Krishnadevaraya University, Anantapur, for their advice.

I thank all my friends, Thiagarajan, Sathish and Family, Senapati, Srinivas and Parents, Arun, Nabi, Rambabu, Viswa Prasad, Selvaraj, Murugan, Suresh Kumar, Debasis Hazra, Prabal, Bhoje Gowd, Samurai, Raghu, Mahua, Gnaneshwar, Anuj Mittal, Mallikarjuna, Rajender, Santhosh, S.K. Pandey, Rajender Reddy, venkatesh, Rambabu, Murali, Swaroop, Ravindra, Pai, Sathyanaraya Reddy, Nagendra, Devaraj, Sathya, Sarika Devi, Rohini Bhor for their friendship and cooperation. I thank all my old friends, Chandra Sekhar and Family, Siva Sankar and Family, Sudhakar, K.S.N. Murthy and Subba Reddy and Family from whom I have received unfailing support and encouragement during many years of studies.

It gives me great pleasure to thank My Parents, Shri U. Subbarayudu and Smt. U. Ramadevi, elder brother Shri U. Subba Rao, younger brother Mr. U. Suresh Babu and sister Ms. U. Subhashini for their love, unfailing support, trust and encouragement.

Finally, my thanks are due to Council of Scientific and Industrial Research, Government of India, for awarding the Senior Research Fellowship, and Dr. S. Sivaram, Director National Chemical Laboratory, to carry out my research work and extending all possible infrastructural facilities, and to allow to submit this work in the form of a thesis for the award of Ph.D. degree. I thank University of Pune for the administrative work done for my thesis.

May 2006 **U. Subramanyam**

CONTENTS

CHAPTER 6. KINETICS OF HEXENE-1 POLYMERIZATION USING [(*N,N*′–DIISOPROPYLBENZENE)-2,3-(1,8-NAPTHYL)-1,4-DIAZABUTA-DIENE] DIBROMONICKEL / METHYLALUMINOXANE CATALYST SYSTEM

CHAPTER 7. SUMMARY AND CONCLUSIONS

LIST OF ABBREVIATIONS

Cp	Cyclopentadiene
DABAn	[(N,N′-diisopropylbenzene)-2,3-(1,8-napthyl)-1,4-diazabutadiene]
DME	Dimethoxyethane
DSC	Differential Scanning Calorimetry
DMA	Dynamic mechanical thermal analysis
GC	Gas Chromatography
GPC	Gel Permeation Chromatography
Ind	Indenyl
Kg	Kilo gram
M_n	Number average molecular weight
M_w	Weight average molecular weight
MWD	Molecular weight distribution
MAO	Methylaluminoxane
MMAO	Modified methylaluminoxane
NMR	Nuclear magnetic resonance
ODCB	*o*-dichlorobenzene
rac	Racemic
T_c	Crystallization temperature
T_m	Melting temperature
Tp	Polymerization temperature
TEAL	Triethylaluminium
TIBAL	Triisobutylaluminium
TMA	Trimethylaluminium
TOF	Turn over frequency
wt %	Weight %

LIST OF TABLES

LIST OF FIGURES

LIST OF SCHEMES

LIST OF CHARTS

CHAPTER 1

TRANSITION METAL CATALYSTS FOR POLYMERIZATION OF α-OLEFINS

1.1. INTRODUCTION

Since the discovery of transition metal catalysts for olefin polymerization by Ziegler and Natta, a great deal of research has been done towards understanding the basic mechanistic steps of this important industrial process[1-3]. Poly(olefin)s are a multibillion dollar a year industry with worldwide production in excess of 80 million tons and is the fastest growing segment of the polymer industry. The design and synthesis of single site olefin polymerization catalysts has developed rapidly in the last few decades with the group IV metallocenes receiving the most attention. The most exciting development in recent years has been the wider exploitation of late transition metal complex chemistry to the synthesis of poly(olefin)s[4]. A large number of studies have also appeared on structure-property-activity relationship of the resultant poly(olefin)s made with a diverse range of catalyst structures. This chapter describes more recent developments in the area of propylene and higher α-olefin (carbon numbers > 4) polymerization by group IV and late transition metal catalysts.

1.2. GROUP IV METALLOCENES

1.2.1. Background

Since the discovery of Ziegler-Natta catalysts in the 1950's polyolefin technology has been revolutionized by new discoveries in periodic intervals. Intense research in this area has resulted in five generations of catalysts, which have found applications in industry[5]. Several excellent reviews on this subject have appeared in the past few years[3,6-9]. To really understand the importance of the "single-site" catalysts, it is necessary to briefly look at the difference between these catalysts and the "multisited" Ziegler-Natta type catalysts. Generally metallocenes are bicomponent systems consisting of group IV transition metal compounds and cocatalysts. The evolution of the metallocene catalyst structures for olefin polymerization is shown in **Table 1.1**.

This discovery of *ansa*-metallocene catalysts for stereospecific polymerization is considered to be a major landmark in homogeneous transition metal catalysts for olefin polymerization. Several catalysts were made by varying the ligand structure surrounding the active center and a correlation of the catalyst structure with catalyst activity and stereospecificity have been established[19]. This led to a better understanding of the

Table 1.1. Development of metallocene research

Year	Milestones
1952	Development of the structure of metallocenes (ferrocene) (**Fishcher** and **Wilkinson**).
1957	Metallocene (Cp_2TiCl_2) as components of Ziegler-Natta catalysts[10,11], low activity with common aluminium alkys (Et_3Al or Et_2AlCl) (**Natta** and **coworkers, Breslow** and **Newburg**).
1973	Addition of small amount of water to increase the activity[12] ($Al:H_2O$ = 1:0.05 upto 1:0.3) (**Reichert, Meyer** and **Breslow**).
1976	Cp_2TiMe_2/TMA/water is highly active for ethylene polymerization[13].
1980	Use separately prepared methylaluminoxane (MAO) as cocatalyst for olefin polymerization[14,15] (**Kaminsky** and **Sinn**).
1982	Synthesis of ansa metallocenes with C_2 symmetry[16] (**Brintzinger**).
1984	Polymerization of propylene using a rac / meso mixture of ansa titanocenes lead to partially isotactic polypropylene[17] (**Ewen**).
1985	Synthesis of highly isotactic polypropylene[18] using chiral ansa zirconocenes produce (**Kaminsky** and **Brintzinger**).
1988	Synthesis of syndiotactic polypropylene[20] using C_s symmetric zirconocenes (**Ewen**).

molecular mechanism of stereochemical control in α-olefin polymerization. In another major development, Ewen et al. synthesized syndiotactic polypropylene in 1988 using C_s symmetric zirconocenes[20]. Metallocene catalysts have several advantages over classical heterogeneous Ziegler-Natta catalysts. These are,

- Very high catalytic activities.
- The 'single site' nature enables synthesis of extremely uniform homo and copolymers (with uniform comonomer distribution) and narrow molecular weight distributions as well as small fraction of extractable oligomers.
- The polymer microstructure can be controlled by changing the symmetry of the metallocene. A number of new polyolefin products with better properties have been made using metallocenes, which were not possible earlier.

- Metallocenes are able to polymerize a large variety of olefins, which were not possible using classical Ziegler-Natta catalysts. They afford efficient copolymerization of less reactive long chain α-olefins, sterically hindered α-olefins, cycloolefins and styrene.

- The main chain termination mechanisms operating with these catalyst systems provide unsaturated chain ends, which can be used for functionalization of polymers/oligomers.

- Metallocenes give excellent control of short as well as long chain branches, influencing the rheological properties and processing.

A number of reviews are available on metallocene catalyzed olefin polymerization[21-36].

1.2.2. Cocatalyst

1.2.2.1. Methylaluminoxane (MAO)

Methylaluminoxane (MAO) was the first highly effective activator of metallocene catalysts[13,14,37]. MAO is prepared by partial and controlled hydrolysis of trimethylaluminium (TMA). Ever since the first reported aluminoxane synthesis in the 1950s[38], most of the literature has shown aluminoxanes as linear chains (**1**) or cyclic rings (**2**) consisting or alternating aluminum and oxygen atoms. The repeat unit is –[Al(CH_3)-O]-. Reddy and Sivaram[25] have reported a detailed methodology for synthesis and characterization of MAO.

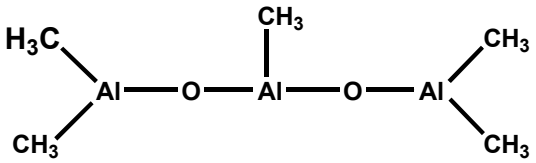

1

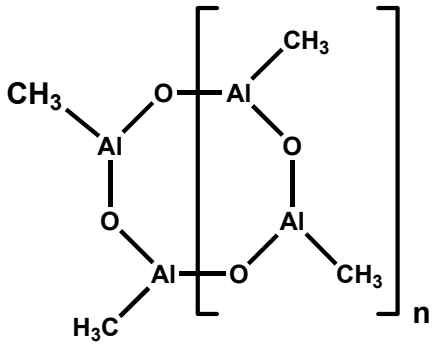

2

The degree of oligomerization generally varies from 5-30 and molecular weight range is 250-1700 daltons as determined by cryoscopic measurements. Me/Al ratio varies from 1.1 to 1.6. Although the details of its oligomeric structure are still under debate, it is generally accepted that the delocalized anion formed upon activation of L_yMX_2 precursors (X = halide, alkyl, or aryl) is a much weaker Lewis base than, e.g. mononuclear $AlR_2X_2^-$ anions derived from AlR_3, and as such, is much less prone to associate with L_yMR^+ active cations in the form of a strong ion couple hindering monomer attack[37].

MAO suffers from two main drawbacks, namely, (a) for opitimum performance it needs to be used in large excess relative to the transition metal species and (b) it contains "free" TMA in equilibrium with the oligomeric species. TMA is a reducing agent and, hence, with transition metal complexes it easily forms Me-bridged dinuclear species. Such species are believed to be catalytically inactive and promote chain transfer reactions in the formation oligomers.

1.2.2.2. Modified methylaluminoxane (MMAO)

MMAO is a modified methylaluminoxane containing 25 % tetraisobutyl dialuminoxane. It has the advantage of improved shelf life with similar activity as that of MAO[39]. Furthermore, commercial modified methylaluminoxane is available from Akzo-Nobel and is prepared by controlled hydrolysis of a mixture of trimethyl aluminum and triisobutyl aluminum. It has good solubility in aliphatic solvents.

1.2.2.3. Boron based catalysts

In 1986, Jordan et. al. reported that MAO free cationic metallocene catalyst system $[CP_2ZrMe(THF)]^+[BPh_4]^-$ can polymerize olefins with high activity in the absence of cocatalysts[40]. The profound effect of counter anions on the reactivity and catalytic activity of cationic early transition-metal complexes is well-established[41-44]. In principle, active homogeneous catalysts can be obtained by the reaction of dialkyl metallocene and Bronsted acidic salts in a 1:1 ratio. The weak coordinating ability of perfluoro analogue $[B(C_6F_5)_4]^-$ leads to a dramatic increase in activity and is the basis of the use of ionic systems $[L_nMR]^+[R'B(C_6F_5)_4]^-$ as highly effective olefin polymerization catalysts[45]. The activation of dialkyl metallocenes with three different non-coordination anions without side reactions has been reported.

(1) $Cp_2Zr(CH_3)_2 + B(C_6F_5)_3 \longrightarrow Cp_2Zr^+(CH_3) + (C_6F_5)_3B(CH_3)^-$
[Marks and coworkers[46]]

(2) $Et(Ind)_2Zr(CH_3)_2 + [Ph_3NHMe_2]^+[BPh_4]^- \longrightarrow Et(Ind)_2Zr(CH_3)^+ + PhNMe_3 + [B(C_6F_5)_4]^- + CH_4$ [Taube and Krukowa[47]]

(3) $Et(Ind)_2Zr(CH_3)_2 + [Ph_3C]^+ [B(C_6F_5)_4]^- \longrightarrow Et(Ind)_2Zr(CH_3)^+ + Ph_3CCCH_3 + [B(C_6F_5)_4]^-$ [Chien et al.[48]]

Compared to metal methyl complexes, benzyl complexes were found to be more stable at higher temperatures[49]. Anions of the type $CB_{11}H_{12}^-$, $[M(C_2B_9H_{11})_2]^-$ (M = Fe, Cp, Ni) have also been used as non-coordinating anions[50,51] with $[Cp_2ZrCH_3]^+$.

1.2.3. Mechanism of Polymerization

1.2.3.1. Nature of active centers

The structure of the active centers in metallocene-based catalysts has been thoroughly studied. Based on various experimental data, the real active species in all metallocene catalysts have been proven to be ion pairs containing cationic species $Cp_2M^+R^-$. First CP_2ZrCl_2 is monoalkylated by MAO to $Cp_2Zr(CH_3)Cl$ and the Cl ligand of the resulting $Cp_2Zr(CH_3)Cl$ is abstracted by MAO to form a catalytically active species[52]. The overall activation scenario for a zirconocenes dichloride with MAO is represented in **Scheme 1.1.**[53,54].

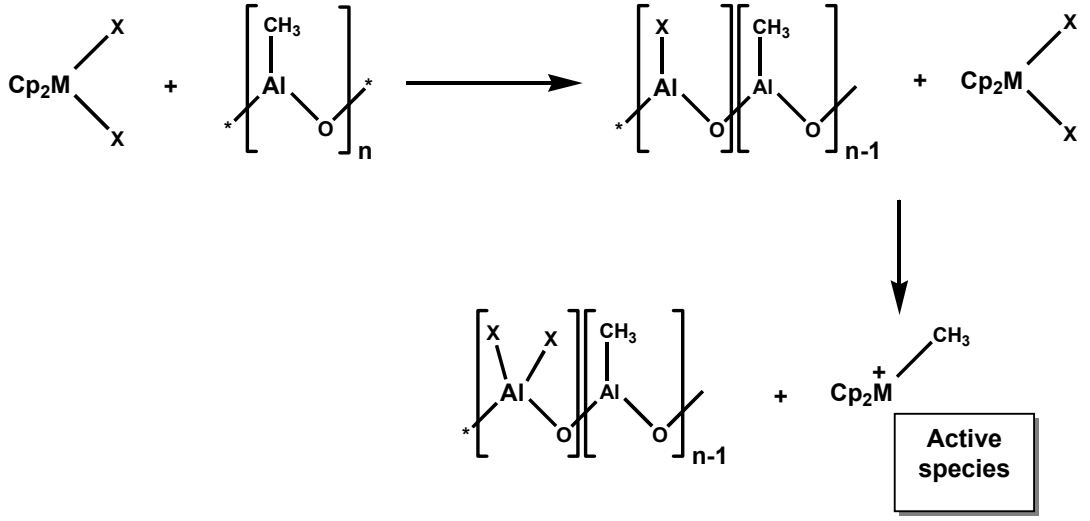

Scheme 1.1. Formation of cationic species (active centers)

These cationic group IV metal complexes are often stabilized by other weak interactions, such as agostic interactions. Direct evidence of the formation of cationic species was reported by Marks and coworkers who studied the reaction of $Cp_2Zr(^{13}CH_3)_2$ and MAO and following ethene insertion with solid state ^{13}CPMAS-NMR[55-59]. Further confirmation was obtained when Jordan et al. isolated and characterized a cationic zirconocene species $[Cp_2ZrMe(THF)]^+$ $[BPh_4]^-$ which was found to be active for ethylene polymerization[40]. This led to the development of several cationic metallocene catalyst systems for olefin polymerization.

1.2.3.2. Polymerization mechanism

The mechanism of polymerization has been the subject of many experimental and theoretical investigations. Cossee's suggestions[60-63], originally developed for olefin polymerization with conventional Z-N catalysts, is generally accepted to be the most plausible mechanism for metallocenes (**Scheme 1.2**)[64,65].

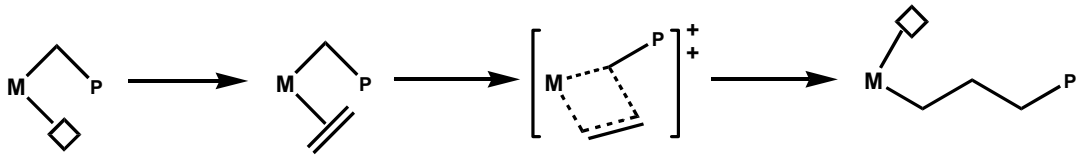

Scheme 1.2. Cossee mechanism (*Direct insertion*)

The key features of the steps insertion mechanism are: (i) that the active metal center bearing the growing alkyl chain must have an available coordination site for the incoming monomer, (ii) the insertion occurs via chain migration to the closet carbon of the olefin double bond, which undergoes *cis* opening with formation of new metal-carbon and carbon-carbon bonds (iii) the new C-C bond is then on the site previously occupied by the coordinated monomer molecule, (iv) the newly formed metal alkyl again reinserts another olefin molecule leading eventually to a polymer. During this process shifting of growing polymer chain to position previously occupied by a coordinated monomer continues until termination of the polymer chain takes place.

1.2.4. Nature of Chain Transfer Reactions

The possible occurrence of chain transfer during olefin polymerization with metallocene/methylaluminoxane catalysts is discussed in this section. The details of chain transfer reaction mechanisms have been reviewed by Resconi and coworkers[66], which are then correlated with zirconocene ligand structure and the polymerization conditions.

1.2.4.1. β-Hydride elimination

Cationic group IV metallocene alkyl complexes rapidly undergo spontaneous β-hydride transfer to the corresponding metal hydrides and alkenes. The types of β-hydride elimination are as follows:

1.2.4.1.1. β-Hydride transfer

1.2.4.1.1.1. β-Hydride transfer to metal (uni- and bi-molecular)

β-Hydride transfer after a primary insertion produces vinylidene-terminated, n-propyl-initiated PP and follows the rate law $R_t = k_{(\beta\text{-}H)0}$ [C], when it is unimolecular (β-hydride transfer to the metal), and $R_t = k_{(\beta\text{-}H)1}$ [C][M], when it is bimolecular (either by concerted β-hydride transfer to the coordinated monomer or by associative displacement). Bercaw[67,68] and Jordan[69,70] have confirmed that both neutral group 3 metallocene alkyl, and cationic group IV metallocene alkyl complexes readily undergo spontaneous β-hydride transfer. **Scheme 1.3** depicts the hydride transfer reactions.

1.2.4.1.1.2. β-Hydride transfer to metal (after secondary olefin insertion)

This can be either unimolecular (β-H transfer to metal) or bimolecular (β-H transfer to monomer), producing a M-H initiating species, and poly(propylene) chain is terminated with either a 4- butenyl (H transfer from terminal CH_3) or a 2-butenyl (H transfer from CH_2) end group (**Scheme 1.4**). In practice, only the internal vinylene unsaturation has been observed[71-74].

β-H transfer after a secondary olefin insertion is an important chain transfer reaction since it is the cause for the drop in molecular weights observed with metallocenes wherein a secondary insertion generates a slower propagating species.

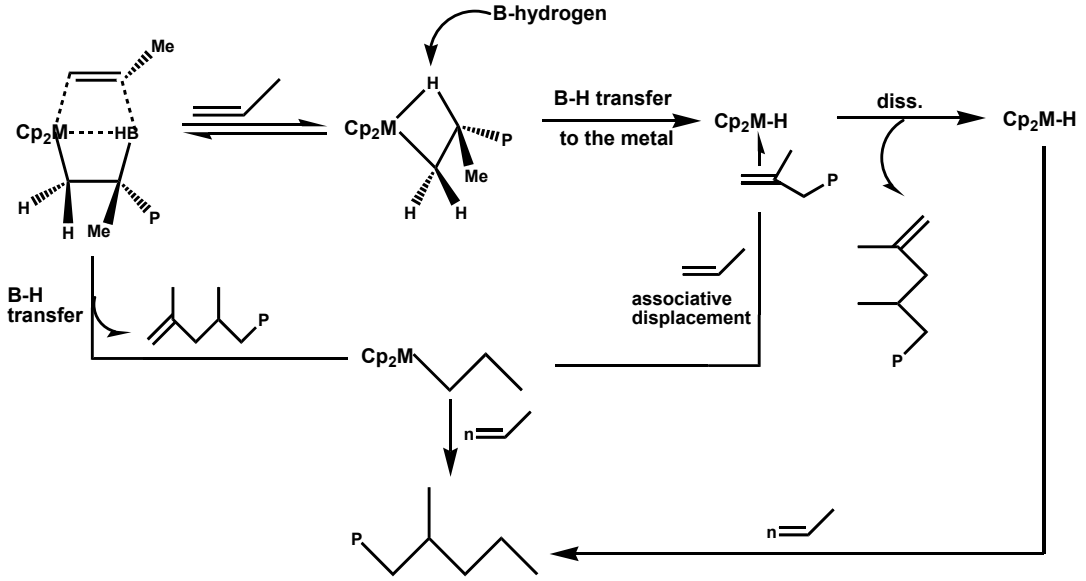

Scheme 1.3. β-Hydride transfer to metal

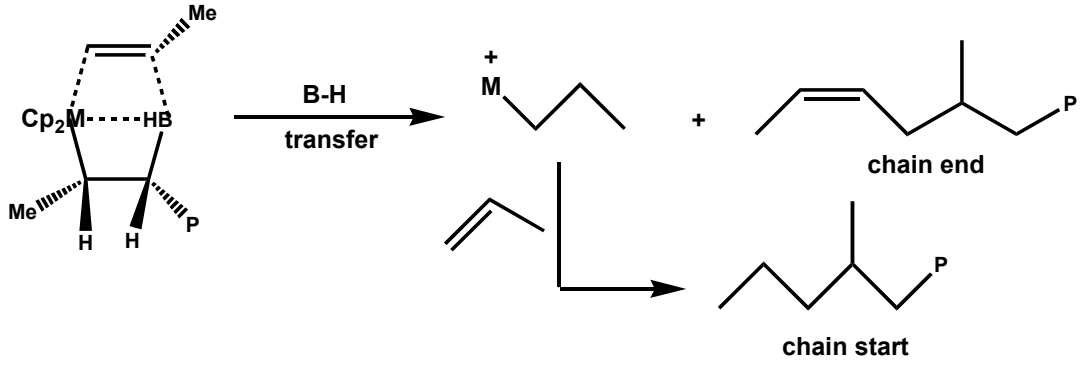

Scheme 1.4. β-Hydride transfer after a secondary propylene insertion

1.2.4.1.2. β-Methyl transfer

β-Methyl transfer, a notable example of C-C bond activation in early transition metal centers, produces PP chains initiated by isobutyl and terminated by the allyl group CH_2=CH-CH_2-$CH(CH)_3$-P (**Scheme 1.5**). Teuben[75,76] and Resconi[77] reported such transfer reactions with $(Me_5Cp)_2$Zr- and Hf catalysts, especially, when the metal has highly substituted cyclopentadienyl ligands[78-81]. Jordan and Bercaw have shown that β-methyl transfer is unimolecular (β-CH_3 transfer to the metal).

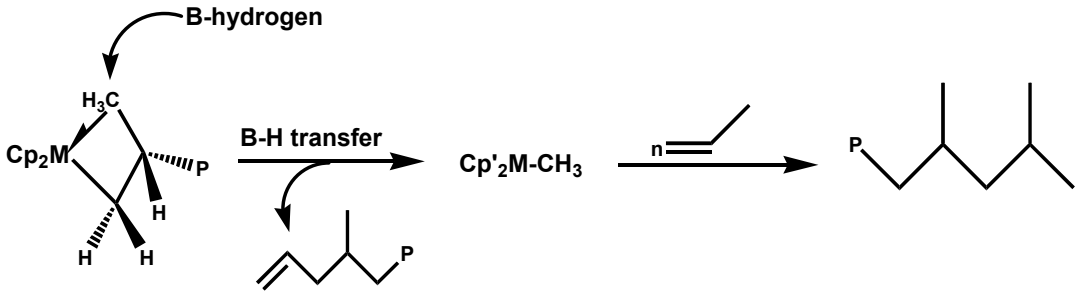

Scheme 1.5. β-Methyl transfer

1.2.4.1.3. Chain transfer to aluminum

Transalkylation to the aluminum cocatalyst produces, after hydrolysis, PP with saturated end groups on both ends (**Scheme 1.6**); in the case of MAO-cocatalyzed olefin polymerization, transalkylation likely occurs with the $AlMe_3$ present in MAO, resulting in isobutyl end groups on both polymer ends. It also occurs with metallocenes at high Al/Zr ratios and under the conditions where the catalyst exhibits low productivity[82-86].

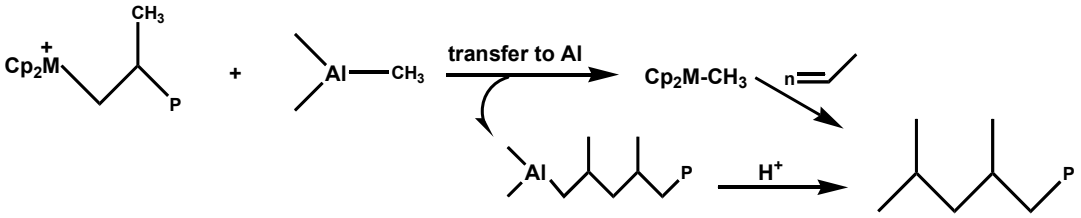

Scheme 1.6. Chain transfer to aluminum

1.2.4.2. Influence of ligand structure and reaction conditions on chain transfer reactions

Effect of nature of metallocene (steric, electronic factors) and polymerization reaction conditions on chain transfer reactions have been very well explored in the literature.

1.2.4.2.1. Steric effect

Chain transfer by β-hydride elimination is most predominant with group IV transition metal catalysts. Steric effect can cause significant increase in the energy of the

transition state associated with β-H elimination due to the non-bonded repulsion between the polymer chain and the ligand. By substituting Cp with bulky indenyl (Ind) or Flu ligands[87] or substituents at the appropriate positions of the ligands, high molecular weight can be achieved[88,89].

1.2.4.2.2. Electronic effect

If the ligands around electron deficient metal atom (Zr or Hf, Ti) become more electron releasing, then the thermodynamic driving force for β-H elimination diminishes. The electron releasing ability increases in the order Flu > Ind > Cp[90].

1.2.4.2.3. Temperature

Since the activation energy of chain transfer reactions is higher than insertion, lowering of polymerization temperature leads to high molecular weight polymer. Kaminsky et al.[91] reported that at T_p below –20 ^oC the transfer reaction is negligible and that the polymerization is first order.

1.2.4.2.4. Catalyst concentration

Average molecular weight decreases with log of increase in catalyst concentration[92].

1.2.4.2.5. [Al / M] ratio

It has been reported that as the Al/Zr ratio increases from 1000 to 10000, the Mw initially increases. Further increase in the ratio does not have significant effect on M_w. But at very high levels of Al/M =. 50,000 to 100000, M_w decreases due to transfer reactions with aluminium.

1.2.4.2.6. Molecular weight distribution (MWD)

Molecular weight and molecular weight distribution are the important properties, which affect mechanical properties as well as the processability of a polymer. Metallocene catalysts, being "single site", produce polymers with a narrow molecular weight distribution (MWD). Typical values of M_w/M_n are 1.6-2.4 for poly(ethylene)s and 1.9-2.6 for poly(propylene)s[93]. Chien and Sugimoto suggested that MWD of 2 might not

be due to 'single site' nature, but two or more active species with similar values of the k_p/k_{tr} ratio[94].

1.2.5. Structure of Polymers

Ewen and coworkers[95-97] and Kaminsky and coworkers[18] described a series of stereoselective metallocene catalyst which define what are now referred to as "Ewen's symmetry rules". These are summarized in **Chart 1.1**. **Scheme 1.7** depicting the four-stereospecific polymerization mechanisms in primary polyinsertion, all of which have been documented with metallocene catalysts.

Scheme 1.7. Mechanism of stereocontrol in primary olefin-1 polyinsertion

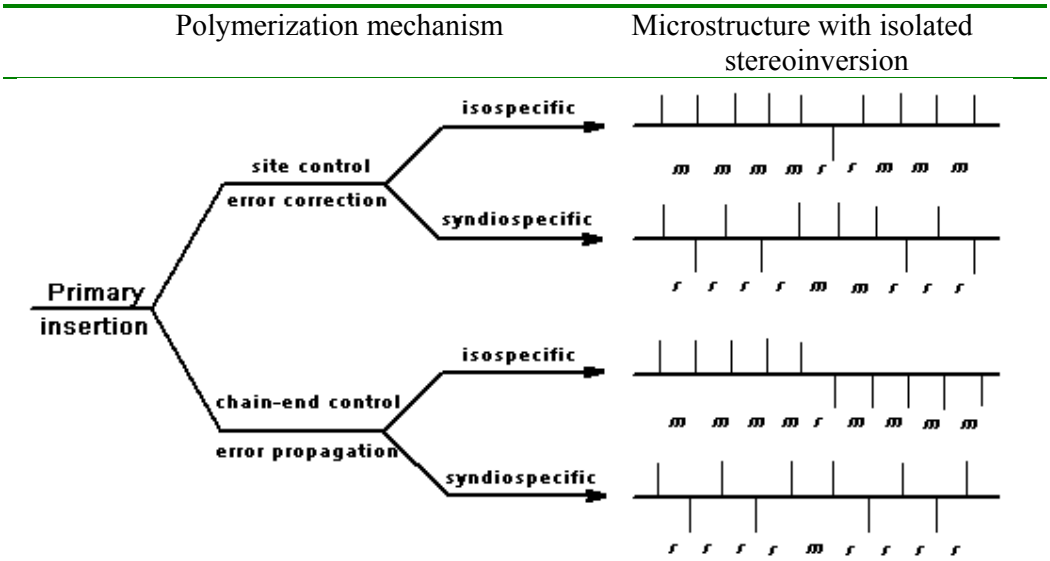

1.2.5.1. Stereo- / regio-specificity of polymers

One of the important features of the insertion mechanism for olefin polymerization is that the active metal center bearing the growing alkyl chain must have an available coordination site for the incoming monomer. It is well known that olefin insertion into metal-carbon bonds is predominantly primary. However, isolated secondary insertions (2,1-insertion or regio defects) are often detectable in metallocene-catalyzed polymerization of propylene. These regio defects play a major role in reducing crystallinity and melting point of isotactic poly(propylene). The relative amounts of these

Chart 1.1. Steric control as a function of metallocene symmetry (*Ewen's symmetry rules*)

Symmetry		Sites	Polymer
C_{2v} *Achiral*	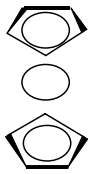	A, A *Homotopic*	Atactic
C_2 *Chiral*	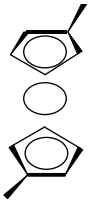	E, E *Homotopic*	Isotactic
C_s *Achiral*	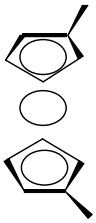	A, A *Diastereotopic*	Atactic
C_s *Prochiral*	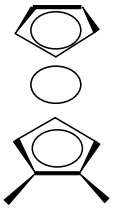	E, -E *Enantiotopic*	Syndiotactic
C_1 *Chiral*	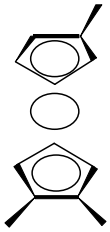	E, A *Diastereotopic*	Hemi-isotactic

regio defects are highly dependent on the nature of metal, ligand structure and polymerization conditions employed. However these regio defects are not well studied, possibly due to their low concentration. For example, a sequence of two secondary

insertions has never been detected. In terms of regiochemistry three propagation reactions can occur, namely, primary on primary chain end, secondary on primary chain end and primary on secondary chain end. The secondary growing chain end is relatively less reactive; however, it can be activated either by hydrogen or by copolymerizing with small amount of ethylene. The secondary growing chain end also undergoes a 3,1-isomerization to form active sites under specified reaction conditions like high temperature and low monomer concentration.

1.2.5.2. Effect of metal on regioselectivity

There are only a few studies carried out on Ti and Hf complexes due to their lower activity. The published literature shows that *rac*-Et(Ind)$_2$TiCl$_2$/MAO is both less stereoselective and regioselective compared to its Zr analogue[98,99]. However change in ligand structure also influences the regio selectivity, for eg. *rac*-Me$_2$Si(2-Me-4-Ph-1-Ind)$_2$TiCl$_2$/MAO has been reported to be more regioselective than its Zr and Hf analogues[100].

1.2.5.3. Effect of cocatalyst on regioselectivity

The nature of co-catalyst does not have any role in regiospecificity. However there may be some variation in the catalyst activity[37].

1.2.5.4. Effect of π-ligands on regio selectivity

The microstructure of low molecular weight atactic poly(propylene) using Cp$_2$ZrCl$_2$ catalyst has been studied in detail. No regioerrors have been detected by ^{13}C NMR[101]. This suggests that Cp$_2$ZrCl$_2$ is highly regioselective and chain propagation cannot proceed after an occasional secondary insertion. Similarly, the more active (MeCp)$_2$ZrCl$_2$ produces atactic poly(propylene) oligomers without detectable internal 2,1-units[66]. The propene oligomerization catalysts (Me$_5$Cp)$_2$ZrCl$_2$ and its Hf analogue are even more regioselective, since secondary units could not be detected even as chain ends. The Me$_2$Si(9-Flu)$_2$ZrCl$_2$ catalyst for high molecular weight atactic poly(propene) is of similar high regioselectivity. (Ind)$_2$ZrCl$_2$ and (H$_4$Ind)$_2$ZrCl$_2$/MAO catalysts, on the contrary, produce low molecular weight atactic poly(propylene) with about 1 % of 3,1-units. Both the C_s symmetric syndiospecific zirconocenes Me$_2$C(Cp)(9-Flu)ZrCl$_2$ and

$Ph_2C(Cp)(9\text{-}Flu)_2ZrCl_2$ show no detectable 2,1-units. However, Busico was able to detect < 0.08% 2,1 units using ^{13}C-enriched propylene in propene polymerization with a similar catalyst system[102].

C_2-symmetric zirconocenes show the greatest variability in terms of both stereo- and regioselectivities, with total regio errors ranging from almost 0-20 % in poly(propylene)[103-105]. Based on the experimental evidence it was concluded that, in the case of C_2-symmetric zirconocenes (i) only the dimethyl-substituted bis-indenyl derivatives allow a significant degree of secondary insertions; (ii) hydrogenation of the indenyl moiety promotes a higher amount of 2,1- to 3,1-isomerization; (iii) substitution in C(2) increases regio selectivity as well as stereo selectivity; and (iv) substitution in C(3) produces highly regioselective catalysts, among the most regioselective of all metallocenes.

1.2.5.5. Effect of monomer concentration on regioselectivity

Even though the total amount of secondary insertions does not depend on monomer concentration, the chemical structure of the chain fragment generated by an isolated secondary unit does depend on both polymerization temperature and monomer concentration.

Busico[106] and Resconi[107] have shown that 2,1- to 3,1-isomerization is a unimolecular process, as the ratio of [2,1]/[3,1] follows a simple first order dependence on monomer concentration and the 2,1-units are more likely to isomerize into 3,1-propene units when the monomer concentration is lowered.

1.2.5.6. Effect of polymerization temperature on regioselectivity

The polymerization temperature is another important variable in determining the microstructure of poly(propylene) obtained from *ansa*-zirconocenes. In liquid propylene monomer, both the amount of secondary insertions and the rate of 2,1- to 3,1-isomerization increase with increasing temperature. For example, for *rac*-$C_2H_4(1\text{-}Ind)_2ZrCl_2$/MAO and *rac*-$C_2H_4(4,7\text{-}Me_2Ind)_2ZrCl_2$/MAO, an increase in temperature from 20 and 70 °C increases the total 2,1-units (including end groups) from 0.4 to 0.7% and from 2.5 to 4.3 %, respectively[108].

1.2.6. Higher α-Olefin Polymerization Using Group IV Metallocenes

Group IV metallocene in combination with MAO have been well investigated for the polymerization of ethylene and propylene due to their commercial significance. Higher α-olefins, have, however, attracted less interest. Polymers of higher α-olefins find several applications due to their special physical properties[15,109-113]. Details of polymerization of higher α-olefins with various stereospecific (aspecific, isospecific and syndiospecific) group IV metallocenes have been summarized in order to understand the reaction mechanism (stereo- or regio-specificity) and the relationship between polymer structure, activity and properties.

1.2.6.1. Aspecific / Isospecific / Syndiospecific polymerization by metallocenes

The initial Kaminsky-Sinn systems based on Cp_2MX_2/MAO (M = Ti, Zr) afforded only atactic polypropylene. In 1984, Ewen found that the Cp_2TiPh_2/MAO system was a catalyst for the isospecific polymerization of propylene (*mmmm* ≅ 50 %) on cooling down the catalyst system below -45 ^oC[114].

Polymerization of hexene-1 using aspecific catalysts (Cp_2ZrCl_2) (**3**) produces low molecular oligomers at higher temperatures[115-118]. However high molecular weight (M_n = 22,690) poly(hexene-1) using Cp_2ZrCl_2/MAO catalyst can be produced at lower polymerization temperatures (-78 °C)[119]. Formation of poly(hexene-1) is shown in **Scheme 1.8**.

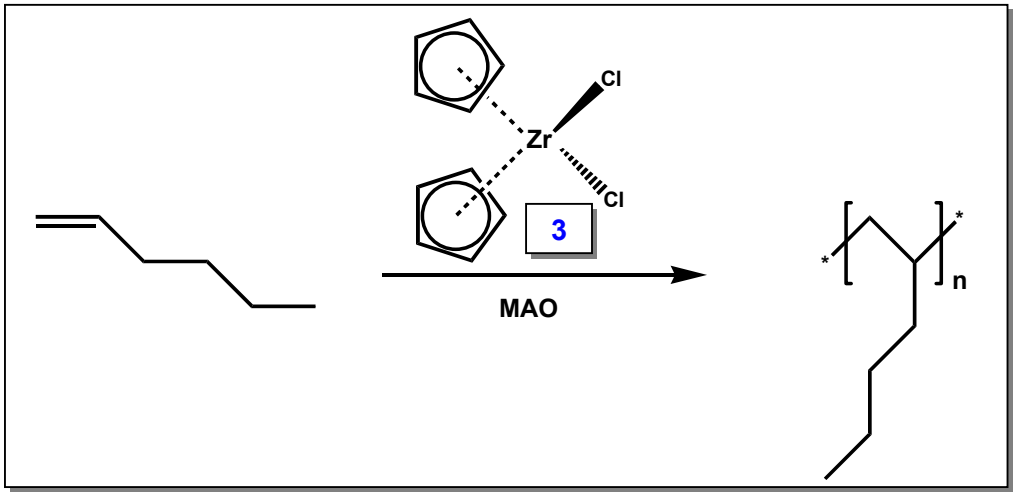

Scheme 1.8. Hexene-1 polymerization using Cp_2ZrCl_2 (**3**)/MAO

It has been noticed that, with decreasing temperature the number average molecular weight (M_n) increases. Microstructure of poly(hexene-1)s prepared at different temperatures revealed that with decreasing polymerization temperature the percentage of isotactic diads increases. With decreasing polymerization temperature the number of NMR signals decreases, indicating mechanism of chain end controlled regio- and stereoselectivity. Microstructure analysis of the low molecular weight oligomers revealed that the major end groups are vinylidene, which arise due to β-hydride transfer to metal.

Chien and coworkers reported[120] that poly(hexene-1)s synthesized using *rac*-$Et(Ind)_2ZrCl_2$ (**4**)/MAO at variable temperatures (T_p = -30 to 50 ^oC) gives high molecular weight (Mw = 18,000-97, 000). Poly(hexene-1)s synthesized using **4** produce high molecular weight (M_w = 20,000-1,00,000) polymer at lower polymerization temperature (T = 0 ^oC). Vinylene end group was observed with this catalyst system[121]. Deffieux and coworkers studied the kinetics of hexene-1 polymerization using **4**/MAO catalyst system in several solvents[122]. Significant enhancement in the activity was observed in polar solvents compared to non-polar solvents.

Chien and coworkers examined the microstructure of isotactic poly(hexene-1) produced at temperature range 25 to -30 ^oC using **4**/$[CPh_3]^+[C(B_6F_5)_4]^-$ catalyst system[123]. Internal vinylene unsaturation, which arises due to β-hydride transfer after 2,1-insertion, was found as the major end group at all temperatures.

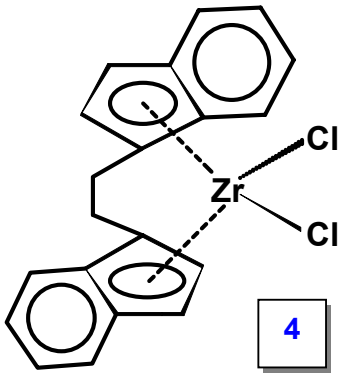

4

In 1997, Naga and Mizunuma reported *rac* and *meso*-$(CH_3)_2Si(2,3,5Me_3Cp)_2ZrCl_2$ (**5**) in combination with MAO and $[CPh_3]^+[C(B_6F_5)_4]^-$ (**6**) used as catalyst for synthesis of poly(hexene-1)s[124]. The obtained molecular weight was

in the range M_w = 60,000-1,34,000 at 40 ^oC and 1 h reaction time. The microstructure of poly(hexene-1) was predominantly atactic.

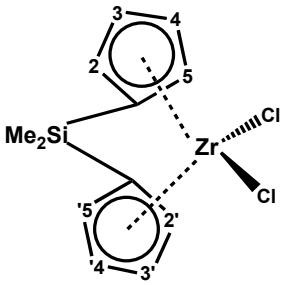

5

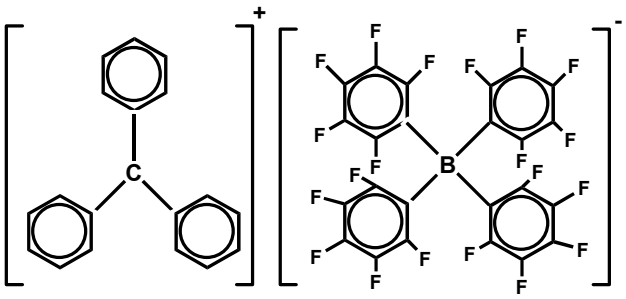

6

Shiono and coworkers reported[125] polymerization of hexene-1 with a mixture of *rac* and *meso*-[dimethylsilylene*bis*(2-methylindenyl)]zirconiumdichloride (**7** and **8)** combination with MAO. Molecular weight of poly(hexene-1) is in the range of 9,000-36,000 at 40 ^oC. The ratio of R_p (*rac*)/R_p (*meso*) (80-160) is remarkably higher than those in propene and butene-1 polymerization. These results might indicate that the *meso* is too sterically hindered for hexene-1 to coordinate to it.

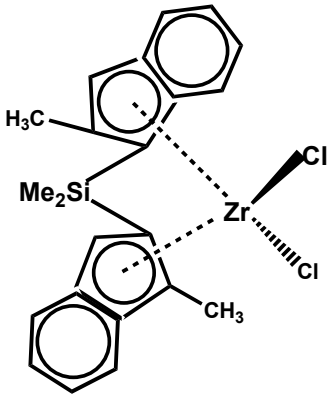

rac

7

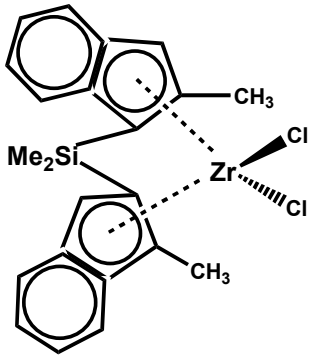

meso

8

Polymerization of hexene-1, octene-1, decene-1, dodecene-1, tetradecene-1, hexadecene-1 and octadecene-1 using *rac*-[(dimethylsilylene)*bis*(η^5-inden-1-ylidene)]zirconiumdichloride (**9**) and *rac*-[(ethylene)bis(η^5-inden-1-ylidene)]hafnium dichloride (**10**) with MAO produces highly isotactic poly(α-olefin)s[126]. The molecular weights of the poly(α-olefin)s synthesized with the zirconocene catalyst are about M_w =

50,000 and those of the hafnocene derived products are higher. The molecular weight distribution was found to be narrow *i.e.* 1.5-2.0. Based on differential scanning calorimetry occurrence of side chain crystallization for the polymers from poly(decene-1) to poly(eicosene-1) has been reported.

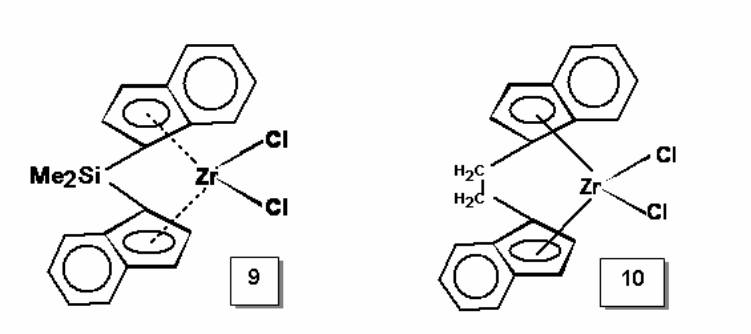

Wahner and coworkers synthesized[127] poly(α-olefin)s ranging from poly(pentene-1) to poly(octadecene-1) with narrow polydispersities using $(CH_3)_2Si$(2-methylbenz[*e*]indenyl)$_2ZrCl_2$ (**11**) and MAO at polymerization temperatures from -15 to 180 ^oC (**Scheme 1.9**). The molar masses of the poly(α-olefin)s range from M_w = 47,000

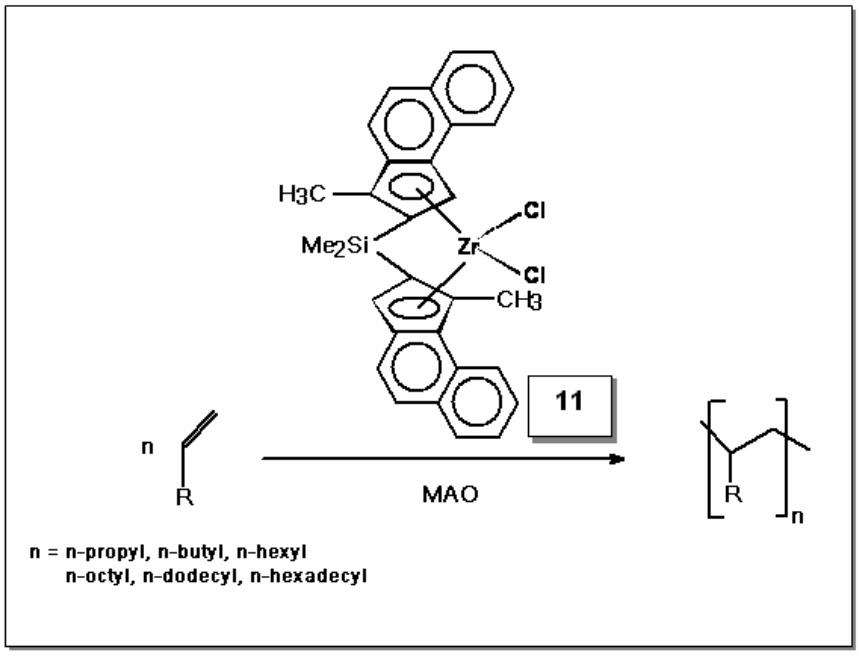

Scheme 1.9. Higher α-olefin polymerization using **11**/MAO

to 3,80,000. The molecular weight of polymers are significantly higher than those of various higher poly(α-olefin)s synthesized with other zirconium-based metallocenes[126,128,129]. It is noticed that the activity of α-olefins in polymerization reaction conditions decreases with increasing chain length. Poly(hexene-1) and poly(octene-1) are amorphous materials without a distinct melting point. However, poly(α-olefin)s with long alkyl chains showed two distinct melting points that are attributtable to the melting of crystals formed by the long side chains and the helical main chain[126,130,131].

Polymerization of higher α-olefins, pentene-1, hexene-1, octene-1 and decene-1 were initiated efficiently by *rac*-$Me_2Si(1\text{-}C_5H_2\text{-}2\text{-}CH_3\text{-}4\text{-}^tBu)_2Zr(NMe_2)_2$ (**12**)/Al(*i*-$Bu)_3$/$[CPh_3][B(C_6F_5)_4]$ catalyst to yield high molecular weight polymers[132]. The [*mm*] triad of polymers decreased with the increased lateral size in the order: poly(propylene) (almost 100 %) > poly(pentene-1) (96 %) > poly(hexene-1) (93 %) > poly(octene-1) (92 %) > poly(decene-1) (86 %). The formation of cationic zirconium species is depicted in **Scheme 1.10**.

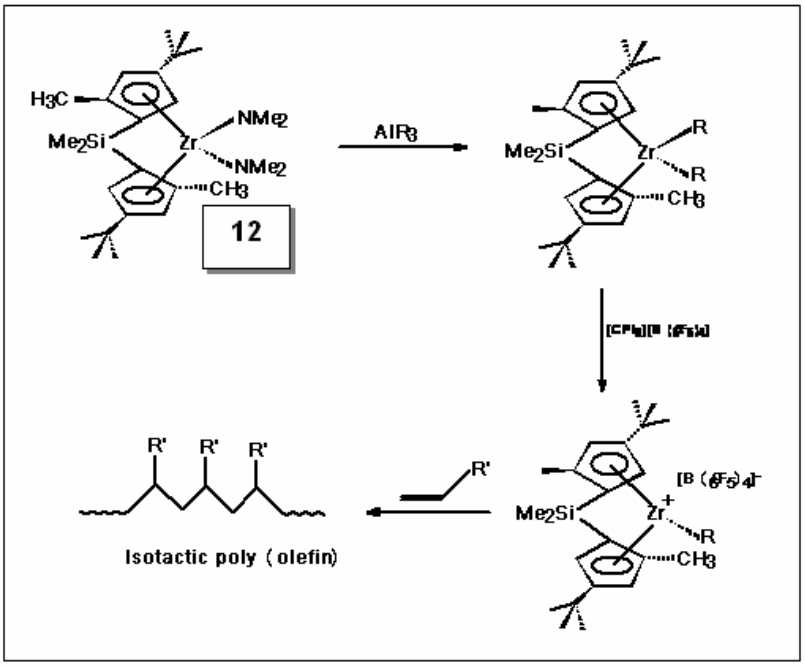

Scheme 1.10. Formation of active species and α-olefin polymerization

Odian and coworkers reported[133] rate of hexene-1 polymerization, polymer molecular weight and microstructure (stereospecificity and regiospecificity) as a function of the temperature and the concentrations of monomer, catalyst, and cocatalyst. Catalyst and coctalyst used was *rac*-(dimethylsilyl)*bis*(4,5,6,7-tetrahydro-1-indenyl)zirconium dichloride (**13a,b**) and MAO respectively. Isotacticity (*mmmm* %) of poly(hexene-1) ranges from 47 to 97 with varying temperature from 100 to 0 °C. The extent of regiospecificity varies from 1.4 to 3.0 %. Increasing concentration of zirconocene and MAO yielded higher extents of reverse addition. The poly(hexene-1) molecular weight decreased modestly with increasing zirconocene concentration at 0 and 50 ^{o}C in line with the higher order dependence of k_{tr} on the zirconium concentration compared to the dependence of R_p on zirconium concentration. The order of dependence on monomer was first-order at 0 ^{o}C.

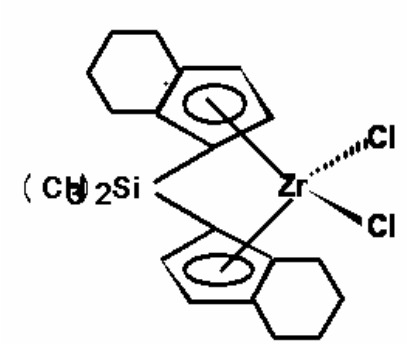

13a

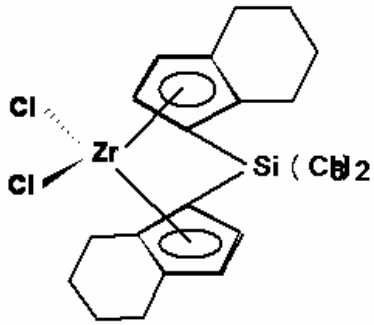

13b

Kaminsky and Hoff reported[134] syndiotactic polymers of pentene-1, hexene-1 and octene-1 using C_s-symmetric metallocene catalysts, i.e. [Ph_2C(Cp)(2,7-*tert*-Bu_2Flu]$ZrCl_2$ (**14**) and [(4-MePh)$_2$C(Cp)(2,7-*tert*-Bu_2Flu)]$ZrCl_2$ (**15**) with MAO as cocatalyst. **14** and **15** produces high molecular weight poly(α-olefin)s (upto 5,50,000 g. mol^{-1}) compare to other metallocenes, which can be ascribed to the phenyl groups in the bridge. For poly(hexene-1), the maximum pented (*rrrr* %) syndiotacticities observed was 87-89 % with both of the catalyst systems.

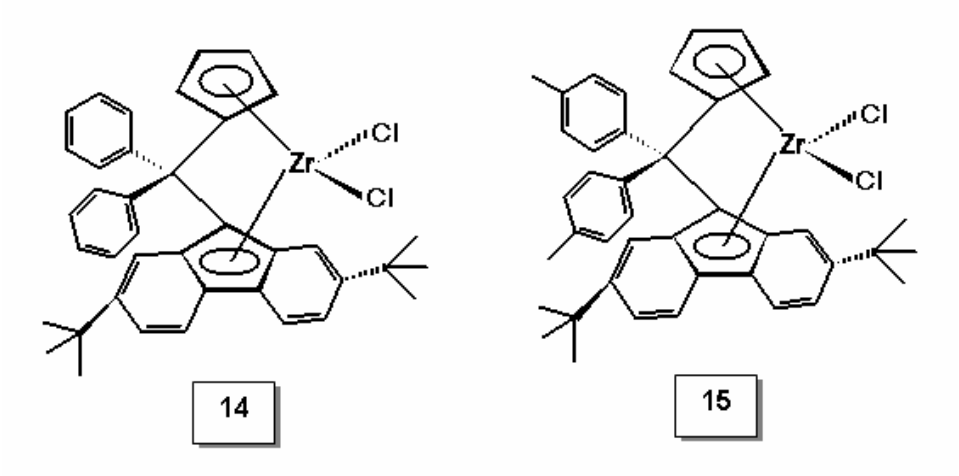

Metallocene catalyzed olefin polymerization under high pressure has recently attracted research interest since a high-pressure polymerization process has become a probable method for the industrial utilization of these catalysts[135-137]. Wakatsuki and coworkers reported[138] the poly(hexene-1)s using a series of Kaminsky-type catalysts with methyl substituents attached to the C_5 rings $(Me_nC_5H_{5-n})_2ZrCl_2$ (where, n = 0, 1, 3, 4, 5) (**16a-e**) with MAO. Poly(hexene-1) with high molecular weight of M_w = 1,570,000 (M_w/M_n=2.44) was obtained by **16d** at an optimum pressure of ca. 250 MPa. The highest activity was observed for **16e**, which polymerized hexene-1 at 500 MPa with a rate of $6.2x10^8$ g(PH) mol $(Zr)^{-1}$ h^{-1}, this is two orders of magnitude higher than at atmospheric pressure. The polymerization activities of zirconocene catalysts increase at 500 MPa in the order, **16a** < **16b** < **16c** < **16d** << **16e**. High molecular weight poly(hexene-1) (M_w = 3,380,000, M_w/M_n = 2.7) was obtained as rubber like solid using $(C_5HMe_4)_2HfCl_2$ (**17**)/MAO at an optimum pressure of ca. 250 MPa.

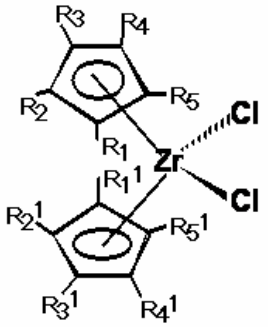

16a: $R_{1\text{-}5} = R^1_{1\text{-}5} = H$
16b: $R_1 = R^1_1 = Me$; $R_{2\text{-}5} = R_{2\text{-}5}{}^1 = H$
16c: $R_{1,2,4} = R^1_{1,2,4} = Me$; $R_{3,5} = R_{3,5}{}^1 = H$
16d: $R_{1\text{-}4} = R^1_{1\text{-}4} = Me$; $R_5 = R_5{}^1 = H$
16e: $R_{1\text{-}5} = R^1_{1\text{-}5} = Me$

Suzuki and coworkers reported[139] high-pressure polymerization of hexene-1 and octene-1 by *ansa*-zirconocene and hafnocene complexes (**18a-e**). Polymerization activities of the complexes were substantially enhanced due to high pressure and the obtained poly(hexene-1)s had extremely high molecular weight ($1.0x10^7$). The germylene-bridged hafnocenes exhibited 4 times higher activity than the silylene-bridged complexes. Investigation on termination process revealed that whereas, bimolecular β-hydride transfer to olefin occurred with zirconocene, unimolecular β-hydride elimination to the metal was the major termination process with hafnocene even under high pressure.

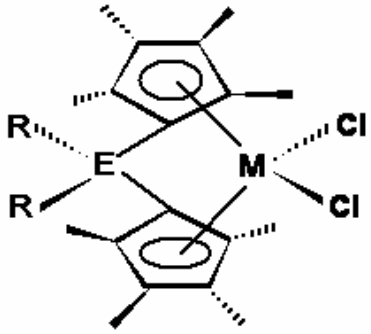

18a: *E = Si; R = Me; M = Zr*
18b: *E = Si; R = Me; M = Hf*
18c: *E = Si; R = Et; M = Hf*
18d: *E = Si; R = Vinyl; M = Hf*
18e: *E = Ge; R = Me; M = Hf*

1.2.7. Polymerization of Higher α-Olefin Using Early and Late Transition Metal Catalysts

Over the last two decades, significant strides have been made in understanding homogeneous single-site catalysts[3,4,24,28,31,35,140-143] for olefin polymerization. Despite the enormous advancement made with single-site catalysts, one limitation remains: the polymerization rate for higher α-olefins generally decreases with the increase in carbon number of monomer due to steric hindrance. Recently, the main focus of research pertaining to higher α-olefin polymerization catalysts has been the discovery of non-metallocenes resulting out of an increased understanding of the factor that are important for stabilizing active metal centers and controlling their activity and selectivity. However, new generation of olefin polymerization catalysts have lead to development of well-defined polyolefins such as highly branched polymers[144-146], alternating copolymers[147-149], narrow molecular weight distribution polymers[150] and high molecular weight polymers[151,152].

1.2.7.1. Higher olefin polymerization by early transition metal (ETM) catalysts: Kinetics and mechanism, chain transfer reactions and polymer structure

Schrock and coworkers reported[153] activation of [(2,4,6-Me_3C_6H-$NCH_2CH_2)_2NR$]$ZrMe_2$ (R = H, Me) (**19a,b**) complex with $[Ph_3C]^+[B(C_6F_5)_4]^-$ for the polymerization of hexene-1 in chlorobenzene at 30 ^oC for a period of 1 h. The molecular weight (M_n = 12,700; PDI = 1.4 and M_n = 29100; PDI = 1.5) of poly(hexene-1) was obtained with **19a** and **19b** respectively. The number average molecular weight of the poly(hexene-1) obtained was consistent with some chain termination, presumably via β-hydride elimination.

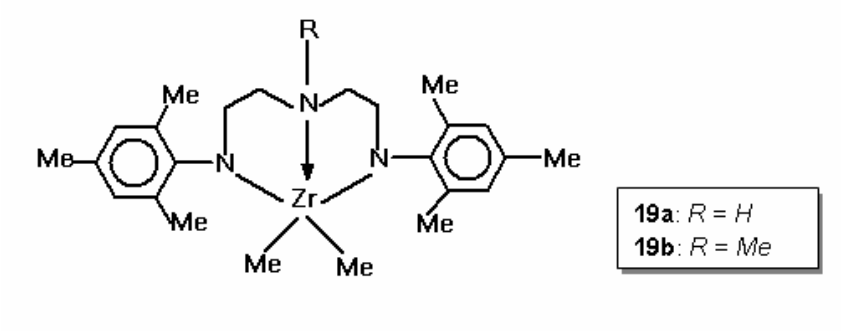

Goldschmidt and coworkers reported[154] dibenzyl complex [ONNO]$Zr(CH_2Ph)_2$ (0.01 mmol) (**20**) along with $B(C_6F_5)_3$ activate hexene-1 (10 mL, neat) polymerization at room temperature. Very fast and complete consumption takes place within 2 min. giving an activity of 15,500 g $mmol^{-1}h^{-1}$. This is the highest reactivity reported for polymerization of hexene-1 under such mild conditions[155,156]. The poly(hexene-1) obtained had a molecular weight of M_w = 1,70,000 and PDI = 2.2. Activation complex (**20**) and $B(C_6F_5)_3$, yielded only oligo(hexene-1) chains, giving a low activity of 23 g $mmol^{-1}h^{-1}$ The extreme reactivity of the catalyst derived form the $[ONNO]^{2-}$ ligand may result from steric effect, e. g. a narrow angle between the growing polymer chain and a coordinated olefin, as well as electronic effects induced by the N-donors being trans to the active positions.

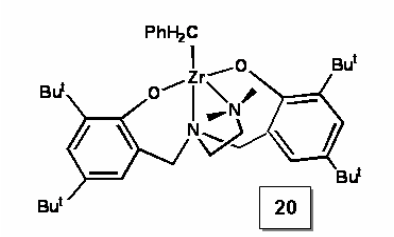

Further Goldsberg and group made several [ONXO]-type amine *bis*(phenolate)zirconium and hafnium complexes (**21a-f**), where X is a heteroatom donor located on a pendant arm for activities in the polymerization of hexene-1, yielding high molecular weight and activity being unprecedented under the conditions employed[157]. The polymerization data are shown in **Table 1.2**. The activity order of the zirconium complexes as a function of the side arm donor was found to be OMe > NMe_2 > SMe. For hafnium series, it is SMe > OMe > NMe_2. However, the highest activity was reported for a hafnium complex under the conditions employed.

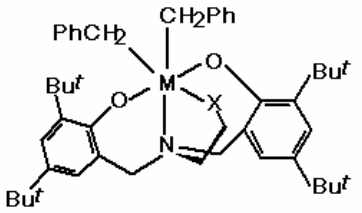

21a: *X = NMe; M = Zr*
21b: *X = NMe_2; M = Hf*
21c: *X = OMe; M = Zr*
21d: *X = OMe; M = Hf*
21e: *X = SMe; M = Zr*
21f: *X = SMe; M = Hf*

Table 1.2. Hexene-1 polymerization data

Catalyst	Solvent	Activity[a]	M_w	M_w/M_n
21a	neat	21,000	35,000	3.5
	heptane	860	1,70,000	2.0
21b	neat	2,200	13,000	3.2
	heptane	200	20,000	1.6
21c	neat	50,000	80,000	3.0
	heptane	1,300	1,60,000	1.4
21d	neat	16,500	1,01,000	2.2
	heptane	700	1,40,000	1.8
21e	neat	9200	1,95,000	2.0
	heptane	450	1,40,000	1.6
21f	neat	35,000	66,000	2.5
	heptane	1,600	2,50,000	1.4

[a] In units of g $mmol^{-1}$ $cat^{-1}h^{-1}$

Nonbridged half-metallocene type group IV transition metal complexes of the type, Cp′M(L)X_2 (Cp′= cyclopentadienyl group; M = Ti, Zr, Hf; L = anionic ligand such as Oar, NR_2, NPR_3; X = halogen, alkyl) have attracted considerable attention as a new type of olefin polymerization catalysts[158-161]. Nomura and Fudo reported[162] that

Cp*$TiMe_2$(O-2,6-$^{i}Pr_2C_6H_3$) (Cp* = C_5Me_5) (**22**) exhibit significant catalytic activity for hexene-1 polymerization even at low temperature of -30 ^{o}C in combination with $Al^{i}Bu_3/[Ph_3C]^{+}[B(C_6F_5)_4]^{-}$ and obtained a polymer with M_w = 1,200,000 and M_w/M_n = 1.5 under these conditions. On the other hand, extremely low activity was observed if $B(C_6F_5)_3$ was used in place of $Ph_3CB(C_6F_5)_3$. The resulting microstructure of poly(hexene-1) was atactic[163] as determined by ^{13}CNMR.

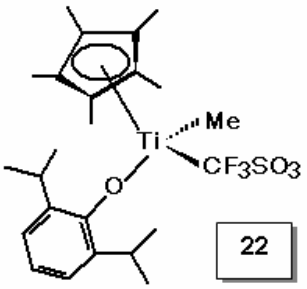

22

Nomura and coworkers reported[164] the synthesis of poly(hexene-1)s using a series of nonbridged (cyclopentadienyl)(ketimide)titanium complexes of the type, Cp′$TiCl_2$(N=C$^{t}Bu_2$) [Cp′= Cp (**23a**), $^{t}BuC_5H_4$ (**23b**) and C_5Me_5 (Cp*, **23c**)] in the presence of MAO as cocatalyst. Cp analogue (**23a**) shown remarkable catalytic activity than the Cp* (**23c**), ^{t}BuCp (**23b**) analogue. The molecular weight of poly(hexene-1)s increased in the order **23a** >> **23b** > **23c**. The steric bulk on Cp′ rather than the electronic effect plays an essential role especially for exhibiting the high catalytic activity.

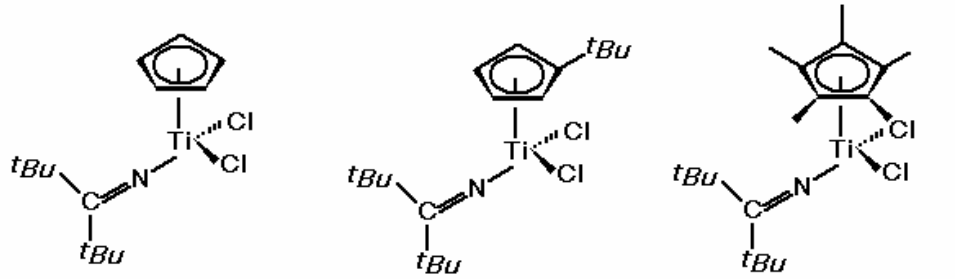

Poly(hexene) (**23a**):
Activity = 16,800 kgPmolTi^{-1}h^{-1}
M_w = 6,17,000
M_w/M_n = 1.6

Poly(hexene) (**23b**):
Activity = 1,310 kgPmolTi^{-1}h^{-1}
M_w = 2,85,000
M_w/M_n = 1.7

Poly(hexene) (**23c**):
Activity = 569 kgPmolTi^{-1}h^{-1}
M_w = 1,30,000
M_w/M_n = 1.6

Goldschmidt and coworkers reported[165] structure-activity trends in amine bis(phenolate) titanium catalysts (**24a-e**) for the polymerization of hexene-1. The activity

of the catalysts of the "OMe" series was low to moderate and was almost independent of the phenolate substituents. In contrast, the activity of the NMe_2 catalysts had a strong dependence on both the steric and electronic character of the phenolate substituents, ranging from mild to highly active. Titanium catalyst (**24e**) led to the most active catalyst and remarkably high molecular weight (M_w > 4,000,000) poly(hexene-1) obtained within 1 h of polymerization at 25°C. The characterization of ultrahigh molecular weight atactic poly(hexene-1) by means of oscillatory rheometry and stress relaxation experiments indicated typical elastomeric behavior at room temperature.

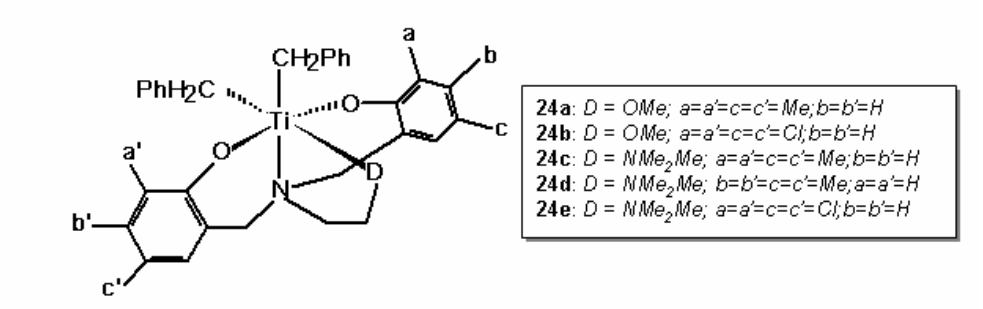

Recently, Fujita and coworkers reported[166,167] polymerization of hexene-1, octene-1 and decene-1 using *bis*[N-(3-*tert*-butylsalicylidene)phenylaminato]titanium (IV) dichloride (**25**) (named as 'FI catalyst') with $^{i}Bu_3Al/Ph_3CB(C_6F_5)_4$ as cocatalyst. **25** produced high molecular weight poly(hexene-1) (M_w = 7,20,000, PDI = 1.68), poly(octene-1) (Mw = 9,50,000, PDI = 1.74), poly(decene-1) (M_w = 8,20,000, PDI = 1.75) at 25 ^{o}C polymerization temperature within 20 min of reaction time, the molecular weight values (7,20,000-9,50,000) being an order of magnitude larger than those obtained by *rac*-$[C_2H_4$-(1-indenyl)$_2]ZrCl_2$ (M_w = 42,000-59,000). ^{13}C NMR revealed that poly(hexene-1) possesses an atactic structure with about 50 mol % of regioirregular units.

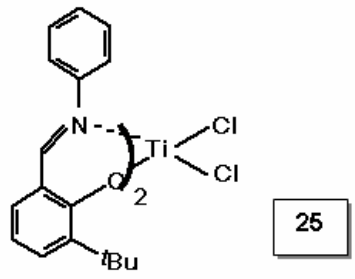

25

Schrock et. al reported[168] that [Mesityl-NH-*o*-C_6H_4N(Ph) CH_2CH_2NMesityl] MMe_2 (M = Zr or Hf) (**26a,b**) with [Ph_3C][$B(C_6F_5)_4$] gives rise to cationic complexes that are active initiators for the polymerization of hexene-1. Poly(hexene-1) synthesized by **26a** and **26b** had molecular weight (M_n = 41,000, PDI = 4.0) and (M_n = 19,000, M_w/M_n = 2.7) respectively at -25 ^oC polymerization temperature. The bimodal nature (GPC trace) of poly(hexene-1) by **26a** is of catalyst deactivation due to CH activation in mesityl methyl group[169,170].

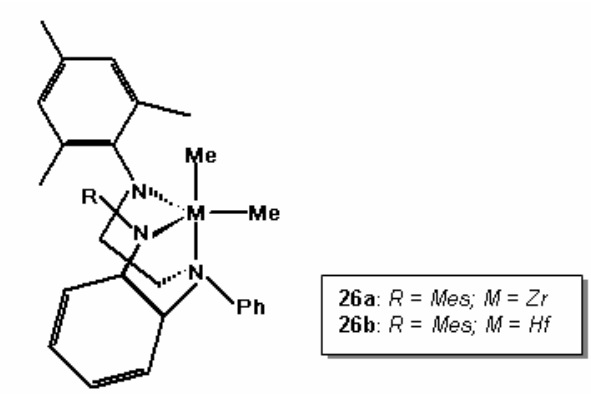

The McConville generation of complexes [$(CH_2)_3${N(2,6-Pr_2^i-C_6H_3)}$_2$$TiCl_2$] (**27a**) ($C_{2v}$)[171] *l*-[$CMe_2${CHMeN(2-$Pr^i$-$C_6H_4$)}$_2$$TiCl_2$] ($C_2$-symmetry) (**27b**)[172] and *u*-[$CHMe_2${CHMeN(2,6-Pr_2^i-C_6H_3)}$_2$$TiCl_2$] ($C_s$-symmetry) (**27c**)[172] polymerize hexene-1 when activated by MAO. The activity of **27a** is very high (115 kg/mmol^{-1}h^{-1}) compare to **27b** (2.2 kg/mmol^{-1}h^{-1}). Poly(hexene-1) obtained within 0.5 min with **27a** had a molecular weight (M_w) of 81,500 and PDI 1.73 as compared to 25,100 (M_w) and 2.0 (PDI) obtained with **27b** for 60 min. NMR analysis confirmed that there were more *mmmm* pentads in poly(hexene-1) produced by **27b** than atactic material produced by **27a**.

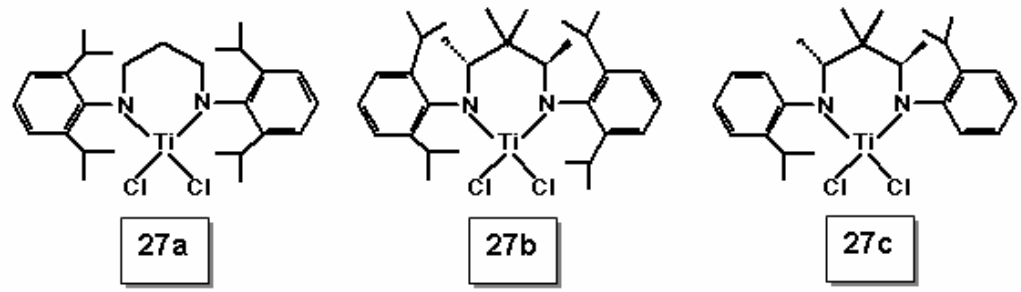

Ultra high molecular weight poly(hexene-1) (M_w = 5,720,000 and M_w/M_n = 1.9) and poly(octene-1) (M_w = 6,050,000 and M_w/M_n = 2.0) have been synthesized using thiobis(phenoxy)titaniumdichloride (**28**) with water modified MMAO[173]. Stereoregular poly(hexene-1)s were obtained.

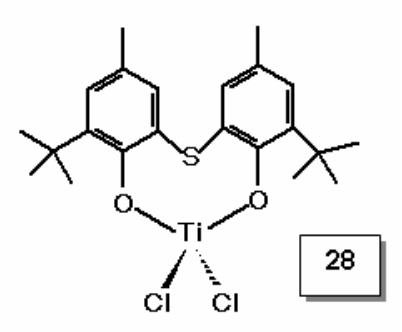

Zirconium and titaniumdiamine *bis*(phenolate) (**29a,b**) in combination with $B(C_6F_5)_3$ catalysts leads to highly active catalyst for hexene-1 polymerization[174]. The dibenzyl Zr complexes of these ligands lead to highly active, but low molecular weight atactic poly(hexene-1). In contrast, the corresponding titanium complexes are highly active and lead to ultrahigh molecular weight poly(hexene-1) (M_w = 1,900,000, M_w/M_n = 2.0) with an isotacticity of 60 %. Electron withdrawing groups on the phenolate rings cause an increase in activity and a small titanium center that is sensitive to ligand steric bulk leads to highly active catalysts.

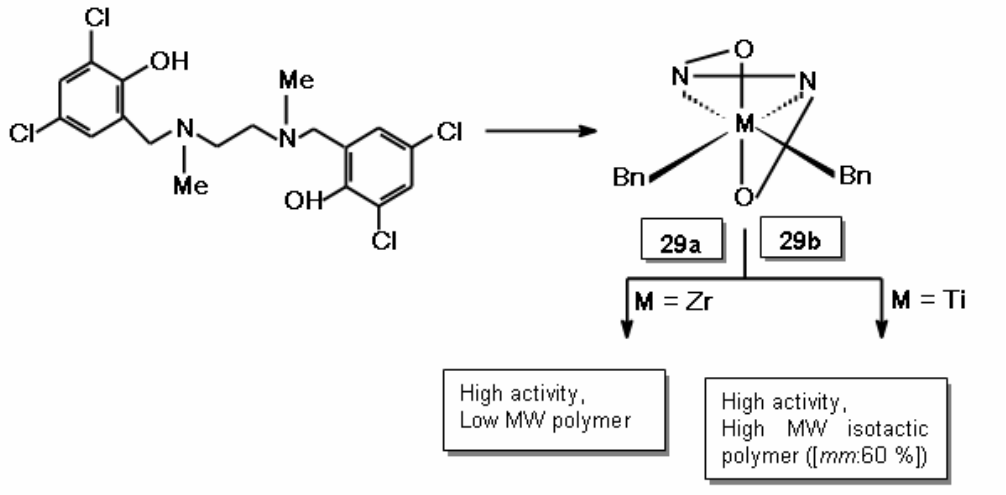

1.2.7.2. Higher olefin polymerization by late transition metal (LTM) catalysts: Kinetics and mechanism, chain transfer reactions and polymer structure

Structure-activity-property relationship for olefin polymerization has been well understood with early transition metal based catalyst systems[3,4,24,28,31,35,140-143]. Transition metal catalysts have played and will continue to play crucial roles in the manufacture of important polymeric materials[175]. Although early transition metal catalysts remain the workhorse of the polyolefin industry, significant advances have been made recently in late transition metal polymerization catalysts[143,144,176-179].The advantage of late transition metal catalysts is that they are more tolerant of polar functional groups in the monomer.

In addition early transition metal catalyst systems offer ease of control of polymer topology[180-187]. By tuning the catalyst structure, polymerization temperature and nature of monomer physical properties can be changed dramatically, from a thermoplastic to an elastomer and eventually to a viscous liquid.

In 1985, Fink and coworkers reported nickelamino*bis*(imino)phosphorane catalyst (**30**) system for the polymerization of α-olefins[188]. This system polymerized pentene-1 to afford methyl-branched polyethylene equivalent to poly(ethylene-alt-propene)[188,189]. The structure of the poly(α-olefin)s is unusual. Polymer contains only methyl branches, with regular spaces along the chain with a separation corresponding to the chain length of the monomer (**Scheme 1.11**). This unusual structure is a consequence of migration of transition metal alkyls along the polyolefin chain followed by insertion, a phenomenon termed as "chain walking". During this migration, transfer reactions (β-hydride elimination) to the monomer can occur, but not insertions. The average molecular weight of the polymer was 1000 g/mol. The degree of polymerization decreases linearly with increasing chain length of the α-olefin.

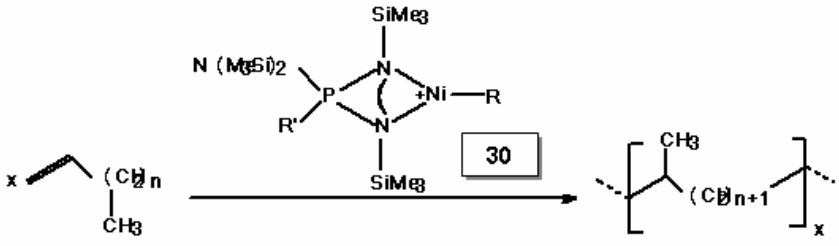

Scheme 1.11. Polymerization of α -olefin using **30**

In 1995, a seminal discovery of the nickel and palladium (α-diimine) catalysts (**31**) was reported by Brookhart and coworkers. This was the result of a collaborative effort on developing a new polymerization catalyst system at DuPont Central Research and Development which was later introduced under the name Verispol process[177,190,191]. Higher α-olefin polymerization using these catalysts produce high molecular weight poly(α-olefin)s, which exhibits different microstructure and physical properties unlike those made by early transition metal catalyst systems. A key feature enabling polymerization to occur to very high molecular weights is retardation of chain transfer by the steric bulk of the *o*-aryl substituents (R^1 or R^2 = ^{i}Pr or Me). The R groups are located in an axial position above and below the square planar coordination plane as a consequence of a perpendicular arrangement of the aryl rings with respect to the latter.

The unique feature of these catalysts is their ability to form highly branched and chain-straightened poly(olefin)s during the homopolymerization of higher α-olefins (**Scheme 1.12**). This leads to less number of branches than the expected. Polymerization of hexene-1 (**31a**, 0.8 M, -10 ^{o}C, 1 h) yields poly(hexene-1)s (M_n = 44,000; M_w/M_n = 1.09; 135 branches/1000 C atoms). Poly(octadecene-1)s produced by **31b** (0.3 M, -10 ^{o}C, 2 h) contains 39 branches with M_n = 19,000, M_w/M_n = 1.14. Poly(octadecene-1)s exhibits two melting points at 32 and 60 ^{o}C. Palladium(II)(α-diimine) (**32**) catalyst for polymerization of long chain α-olefin (octadecene-1) leads to a semicrystalline polymer (T_m = 72 and 86 ^{o}C) with 34 branches per 1000 C atoms[192].

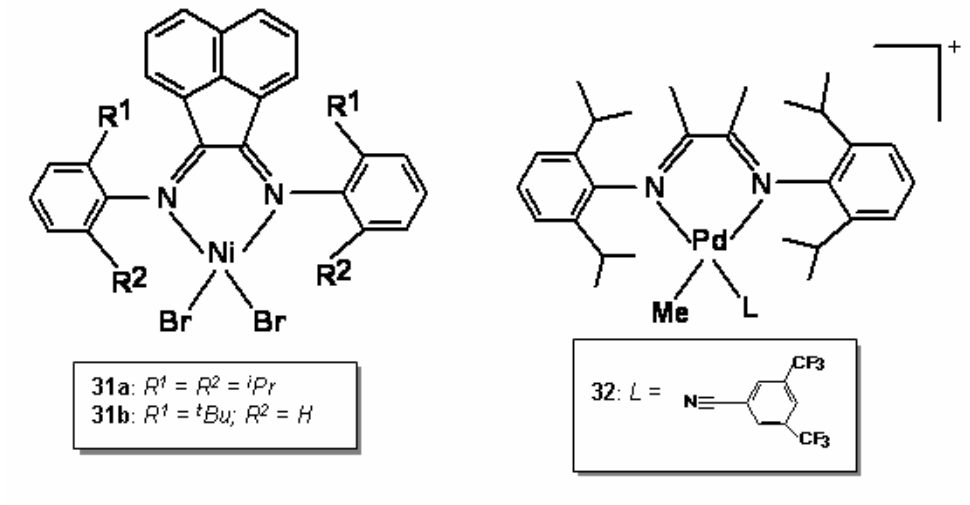

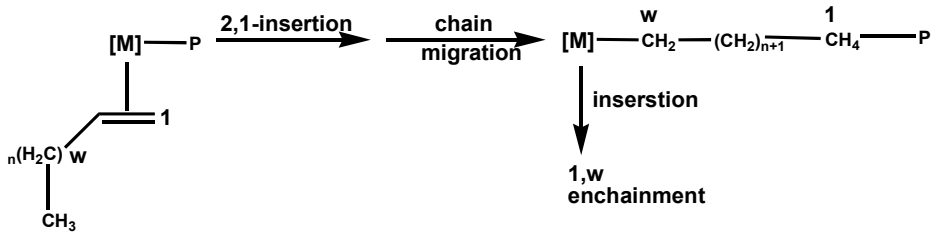

Scheme 1.12. Olefin-1 polymerization using **31**, **32**

Yu and coworkers reported[193] that the polymerization of hexene-1 at high pressure (500 MPa) using nickel(α-diimine) (**33**) (similar to **31a**, methyl group instead of acenapthene) gave higher molecular weights (M_w = 1,250,000, M_w/M_n = 1.86) only at low monomer concentrations (1.2 M). The yield of poly(hexene-1)s was five times higher at 500 MPa at 1 h as compared to 0.1 MPa. At high-pressure polymerizations, chain walking is more frequently interrupted by chain transfer reactions; which leads to increase number of branches.

Recently, Guan and coworkers developed a cyclophane based Ni^{II}-(α-diimine) complex (**34**), which has been shown to be a highly active and robust catalyst for hexene-1 polymerization at high temperature[194]. Poly(hexene-1)s made with **34** produced higher molecular weight even at higher temperature compare to poly(hexene-1)s synthesized by **31a**. Comparative data have been shown in **Table 1.3**. Improved performance at high temperature is attributed to the unique cyclophane framework of the catalyst ligand, which prevents catalyst deactivation and provide efficient steric blocks at the axial sites, suppressing associative chain transfer by monomer from axial direction[195]. Significantly less number of branches with poly(hexene-1) indicates that the higher percentage insertion of 2,1-fashion followed by 1,ω-enchainment is predominant. This also leads to having longer linear segments, resulting in crystalline domains and exhibiting melting endotherm (T_m = 62 ^oC).

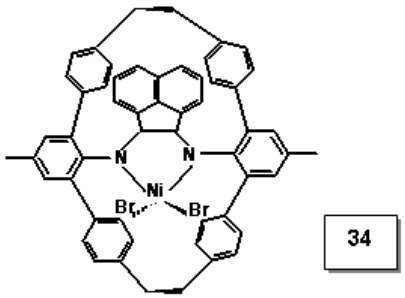

34

Table 1.3. Hexene-1 polymerization using **31a** and **34**/MMAO

Catalyst	Temp., (^oC)	TOF	M_n	M_w/M_n	Branches/ 1000 C atoms	DSC
31a	25	1505	534000	1.50	108	- 54 (T_g)
	50	753	461000	1.45	110	- 57 (T_g)
34	25	1331	510000	1.22	57	- 34 (T_g), 62 (T_m)
	50	1901	647000	1.13	58	-38 (T_g), 58 (T_m)

1.2.8. LIVING POLYMERIZATION OF α-OLEFINS

Polymer synthesis is increasingly driven by the need to accomplish greater control of molecular and supramolecular structures. This includes, the preparation of polymers with novel topology such as highly regular comb shaped, dendritic structure as well as various type of block, star polymers and copolymers, which may microphase, separate into domains of various geometries. The potential application of a polymer is determined by its physical and mechanical properties, which in turn, is defined by its topological structure. Synthesis of well-defined topology for poly(olefin)s requires high chemoselectivity, regioselectivity and stereoselectivity. High chemoselectivity is observed in living polymerizations when chain growth is not disturbed by any chain breaking reactions.

Living polymerization techniques[196-198] allow synthesis of well defined polymers with predictable molecular weights and narrow molecular weight distributions, end functionalized polymers and synthesis of a wide array of polymer architectures. Living polymerization is currently an area of intense research. Several terminologies like, controlled polymerization, living, living/controlled, pseudo-living, living polymerization with reversible deactivation and others are scattered throughout the literature[199]. Features of an ideal living polymerization are discussed below.

1.2.8.1. Nature of catalyst and cocatalyst

Progress in the coordination polymerization of α-olefins can be ascribed to the better understanding of the reaction mechanism and to the correct choice of catalyst and

cocatalyst systems. The common feature of α-olefin polymerization by transition (early and late) metal catalyst in combination with MAO, leads to the chain transfer and elimination reactions resulting in the formation new polymer chain[66]. Details of chain transfer and termination reactions are discussed in the Section 1.2.3.3. Olefin polymerization by metallocene catalysts/MAO, consecutive alkene insertion into the M-C bond connecting the catalyst and polymer chain proceeds until *β*-hydride and/or *β*-alkyl elimination[200]. The presence of aluminum alkyls provides a major termination route via transfer to the aluminum center. Several approaches to suppress transfer reactions have been reported. In this regard introducing boranes (replacement of aluminum alkyls) that are weakly coordinating anions has made significant contribution to living olefin polymerization[201].

In 2003, Sita and coworkers reported[202] a degenerative transfer- living olefin polymerization by neutral dimethyl pentamethylcyclopentadienylzirconium acetamidinate (**35**) complexes with boranes as catalyst systems. This involves reversible methyl group exchange between cationic (active) and neutral (dormant) end groups (**Scheme 1.13**), which leads to narrow molecular weight poly(α-olefin)s. The great advantage of this degenerative transfer- living process is that, borane (cocatalyst) to metal catalyst ratio is 1:1. Based on this process a range of stereoblock polyolefins of narrow polydispersity and specific microstructures with respect to their relative stereoblock lengths were synthesized.

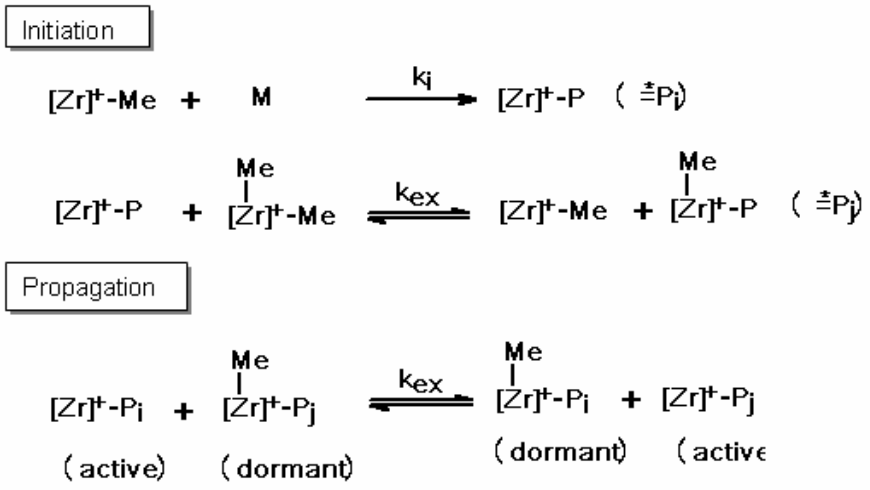

Scheme 1.13. Initiation and propagating species with **35** and $[PhNMe_2H][B(C_6F_5)_4]$

1.2.8.2. Influence of reaction conditions on extent of livingness

Several strategies have been used to decrease the rate of chain termination relative to that of propagation to enhance the livingness of polymerization. Lowering polymerization temperature results in reduced probability of β-hydrogen and alkyl elimination processes, which are unimolecular in nature. The main disadvantage of using low temperature is the precipitation of polymers from solution, which can hinder the controlled nature of a living polymerization.

1.2.8.3. Experimental criteria used to establish living nature of α-olefin polymerization

The following are the generally accepted criteria for living olefin polymerization. All these conditions and kinetic parameters have already been well established for living carbocationic polymerization by Kennedy and coworkers[203] and living radical polymerization by Matyajaszewski and coworkers[204]. Sivaram and coworkers have reported the kinetics of living MMA polymerization by anionic polymerization techniques[205,206].

(A) Initiation should be much faster than propagation and termination. First order monomer consumption plot should be linear. This signifies absence of catalyst deactivation as well as termination reactions during polymerization. Polymerization proceeds to complete monomer consumption.

(B) Degree of polymerization versus monomer conversion plot should be linear. The curve should pass through origin. Molecular weights must precisely controlled.

(C) Poly(α-olefin)s should have narrow molecular weight distribution ($M_w/M_n = 1$) implying the number of active centers remain the same throughout the polymerization.

(D) Should be possible to synthesize block copolymers by sequential monomer addition and end-functionalized polymers.

1.2.8.4. Synthesis and characterization of α-olefin block copolymers

In 1998, Kim and coworker reported[207] the use of *2,2'*-ethylenebis(*N,N'*-(triisopropylsilyl)anilinido)dialkylzirconium (**36**) in combination with $B(C_6F_5)_3$ for the synthesis of hexene-1/octene-1 block copolymer by sequential addition of hexene-1 and

octene-1 at 0 ^{o}C (M_n = 1,08,700; M_w/M_n = 1.21) (**Scheme 1.14**). A high molecular weight atactic block copolymer with narrow molecular weight distribution was obtained.

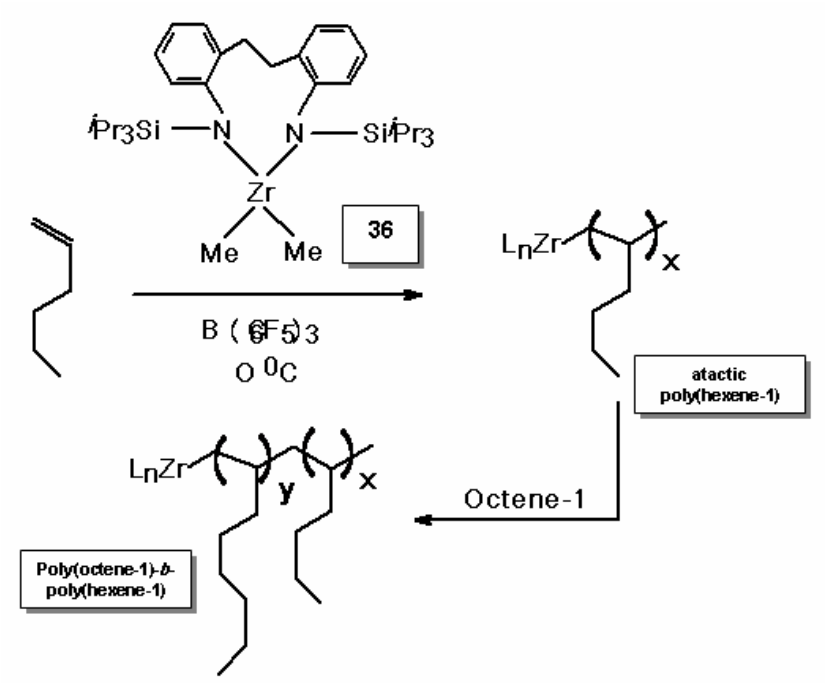

Scheme 1.14. Hexene-1/octene-1 block copolymer synthesis using **36**/$B(C_6F_5)_3$

Kol and coworkers[208] reported synthesis of block copolymers of hexene-1 and octene-1 in chlorobenzene at room temperature using C_2-symmetric titanium catalyst (**37**) with $B(C_6F_5)_3$. The resulting poly(hexene-1-*co*-octene-1) (**Scheme 1.15**) has moderate molecular weights (M_n = 11,600) with a molecular weight distribution 1.2. ^{13}C NMR spectrum confirmed the atactic nature of the copolymer.

Brookhart and Gottfried reported[192] synthesis of poly(ethylene-*b*-octadecene-1)s and poly(octadecene-1-*b*-ethylene)s using late transition palladium(α-diimine) catalyst system (**32**). The copolymer microstructure differed depending on the order of introduction of the monomer blocks. Poly(ethylene-*b*-octadecene-1)s with a M_n = 50,000; M_w/M_n = 1.22; 53 branches/1000 carbon atoms and poly(octadecene-1-*b*-ethylene)s with a M_n = 23,000; M_w/M_n = 1.10; 66 branches/1000 carbon atoms were obtained.

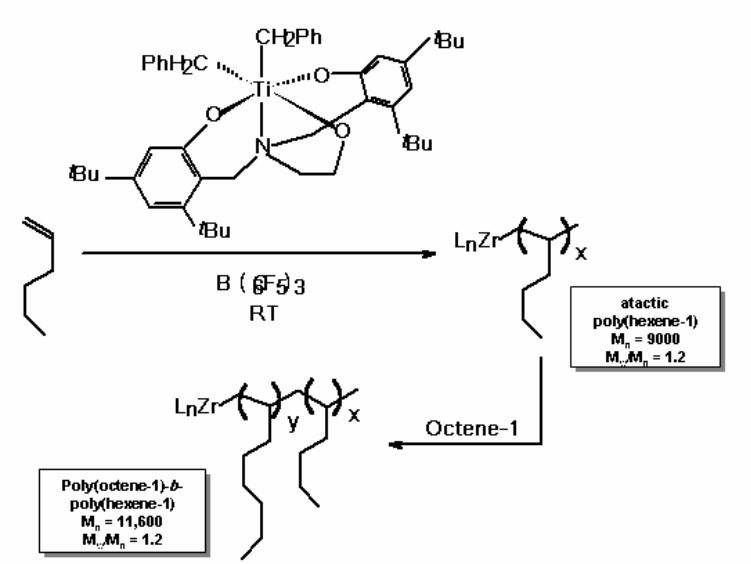

Scheme 1.15. Hexene-1/octene-1 block copolymer synthesis using **37**/$B(C_6F_5)_3$

1.3. CONCLUSIONS

Single site group IV metallocene based catalyst (Ti, Zr and Hf) systems have been well studied for the polymerization of α-olefins in the last decade. Metallocene based innovations with respect to both catalyst and polymer development have been very significant and the relationship of catalyst-activity-polymer property has reached a high level of achievement, both, academically as well as from an industrial point of view. The most striking feature of group IV metallocene catalysts is their capability to control polymer microstructures.

The concept of single site catalyst has been expanded successfully to bridged half-sandwich complexes and a rapidly increasing number of complexes containing chelating ligands for the polymerization of α-olefins. For many years the major focus of catalyst development in relation with development of high molecular weight poly(α-olefin)s was placed upon early transition metals such as Ti, Zr, Hf, V and Cr.

New generation of catalysts of group VIII metal-based systems, i.e., nickel- and palladium(α-diimine) for the polymerization of α-olefins, olefin containing polar groups and cyclic olefins has been of more recent interest. The concept of "chain running" (or)

"chain walking" (or) "chain straightening" has made possible synthesis of polymers with various topologies.

The kinetics of living polymerization using group IV and VIII transition metal catalysts has been recently explored to understand the insertion mechanisms of olefins at the M-C bond. Catalysts have been developed in order to suppress the chain transfer and termination reactions for the synthesis of well-defined polymers and block copolymers.

In spite of all these developments, the stereo- and regio- chemistry of poly(α-olefin)s and the process of insertion of α-olefin into M-C in the synthesis of poly(α-olefin)s by group IV and VIII is still not clearly understood in the literature. Research needs to be focused on precise synthesis of novel polymeric materials (chain size, uniformity, topology, microstructure, composition and functionality).

1.4. REFERENCES

(1) Boor, J. *Ziegler-Natta catalysts and Polymerization*, Academic Press, New York, **1979**.

(2) Barbe, P. C.; Cecchin, G.; Noristi, L. *Adv. Polym. Sci*. **1978**, *81*, 3.

(3) Brintzinger, H. H.; Fischer, D.; Mulhaupt, R.; Rieger, B.; Waymouth, R. M. *Angew. Chem., Int. Ed. Engl.* **1995**, *34*, 1143.

(4) Britovsek, G. J. P.; Gibson, V. C.; Wass, D. F. *Angew. Chem., Int. Ed.* **1999**, *38*, 429.

(5) Albizzati, E.; Galimberti, M. *Catal. Today* **1998**, *41*, 159.

(6) Mashima, K.; Nakayama, Y.; Nakamura, A. *Adv. Polym. Sci*. **1997**, *133*, 1.

(7) Kaminsky, W.; Arndt, M. *Adv. Polym. Sci*. **1996**, *127*, 143.

(8) Gupta, V. K.; Satish, S.; Bhardwaj, I. S. *J. Mat. Sci. -Rev. Macromol. Chem. Phys*. **1994**, *C34 (3)*, 439.

(9) Chandrasekhar, S. B.; Sivaram, S. *Current Science* **2000**, 78, 1325.

(10) Natta, G.; Pino, P.; Mazzanti, G.; Giannini, U. J. *J. Am. Chem. Soc.* **1957**, *79*, 2997.

(11) Breslow, D. S.; Newburg, N. R. *J. Am. Chem. Soc.* **1957**, *79*, 5072.

(12) Reichert, K. H.; Meyer, K. R. *Makromol. Chem.* **1973**, *169*, 163.

(13) Andresen, A.; Cordes, H. G.; Herwig, J.; Kaminsky, W.; Merck, A.; Mottweiler, R.; Pein, J.; Sinn, H.; Vollmer, H. J. *Angew. Chem., Int. Ed. Engl.* **1976**, *15*, 630.

(14) Sinn, H.; Kaminsky, W.; Vollmer, H. J.; Woldt, R. *Angew. Chem., Int. Ed. Engl.* **1980**, *19*, 390.

(15) Sinn, H.; Kaminsky, W. *Adv. Organomet. Chem.* **1980**, *18*, 99.

(16) Wild, F. R. W. P.; Zsolnai, L.; Huttner, G.; Brintzinger, H. H. *J. Organomet. Chem.* **1982**, *232*, 233.

(17) Ewen, J. A. *J. Am. Chem. Soc.* **1984**, *106*, 6355.

(18) Kaminsky, W.; Kulper, K.; Brintzinger, H. H.; Wild, F. R. W. P. *Angew. Chem., Int. Ed. Engl.* **1985**, *24*, 507.

(19) Spaleck, W.; Aulbach, M.; Bachmann, B.; Kuber, F.; Winter, A. *Macromol. Symp.* **1995**, *89*, 237.

(20) Ewen, J. A.; Jones, R. L.; Razavi, A.; Ferrara, J. P. *J. Am. Chem. Soc.* **1988**, *110*, 6255.

(21) Sinclair, K. B.; Wilson, R. B. *Chem. Ind. (London)* **1994**, 857.

(22) Montagna, A. A.; Dekmezian, A. H.; Burkhart, R. M. *Chemtech* **1997**, *27*, 26.

(23) Hackmann, M.; Rieger, B. *Cattech* **1997**, *1*, 79.

(24) Brintzinger, H. H.; Fischer, D.; Mulhaupt, R.; Rieger, B.; Waymouth, R. M. *Angew. Chem., Int. Ed. Engl.* **1995**, *34*, 1143.

(25) Reddy, S. S.; Sivaram, S.; *Prog. Polym. Sci.* **1995**, *20*, 309.

(26) Horton, A. D. *TRIP* **1994**, *2*, 158.

(27) Kaminsky, W.; Arndt, M. *Adv. Polym. Sci.* **1997**, *127*, 143.

(28) Soga, K.; Shiono, T. *Prog. Polym. Sci.* **1997**, *22*, 1503.

(29) Huang, J.; Reuspel, G. L. *Prog. Polym. Sci.* **1995**, *20*, 459.

(30) Kaminsky, W. *Macromol. Chem. Phys.* **1996**, *197*, 3907.

(31) Bochmann, M. *J. Chem. Soc. Dalton. Trans.* **1996**, 25

(32) Fink, G.; Mulhaupt, R.; Brintzinger, H. H.*"Ziegler Catalysts"*; Springer: Berlin, **1995**.

(33) Hamielec, A. E.; Soares, J. B. P. *Prog. Polym. Sci.* **1996**, *21*, 651.

(34) Mashima, K.; Nakayama, Y.; Nakamura, A. *Adv. Polym. Sci.* **1997**, *133*, 1.

(35) Kaminsky, W. *J. Chem. Soc. Dalton. Trans.* **1998**, 1413.

(36) Jordan, R. F. *Adv. Organomet. Chem.* **1991**, *32*, 325.

(37) Chen, E. Y. X.; Marks, T. J. *Chem. Rev*. **2000**, *100*, 13914.

(38) Andrianov, K. A.; Zhadanov, A. A. *J. Polym. Sci*. **1958**, *30*, 513.

(39) Small, B. L.; Brookhart, M. *J. Am. Chem. Soc.* **1998**, *120*, 7143.

(40) Jordan, R. F.; Bajgur, C. S.; Willet, R.; Scott, B. *J. Am. Chem. Soc.* **1986**, *108*, 7410.

(41) (a) Reed, C. A. *Acc. Chem. Res*. **1998**, *31*, 133. (b) Strauss, S. H. *Chem. Rev*. **1993**, *93*, 927.

(42) (a) Bochmann, M.; Jaggar, A. J. *J. Organomet. Chem*. **1992**, *424*, C5. (b)

Bochmann, M. *Angew. Chem., Int. Ed. Engl*. **1992**, *31*, 1181.

(43) Yang, X.; Stern, C. L.; Marks, T. J. *Organometallics* **1991**, *10*, 840.

(44) Chien, J. C. W.; Song, W.; Rausch, M. D. *J. Polym. Sci., Part A: Polym. Chem*. **1994**, *32*, 2387.

(45) (a) Yang, X.; Stern, C. L.; Marks, T. J. *J. Am. Chem. Soc*. **1991**, *113*, 3623. (b) Ewen, J. A.; Elder, M. *J. Makromol. Chem., Macromol. Symp*. **1993**, *66*, 179.

(46) Yang, X.; Stern, C. L.; Marks, T. J. *J. Am. Chem. Soc.* **1991**, *113*, 3613.

(47) Taube, R.; Krukowa, L. J. *J. Organomet. Chem.* **1988**, *347*, C9.

(48) Chien, J. C. W.; Tsai, W. M.; Rausch, M. D. *J. Am. Chem. Soc.* **1991**, *113*, 8570.

(49) Bochmann, M.; Lancaster, S. J. *Organometallics* **1993**, *12*, 633.

(50) Crowther, D. J.; Borkowsky, S. L.; Swenson, D.; Meyer, T. Y.; Jordan, R. F. *Organometallics* **1993**, *12*, 2897.

(51) Hlatky, G. G.; Eckman, R. R.; Turner, H. W. *Organometallics* **1992**, *11*, 1413.

(52) Cam, D.; Giannini, U. *Makromol. Chem.* **1992**, *193*, 1049.

(53) Kaminsky, W. *Makromol. Chem. Phys.* **1996**, *197*, 3907.

(54) Kaminsky, W.; Strubel, C. *J. Mol. Catal. A* **1998**, *128*, 191.

(55) Sishta, C.; Hurthorn, R. M.; Marks, T. J. *J. Am. Chem. Soc.* **1992**, *114*, 1112.

(56) Toscano, P. J.; Marks, T. J. *J. Am. Chem. Soc.* **1985**, *107*, 653.

(57) Finch, W. C.; Gillespie, R. D.; Hedden, D.; Marks, T. J. *J. Am. Chem. Soc.***1990**, *112*, 6221.

(58) Dahmen, K. H.; Hedden, D.; Burwell, R. L. J.; Marks, T. J. *Langmuir* **1988**, *4*, 1212.

(59) Toscano, P. J.; Marks, T. J. *Langmuir* **1986**, *2*, 820.

(60) Cossee, P. *J. Catal.* **1964**, *3*, 80.

(61) (a) Arlman, E. J.; Cossee, P. *J. Catal.* **1964**, *3*, 99. (b) Cossee, P. *J. Catal.* **1964**, *3*, 80.

(62) Cossee, P. *Tetrahedron Lett*. **1960**, *17*, 12.

(63) Cossee, P. *Tetrahedron Lett*. **1960**, *17*, 17.

(64) Castonguay, L. A.; Rappe, A. K. *J. Am. Chem. Soc.* **1992**, *114*, 5832.

(65) Kawamura-Kuribayashi, H.; Koga.N.; Morokuma, K. *J. Am. Chem. Soc.* **1992**, *114*, 8687.

(66) Resconi, L.; Camurati, I.; Sudmeijer, O. *Top. Catal*. **1999,** *7*, 145.

(67) Burger, B. J.; Thompson, M. E.; Cotter, W. D.; Bercaw, J. E. *J. Am. Chem. Soc*. **1990**, *112*, 1566.

(68) Hajela, S.; Bercaw, J. E. *Organometallics* **1994**, *13*, 1147.

(69) Alelyunas, Y. W.; Guo, Z.; Lapointe, R. E.; Jordan, R. F. *Organometallics* **1993**, *12*, 544.

(70) Guo, Z.; Swenson, D.; Jordan, R. F. *Organometallics* **1994**, *13*, 1424.

(71) Resconi, L.; Fait, A.; Piemontesi, F.; Colonnesi, M.; Rychlicki, H.; Zeigler, R. *Macromolecules* **1995**, *28*, 6667.

(72) Resconi, L.; Piemontesi, F.; Camurati, I.; Balboni, D.; Sironi, A.; Moret, M.; Rychlicki, H.; Zeigler, R. *Organometallics* **1996**, *15*, 5046.

(73) Jungling, S.; Mulhaupt, R.; Stehling, U.; Brintzinger, H. H.; Fisher, D.; Langhauser, F. *J. Polym. Sci., Part A: Polym. Chem*. **1995**, *33*, 1305.

(74) Schneider, M. J.; Mulhaupt, R. *Macromol. Chem. Phys*. **1997**, 198, 1121.

(75) Eshuis, J. J. W.; Tan, Y. Y.; Teuben, J. H.; Renkema, J. *J. Mol. Catal*. A **1990**, *62*, 277.

(76) Eshuis, J. J. W.; Tan, Y. Y.; Meetsma, A.; Teuben, J. H.; Renkema, J.; Evens, G. G. *Organometallics* **1992**, *11*, 362.

(77) Resconi, L.; Piemontesi, F.; Franciscono, G.; Abis, L.; Fioranti, T. *J. Am. Chem. Soc*. **1992**, *114*, 1025.

(78) Resconi, L.; Piemontesi, F.; Camurati, I.; Sudmeijer, O.; Nifantév, I. E.; Ivchenko, P. V.; Kuz'mina, L. G. *J. Am. Chem. Soc*. **1998**, *120*, 2308.

(79) Resconi, L.; Jones, R. L.; Rheingold, A. L.; Yap, G. P. A. *Organometallics* **1996**, *15*, 998.

(80) Resconi, L.; Piemontesi, F.; Camurati, I.; Balboni, D.; Sironi, A.; Moret, M.; Rychlicki, H.; Ziegler, R. *Organometallics* **1996**, *15*, 5046.

(81) Yang, X.; Stern, C. L.; Marks, T. J. *Angew. Chem., Int. Ed. Engl*. **1992**, *31*, 1375.

(82) Chein, J. C. W, Wang, B. P. *J. Polym. Sci., Part A: Polym. Chem*. **1988**, *26*, 3089.

(83) Chien, J. C. W.; Razavi, A. *J. Polym. Sci., Part A: Polym. Chem*. **1988,** *26*, 2369.

(84) Chien, J. C. W, Wang, B. P. *J. Polym. Sci., Part A: Polym. Chem*. **1990,** *28*, 15.

(85) Resconi, L.; Bossi, S.; Abis, L. *Macromolecules* **1990**, *23*, 4489.

(86) Naga, N.; Mizunuma, K. *Polymer* **1998**, *39*, 5059.

(87) Siedle, A. R.; Lamanna, W. M.; Newmark, R. A.; Stevens, J.; Richardson, D. E.; Ryan, M. *Macromol. Chem. Macromol. Symp.* **1993**, *66*, 215.

(88) Roll, W.; Brintzinger, H. H.; Rieger, B.; Zolk, R. *Angew. Chem., Int. Ed. Engl.* **1990**, *29*, 279.

(89) Burger, P.; Hortmann, K.; Brintzinger, H. H. *Macromol. Chem. Macromol. Symp.* **1993**, *66*, 127.

(90) Siedle, A. R.; Lamanna, W. M.; Newmark, R. A.; Stevens, J.; Richardson, D. E.; Ryan, M. *Macromol Chem Macromol Symp*. **1993**, *66*, 215.

(91) Kaminsky, W.; Sinn, H.; Woldt, R. *Macromol. Chem. Rapid. Commun.* **1983**, *4*, 417.

(92) Kaminsky, W.; Kulper, K.; Niedoba, S. *Macromol. Chem. Macromol. Symp.* **1986**, *3*, 377.

(93) Kaminsky, W.; Steiger, R. *Polyhedron* **1988**, *7(22/23)*, 2375.

(94) Chien, J. C. W.; Sugimoto, M. *J. Polym. Sci., Polym. Chem. Ed.* **1991**, *29*, 459.

(95) Halterman, R. L. *Chem. Rev*. **1992**, *92*, 965.

(96) Ewen, J. A.; Elder, M. J.; Jones, R. L.; Haspeslagh, L.; Atwood, J. L.; Bott, S. G.; Robinson, K. *Makromol. Chem., Macromol. Symp*. **1991**, *48/49*, 253.

(97) Ewen, J. A.; Jones, R. L.; Razavi, A.; Ferrara, J. *J. Am. Chem. Soc*. **1988**, *110*, 6255.

(98) Zambelli, A.; Longo, P.; Ammendola, P.; Grassi, A. Gazz. *Chim Ital*. **1986**, *116*, 731.

(99) Tsutsui, T.; Ishimaru, N.; Mizuno, A.; Toyota, A.; Kashiwa, N. *Polymer* **1989**, *30*, 1350.

(100) Ewen, J. A, Zambelli, A.; Longo, P.; Sullivan, J. M. *Macromol. Rapid Commn*. **1998**, *19*, 71.

(101) Tsutsui, T.; Mizuno, A.; Kashiwa, N. *Polymer* **1989**, *30*, 428.

(102) Busico, V.; Cipullo, R.; Talarico, G.; Segre, A. L.; Caporaso, L. *Macromolecules* **1998**, *31*, 8720.

(103) Spaleck, W.; Antberg, M.; Aulbach, M.; Bachmann, B.; Dolle, V.; Haftka, S.; Ku¨ ber, F.; Rohrmann, J.; Winter, A. In Ziegler Catalysts; Fink, G.; Mulhaupt, R.; Brintzinger, H. H. Eds; *Springer-Verlag: Berlin*. **1995**; p 83.

(104) Resconi, L.; Balboni, D.; Baruzzi, G.; Fiori, C.; Guidotti, S. *Organometallics* **2000**, *19*, 420.

(105) Resconi, L.; Piemontesi, F.; Camurati, I.; Sudmeijer, O.; Nifantev, I. E.; Ivchenko, P. V.; Kuzmina, L. G. *J. Am. Chem. Soc*. **1998**, *120*, 2308.

(106) Busico, V.; Cipullo, R.; Chadwick, J. C.; Modder, J. F.; Sudmeijer, O. *Macromolecules* **1994**, *27*, 7538.

(107) Resconi, L.; Fait, A.; Piemontesi, F.; Colonnesi, M.; Rychlicki, H.; Zeigler, R. *Macromolecules* **1995**, *28*, 6667.

(108) Resconi, L.; Colonnesi, M.; Rychlicki, H.; Piemontesi, F.; Camurati, I. ISHC, *11th International symposium on homogeneous catalysis*; P 128, St Andrews, Scotland; **1998**.

(109) Sinn, H.; Kaminsky, W. *Adv. Organomet. Chem*. **1980**, *18*, 99.

(110) Pino, P.; Mulhaupt, R. *Angew. Chem., Int. Ed. Engl*. **1980**, *19*, 857.

(111) Kaminsky, W. *Catal. Today*. **1994**, *20*, 257.

(112) Mohring, P. C.; Coville, N. J. *J. Organomet. Chem*. **1994**, *479*, 1.

(113) Sinclair, K. B.; Wilson, R. B. *Chem. Ind*. **1994**, 857.

(114) Ewen, J. A. *J. Am. Chem. Soc*. **1984**, *106*, 6355.

(115) Janiak, C.; Lange, K. C H.; Marquardt, P. *Macromol Rapid Commn*. **1995,** *16*, 643.

(116) Yanjrappa, M. J. *Ph.D. Thesis*, University of Pune, December **2002**.

(117) Hungenberg, K. D.; Kerth, J.; Langhauser, F.; Muller, H. J.; Muller, P. *Die Angewandte Makromolekulare Chemie*. **1995**, *227*, 158.

(118) Janiak, C.; Lange, K. C. H.; Marquardt, P.; Kruger, R. P.; Hanselmann, R. *Macromol. Chem. Phy*. **2002,** *203*, 129.

(119) Frauenrath, H.; Keul, H.; Hocker, H. *Macromol. Rapid. Commun*. **1998**, *19*, 391.

(120) Chien, J. C. W.; Gong, B. M. *J. Polym. Sci., Part A: Polym. Chem*. **1993**, *31*, 1747.

(121) Selectivity in Catalysts. *ACS Symposium series*. **1993**, *517*, 156.

(122) Coevoet, D.; Cramail, H.; Deffieux, A. *Macromol. Chem. Phys*. **1996**, *197*, 855.

(123) Babu, G. N.; Newmark, R. A.; Chien, J. C. W. *Macromolecules* **1994**, *27*, 3383.

(124) Naga, N.; Mizunuma, K. *Macromol. Rapid. Commun*. **1997**, *18*, 581.

(125) Naga, N.; Shiono, T.; Ikeda, T. *Macromol. Chem. Phys*. **1999**, *200*, 1587.

(126) Henschke, O.; Knorr, J.; Arnold, M. *J. Macromol. Sci., Pure. Appl. Chem*. **1998**, *A35*, 473.

(127) Brull, R.; Pasch, H.; Raubenheimer, H. G.; Wahner, U. M. *J. Polym. Sci., Part A: Polym. Chem*. **2000**, *38*, 2333.

(128) Asanuma, T.; Nishimori, Y.; Ito, M.; Uchikawa, N.; Shiomura, T. *Polym. Bull*. **1991**, *25*, 567.

(129) Wahner, U. M.; Brull, R.; Pasch, H.; Raubenheimer, H. G.; Sanderson, R. *Angew. Makromol. Chem*. **1999**, *270*, 49.

(130) Krenstel, B. A.; Kissin, Y. V.; Kleiner, V. J.; Stotskaya, L. L. *In Polymers and Copolymers of Higher α-olefins*, **1997,** *Chapter 4*, p 85.

(131) Wang, J. S.; Porter, R. S.; Knox, J. R. *Polym. J*. **1978**, *10*, 619.

(132) Kim, I. L.; Zhou, J.; Chung, H. *J. Polym. Sci., Part A: Polym. Chem*. **2000**, *38*, 1687

(133) Zhao, X.; Odian, G.; Rossi, A. *J. Polym. Sci., Part A: Polym. Chem*. **2000**, *38*, 3802.

(134) Hoff, M.; Kaminsky, W. *Macromol. Chem. Phys*. **2004**, *205*, 1167.

(135) Suzuki, N.; Mise, T.; Yamaguchi, Y.; Chihara, T.; Ikegami, Y.; Ohmori, H.; Matsumoto, A.; Wakasuki, Y. *J. Organomet. Chem*. **1998**, *560*, 47.

(137) Yamaguchi, Y.; Suzuki, N.; Fries, A.; Mise, T.; Koshino, H.; Ikegami, Y.; Ohmori, H.; Matsumoto, A. *J. Polym. Sci., Part A: Polym. Chem*. **1999**, *37*,

283.

(137) Suzuki, N.; Yamaguchi, Y.; Fries, A.; Mise, T. *Macromolecules* **2000**, *33*, 4602.

(138) Fries, A.; Mise, T.; Matsumoto, A.; Ohmori, H.; Wakatsuki, Y. *Chem. Commun*. **1996**, 783.

(139) Suzuki, N.; Masubuchi, Y.; Yamaguchi, Y.; Kase, T.; Miyamoto, T. K.; Horiuchi, A.; Mise, T. *Macromolecules* **2000**, *33*, 754.

(140) Alt, H. G.; Koeppl, A. *Chem. Rev*. **2000**, *100*, 1205.

(141) Coates, G. W. *Chem. Rev*. **2000**, *100*, 1223.

(142) Resconi, L.; Cavallo, L.; Fait, A.; Piemontesi, F. *Chem. Rev*. **2000**, *100*, 1253.

(143) Britovsek, G. J. P.; Gibson, V. C.; Wass, D. F. *Angew. Chem., Int. Ed. Engl*. **1999**, *38*, 428.

(144) Ittel, S. D.; Johnson, L. K.; Brookhart, M. *Chem. Rev*. **2000**, *100*, 1169.

(145) Johnson, L. K.; Killian, C. M.; Brookhart, M. *J. Am. Chem. Soc*. **1995**, *117*, 6414.

(146) Guan, Z.; Cotts, P. M.; McCord.; McLain, S. J. *Science* **1999**, *283*, 2059.

(147) Miyatake, T.; Mizunuma, K.; Kakugo, M. *Makromol. Chem. Macromol. Symp*. **1993**, *66*, 203.

(148) Fujita, M.; Coates, G. W. *Macromolecules* **2002**, *35*, 9640.

(149) Yoshida, Y.; Saito, J.; Mitani, M.; Takagi, Y.; Matsui, S.; Ishii, S. I.; Nakano, T.; Kashiwa, N.; Fujita, T. *Chem. Commun*. **2002**, *1298*.

(150) Coates, G. W.; Hustad, P. D.; Reinartz, S. *Angew. Chem., Int. Ed. Engl*. **2002**, *41*, 2236.

(151) Miyatake, T.; Mizunuma, K.; Seki, Y.; Kakugo, M. *Makromol. Chem. Rapid. Commun*. **1989**, *10*, 349.

(152) Saito, J.; Suzuki, Y.; Fujita, T. *Chem. Lett*. **2003**, *32*, 236.

(153) Liang, L. C.; Schrock, R. R.; Davis, W. M.; McConville, D. H. *J. Am. Chem. Soc*. **1999**, *121*, 5797.

(154) Tshuva, E. Y.; Goldberg, I.; Kol, M.; Weitman, H.; Goldschmidt, Z. *Chem. Commun*. **2000**, 379.

(155) Scollard, J. D.; McCoville, D. H.; Payne, N. C.; Vittal, J. J. *Macromolecules* **1996**, *29*, 5241.

(156) Chen, Y. X.; Fu, P. F.; Stern, C. L.; Marks, T. J. *Organometallics* **1997**, *16*, 5958.

(157) Tshuva, E. Y.; Groysman, S.; Goldberg, I.; Kol, M. *Organometallics* **2002**, *21*, 662

(158) Ewart, S. W.; Baird, M. C. *Top. Catal*. **1999**, *7*, 1.

(159) Baird, M. C. *Chem. Rev*. **2000**, *100*, 1471.

(160) Nomura, K.; Naga, M.; Miki, K.; Yanagi, K.; Imai, A. *Organometallics* **1998**, *17*, 2152.

(161) Nomura, K.; Oya, K.; Komatsu, T.; Imanishi, Y. *Macromolecules* **2000**, *33*, 3187.

(162) Nomura, K.; Fudo, A. *Inorg. Chim. Acta*. **2003**, *345*, 37.

(163) Nomura, K.; Komatsu, T.; Imanishi, Y. *J. Mol. Catal. A* **2000**, *159*, 127.

(164) Nomura, K.; Fujita, K.; Fujiki, M. *J. Mol. Catal. A* **2004**, *220*, 133.

(165) Groysman, S.; Tshuva, E. Y.; Goldberg, I.; Kol, M.; Goldschmidt, Z.; Shuster, M. *Organometallics* **2004**, *23*, 5291.

(166) Saito, J.; Mitani, M.; Matsui, S.; Kashiwa, N.; Fujita, T. *Macromol. Rapid. Commun*. **2000**, *21*, 1333

(167) Saito, J.; Suzuki, Y.; Fujita, T. *Chem. Lett*. **2003**, *32*, 236.

(168) Tonzetich, Z. J.; Lu, C. C.; Schrock, R. R.; Hock, A. S.; Bonitatebus, P. J. *Organometallics* **2004**, *23*, 4362.

(169) Schrock, R. R.; Casado, A. L.; Goodman, J. T.; Liang, L. C.; Bonitatebus, P. J.; Davis, W. M. *Organometallics* **2000**, *19*, 5325.

(170) Schrock, R. R.; Bonitatebus, P. J.; Schrodi, Y. *Organometallics* **2001**, *20*, 1056.

(171) Scollard, J. D.; McConville, D. H.; Payne, N. C.; Vittal, J. J. *Macromolecules* **1996**, *29*, 5241.

(172) Heatley, F.; Mair, F. S.; Pritchard, R. G.; Woods, R. J. *J. Org. Chem*. **2005**, *690*, 2078.

(173) Fujita, M.; Seki, Y.; Miyatake, T. *J. Polym. Sci., Part A: Polym. Chem*. **2004**, *42*, 1107.

(174) Segal, S.; Goldberg, I.; Kol, M. *Organometallics* **2005**, *24*, 200.

(175) Grubbs, R. H.; Tumas, W. *Science* **1989**, *243*, 907.

(176) Gibson, V. C.; Spitzmesser, S. K. *Chem. Rev*. **2003**, *103*, 283.

(177) Johnson, L. K.; Killian, C. M.; Brookhart, M. *J. Am. Chem. Soc*. **1995**, *117*, 6414.

(178) Johnson, L. K.; Mecking, S.; Brookhart, M. *J. Am. Chem. Soc*. **1996**, *118*, 267.

(179) Younkin, T. R.; Connor, E. F.; Henderson, J. I.; Friedrich, S. K.; Grubbs, R. H.; Bansleben, D. A. *Science* **2000**, *287*, 460.

(180) Guan, Z. *Chem. -Eur. J*. **2002**, *8*, 3086.

(181) Guan, Z. *J. Am. Chem. Soc*. **2002**, *124*, 5616.

(182) Guan, Z. *Polym. Mater. Sci. Eng*. **1999**, *80*, 50.

(183) Guan, Z. *U. S. Pat. 5,76,7211*, **1998**.

(184) Guan, Z.; Cotts, P. M.; McCord, E. F.; McLain, S. J. *Macromolecules* **2000**, *33*, 6945.

(185) Chen, G.; Ma, S. X.; Guan, Z. *J. Am. Chem. Soc*. **2003**, *125*, 6697.

(186) Guan, Z.; Marshall, W. *Organometallic* **2002**, *21*, 3580.

(187) Zhibin, G. *J. Polym. Sci., Part A: Polym. Chem*. **2003**, *41*, 3680.

(188) Mohring, V. M.; Fink, G. *Angew. Chem., Ind. Ed. Engl*. **1985**, *24*, 1001.

(189) Schubbe, R.; Angermund, K.; Fink, G.; Goddard, R. *Macromol. Chem. Phys*. **1995**, *196*, 467.

(190) Killian, C. M.; Tempel, D. J.; Johnson, L. K.; Brookhart, M. *J. Am. Chem. Soc*. **1996**, *118*, 11664.

(191) Johnson, L. K.; Killian, C. M.; Arthur, S. D.; Feldman, J.; McCord, E. F.; McLain, S. J.; Kreutzer, K. A.; Bennett, A. M. A.; Coughlin, E. B.; Ittel, S. D.; Parthasarathy, A.; Templel, D. J.; Brookhart, M. Patent Appl. *WO 9623-10*, **1996**.

(192) Gottfried, A. C.; Brookhart, M. *Macromolecules* **2003**, *36*, 3085.

(193) Suzuki, N.; Yu, J.; Masubuchi, Y.; Horiuchi, A.; Wakatsuki, Y. *J. Polym. Sci., Part A. Polym. Chem*. **2003**, *41*, 293.

(194) Camacho, D. H.; Guan, Z. *Macromolecules* **2005**, *38*, 2544.

(195) Camacho, D. H.; Salo, E. V.; Ziller, J. W.; Guan, Z. *Angew. Chem., Int. Ed*. **2004**, *43*, 1821.

(196) Odian, G. G. *Principles of Polymerization*, 3rd ed.; John Wiley & Sons, Inc.: New York, **1991**.

(197) Webster, O. W. *Science* **1991**, *251*, 887.

(198) Szwarc, M. *J. Polym. Sci., Part A*: *Polym. Chem.* **1998**, *36*, IX-XV.

(199) Darling, T. R.; Davis, T. P.; Fryd, M.; Griney, A. A.; Haddleton, D. M.; Ittel, S. D.; Matheson, R. R.; Matheson, Jr.; Moad, G.; Rizzardo, E. *J. Polym. Sci., Part A: Polym. Chem*. **2000**, *38*, 1706.

(200) Grubbs, R. H.; Coates, G. W. *Acc. Chem. Res*. **1996**, *29*, 85.

(201) Chen, E. Y. X.; Marks, T. J. *Chem. Rev*. **2000**, *100*, 1391.

(202) Zhang, Y.; Keaton, R. J.; Sita, L. R. *J. Am. Chem. Soc*. **2003**, *125*, 9062.

(203) Kennedy, J. P. *J. Polym. Sci., Part A: Polym. Chem*. **1999**, *37*, 2285 and reference therein.

(204) Greszta, D.; Mardare, D.; Matyjaszewki, K. *Macromolecules* **1994**, *27*, 638.

(205) Baskaran, D.; Sivaram, S. *Macromolecules* **1997**, *30*, 1550.

(206) Baskaran, D.; Muller, A. H. E.; Sivaram, S. *Macromolecules* **1999**, *32*, 1356.

(207) Jeon, Y.M.; Park, S. J.; Heo, J.; Kim, K. *Organometallics* **1998**, *17*, 3161.

(208) Tshuva, E. Y.; Goldberg, M.; Kol, M.; Weitman, H.; Goldschmidt, Z. *Chem. Commun*. **2000**, 237.

CHAPTER 2

SCOPE AND OBJECTIVES

2.1. INTRODUCTION

Late transition metal nickel(II) and palladium(II) α-diimine catalysts produce poly(α-olefin)s which exhibit different structural features as compared to those prepared by Ziegler-Natta or metallocene catalysts[1-6]. The differences in their structural properties are attributed to the existence of various unconventional branches arising due to insertion of many methylene units in the backbone and side chain. The unique feature of these catalysts is their ability to form highly branched and chain-straightened poly(olefin)s during the homopolymerization of α-olefin.

Brookhart and coworkers[2-4] reported that nickel(α-diimine) catalyst polymerizes ethylene and other α-olefins to high molecular weight polymers with unconventional microstructures. Poly(α-olefin)s made with these catalysts had fewer branches than those expected from an 1,2-insertion. Poly(propylene)s thus prepared showed the presence of different types of sub units including long branches, branches on branches, isobutyl branches and highly variable levels of 1,3-enchainments[7]. The proposed mechanism for the behavior of the catalyst involves the migration of the metal followed by β-hydride elimination during polymerization. The extent of metal migration determines the nature of branches formed and the extent of 1,ω-enchainment. Fink et. al. proposed the concept of chain running initially in their study of the synthesis of poly(α-olefin)s by nickel catalysts[8,9]. According to literature[1a,7] α-olefins, other than propylene, cannot insert into metal-secondary carbon.

Living polymerization methods allow the synthesis of polymers with precisely controlled molecular weight, narrow molecular weight distribution, ability to synthesize end functionalized polymers, and well defined block copolymers. Whereas tremendous advances in living/controlled polymerizations have been made by using anionic[10], cationic[11], and radical based[12-14] systems, there are relatively fewer examples of living olefin polymerization using transition metal catalysts[15-20]. The living polymerization of α-olefins has been achieved only in rare instances and at very low temperatures. Living polymerizations are characterized by the fact that each catalyst only forms one chain in contrast to common α-olefin polymerization catalysts that can produce thousands of chains as a result of periodic chain transfer or termination events.

α-Olefin polymerizations using metallocene catalysts systems are intrinsically endowed with chain transfer and elimination reactions that terminate the growth of a polymer chain and result in the initiation of a new polymer chain by the catalyst[21,22]. When alkylaluminum cocatalysts are employed, an additional termination route, namely, chain transfer to aluminum, is introduced[22]. At lower polymerization temperature, some of these chain breaking reactions can be retarded leading to "quasi-living" or at least controlled polymerization behavior. The development of weakly coordinating anions has opened up new opportunities in living olefin polymerizations[23]. Significant amount of research in the quest for living olefin polymerization catalysts has centered on complexes based on the Group IV metals. Non-metallocene systems based on nitrogen and oxygen donor ligands have also received considerable attention[24].

A major breakthrough in living olefin polymerization occurred in 1995 with the discovery of a new family of the late transition nickel or palladium(α-diimine) complexes[2,4]. Since chain running is a distinguishing mechanistic feature of palladium and nickel catalysts, polymerization of higher α-olefins leads to chain straightening, as indicated by a branching content that is lower than expected. The unique combination of living α-olefin polymerization behavior with the formation of chain straightened poly(α-olefins)s provided the means to prepare near monodisperse elastomeric α-olefin-based block copolymers.

2.2. OBJECTIVES OF THE PRESENT WORK

The objective of the present work is to explore aspects of synthesis, structure and property of poly(α-olefin)s using late transition nickel(α-diimine) catalysts.

1. Stereo- and regiochemistry are of major interest in the mechanistic understanding of the polymerization mechanism. Late transition nickel(α-diimine) catalysts polymerize α-olefins to high molecular weight poly(α-olefin)s. The microstructure of these polymers is different from those prepared from other transition metal catalysts. This chapter examines in detail the structure of poly(hexene-1)s prepared using [*N*,*N*´-diisopropylbenzene)-2,3-(1,8-napthyl)1,4-diazabutadiene]

dibromonickel/methylaluminoxane (MAO) catalyst. The effect of reaction conditions on the structure of poly(hexene-1)s was studied using high resolution NMR spectroscopy. A comparison of the structural features of poly(hexene-1)s is made with those of poly(octene-1)s, poly(decene-1)s and poly(tetradecene-1)s prepared using the same catalyst.

2. Late transition metal catalysts polymerize α-olefins into poly(*α*-olefin)s with less number of branches than expected. This has been explained by the concept of chain running during polymerization. This leads to number of methylenes in backbone as well as side chain. The consequences of these on the properties of polymers are of interest to study. Poly(octadecene-1)s were synthesized using [*N*,*N*′-diisopropyl benzene)-2,3-(1,8-napthyl)1,4-diazabutadiene]dibromonickel/methylaluminoxane (MAO) catalyst. A detailed investigation on the effect of chain running on physical properties of poly(octadecene-1)s using ^{1}H, ^{13}C NMR, DSC and DMTA was undertaken.

3. *α*-Olefin polymerization with transition metal (early and late) catalysts in combination with methylaluminoxane give poly(*α*-olefin)s with variable molecular weights depending on rate of terminative or transfer reactions with respect to propagation rates. Kinetics provides the main evidence to understand the behavior of catalyst systems during polymerization. Living polymerization of α-olefins is of great interest for the synthesis of polymers with precisely controlled molecular weight, narrow molecular weight distribution, end functionalization and well defined block copolymers. Kinetic evidences in favor of living nature of a catalyst system for *α*-olefin polymerization are not well documented in the literature. This chapter deals with the kinetics of homopolymerization of hexene-1 using [*N*,*N*′-diisopropyl benzene)-2,3-(1,8-napthyl)1,4-diazabutadiene]dibromonickel/methylaluminoxane (MAO) catalyst. Kinetic parameters, k_p (rate of propagation), k_{ter} (rate of termination) and k_{tr} (rate of transfer) were determined.

2.3. REFERENCES

(1) (a) Ittel, S. D.; Johnson, L. K.; Brookhart, M. *Chem. Rev*. **2000**, *100*, 1169. (b) Britovsek, G. J. P.; Gibson, V. C.; Wass, D. F. *Angew. Chem., Int. Ed. Engl*. **1999**, *38*, 428.

(2) Johnson, L. K.; Killian, C. M.; Brookhart, M. *J. Am. Chem. Soc*. **1995**, *117*, 6414.

(3) Johnson, L. K.; Killian, C. M.; Arthur, S. D.; Feldman, J.; McCord, E. F.; McLain, S. J.; Kreutzer, K. A.; Bennett, A. M. A.; Coughlin, E. B.; Ittel, S. D.; Parathasarathy, A.; Tempel, D. J.; Brookhart, M. S. *Pat. Appl. WO* 9623-10, **1996**.

(4) Killian, C. M.; Tempel, D. J.; Johnson, L. K.; Brookhart, M. *J. Am. Chem. Soc*. **1996**, *118*, 11664.

(5) Mecking, S. *Angew. Chem., Int. Ed*. **2001**, *40*, 534.

(6) Mader, D.; Heinemann, J.; Mulhaupt, R. *Macromolecules* **2000**, *33*, 1254.

(7) McCord, E. F.; McLain, S. J.; Nelson, L. T. J.; Arthur, S. D.; Coughlin, E. B.; Ittel, S. D.; Johnson, L. K.; Tempel, D.; Killian, C. M.; Brookhart, M. *Macromolecules* **2001**, *34*, 362.

(8) Schubbe, R.; Angermund, K.; Fink, G.; Goddard, R. *Macromol. Chem. Phys*. **1995**, *196*, 467.

(9) Mohring, V. M.; Fink, G. *Angew. Chem., Ind. Ed. Eng*. **1985**, *24*, 1001.

(10) *Anionic polymerization: Principles and practical applications* (Ed.: Hsieh, H. L.; Quirk, R. P.), Marcel Dekker, New Yark, **1996**.

(11) *Cationic polymerizations: Mechanisms, Synthesis, and applications*, (Ed.: Matyjaszewski, K), Marcel Dekker, New Yark, **1996**.

(12) Hawker, C. J.; Bosman, A. W.; Harth, E. *Chem. Rev*. **2001**, *101*, 3661.

(13) Kamigaito, M.; Ando, T.; Sawamoto, M. *Chem. Rev*. **2001**, *101*, 3689.

(14) Matyjaszewski, K.; Xia, J. H. *Chem. Rev*. **2001**, *101*, 2921.

(15) Murray, M. C.; Baird, M. C. *J. Mol. Catal A. Chem*. **1998**, *128*, 1.

(16) Resconi, L.; Piemontesi, F.; Franciscono, G.; Abis, L.; Fiorani, T. *J. Am. Chem. Soc*. **1992**, *114*, 1025.

(17) Hagihara, H.; Shiono, T.; Ikeda, T. *Macromolecules* **1998**, *31*, 3184.

(18) Scollard, J. D.; Mc Conville, D. H. *J. Am. Chem. Soc*. **1996**, *118*, 10008.

(19) Jeon, Y. M.; Park, S. J.; Heo, J.; Kim, K. *Organometallics* **1998**, *17*, 3161.

(20) Jayaratne, K. C.; Sita, L. R. *J. Am. Chem. Soc*. **2000**, *122*, 958.

(21) Grubbs, R. H.; Coates, G. W. *Acc. Chem. Res*. **1996**, *29*, 85.

(22) Resconi, L.; Cavallo, L.; Fait, A.; Piemontesi, F. *Chem. Rev*. **2000**, *100*, 1253.

(23) Chen, E. Y. X.; Marks, T. J. *Chem. Rev*. **2000**, *100*, 1391.

(24) (a) Britovsek, G. J. P.; Gibson, V. C.; Wass, D. F. *Angew. Chem*. **1999**, *111*, 448. (b) Britovsek, G. J. P.; Gibson, V. C.; Wass, D. F. *Angew. Chem., Int. Ed. Engl*. **1999**, *38*, 428.

CHAPTER 3

EXPERIMENTAL METHODS

INTRODUCTION

Synthesis of transition metal complexes and polymerization of olefins necessitates scrupulous purification of the all the ingredients involved in catalyst preparation as well as polymerization reactions. The monomers, solvents and other reagents have to be purified and dried in multiple steps to eliminate traces of impurities, especially, the protic ones. All manipulations of air- and/or moisture-sensitive compounds were performed using high vacuum or Schlenk techniques. All manipulations involving solid, air and moisture sensitive compounds were performed inside an inert atmosphere glove box (Labconco model 50004 and M. Braun/labmaster 100) continuously purged with high purity nitrogen from a generator (Spantech model NG 300-1, England). Argon and nitrogen were purified by passage through columns of 4 Å and 3 Å molecular sieves. The reactions are conducted under inert atmosphere of dry nitrogen or argon gas.

In this chapter, materials used, purification and drying of reagents, synthesis of catalysts, polymerization methods and polymer characterization techniques used in the present study are discussed.

3.2. MATERIALS USED

The list of chemicals used for experiments has been summarized in **Table 3.1**.

Table 3.1. List of chemicals

Name of chemical	Formula/ Abbreviation	Grade/ Purity	Source
Acenaphthenequinone		Tech.	Aldrich, USA
Acetone	CH_3COCH_3	AR	S.d. fine. Chem. Ltd. India
Benzophenone	$(C_6H_5)_2CO$	99 %	Aldrich
Benzeze-d_6	C_6D_6	99 %	Aldrich
bis(cyclopentadienyl)zirconium dichloride	$(Cp)_2ZrCl_2$		Aldrich

Calcium hydride	CaH_2	95 %	Aldrich
Chloroform	$CHCl_3$	LR	S.d. Fine. Chem. Ltd. India
Cyclohexane	C_6H_{12}		Merck, India
Decene-1	$C_{10}H_{20}$		Aldrich
Dodecene-1	$C_{12}H_{24}$		Aldrich
o-Dichlorobenzene	ODCB		S.d. Fine. Chem. Ltd. India
Dichloromethane	CH_2Cl_2	LR	Merck, India
Diethylaluminumchloride	$(C_2H_5)_2AlCl$ (DEAC)		Schering A-G, Germany
Diethyl ether	$(C_2H_5)_2O$	LR	S.d. Fine. Chem. Ltd. India
2,6-diisopropylaniline	$[(CH3)_2CH]_2C_6H_3NH_2$	90 %	Aldrich
1,2-dimethoxyethane	$C_2H_4(OCH_3)_2$ (DME)	99+ %	Aldrich
Ethanol	C_2H_5OH	Commercial	S.d. Fine. Chem. Ltd. India
rac-ethylene bis(indenyl)zirconium dichloride	*rac*-$Et(Ind)_2ZrCl_2$		Witco GmbH, Germany
Hexane	$CH_3(CH_2)_4CH_3$	AR	S.d. Fine. Chem. Ltd. India
Hexadecene-1	$C_{16}H_{32}$		Aldrich
Hexene-1	C_6H_{12}	99 %	Aldrich
Hydrochloric acid	HCl	LR	S.d. Fine. Chem. Ltd. India
Irganox 1010	$C_{16}H_{24}N_{10}O_4$	antioxidant	Ciba-Giegy
Isopropanol	$(CH_3)_2CHOH$	LR	Ranbaxy, India
Magnesium turnings	Mg	98 %	Aldrich
Magnesium dichloride-Titanium tetrachloride	$MgCl_2$-$TiCl_4$	Mg, 17-19 wt.%; Ti, 2.9-3.3 wt. %	Union Carbide, USA
Methanol	CH_3OH	AR	S.d. Fine. Chem. Ltd. India

Methylaluminoxane	MAO	10 wt % solution in toluene	Witco GmbH, Germany
Molecular sieves (4 Å and 3 Å)	$Na_{12}[(AlO_2)_{12}(SiO_2)_{12}].xH_2O$		S.d. Fine. Chem. Ltd. India
Nickel(II)Bromide	$NiBr_2$	Anhydrous, 99.99+ %	Aldrich
Octadecene-1	$C_{18}H_{36}$		Aldrich
Octene-1	C_8H_{16}		Aldrich
Pentane	$CH_3(CH_2)_3CH_3$	LR	S.d. Fine. Chem. Ltd. India
Sodium metal	Na	LR	S.d. Fine. Chem. Ltd. India
Tetradecene-1	$C_{14}H_{28}$		Aldrich
Toluene	$C_6H_5CH_3$	Sulfur free, LR	S.d. Fine. Chem. Ltd. India
1,2,4-Trichlorobenzene	$C_6H_3Cl_3$	Spectrophotometric grade	Aldrich
Triisobutylaluminum	TIBAL		Witco GmbH, Germany
Trimethylaluminum	TMA		Schering A.-G., Germany
Zirconocene dichloride	Cp_2ZrCl_2	98+ %	Aldrich

3.3. PURIFICATION AND DRYING

All solvents and reagents were purified and dried under dry nitrogen atmosphere by standard procedures[1]. Toluene, cyclohexane, and diethylether were distilled from sodium benzophenone ketyl radical. Dichloromethane was dried and distilled from phosphorus pentoxide. 1,2-dichlorobenzene was dried and distilled from calcium hydride and stored over 4 Å molecular sieves. Monomers (hexene-1, octene-1, decene-1, dodecene-1, tetradecene-1, hexadecene-1 and octadecene-1) were dried and distilled from calcium hydride. MAO (Witco GmbH), 10 wt % in toluene was used as

received. Cp_2ZrCl_2 and *rac*-$C_2H_5(Ind)_2ZrCl_2$ were obtained from Witco GmbH, Germany and used as received.

3.4. Synthesis of [(N,N′-diisopropylbenzene)-2,3-(1,8-naphthyl)-1,4-diazabutadiene) dibromonickel catalyst[2]

3.4.1. Synthesis of [(N,N′-diisopropylbenzene)-2,3-(1,8-naphthyl)-1,4-diazabutadiene]

4 mL (21 mmol) of 2,6-diisopropylaniline and 20 mL of methanol were taken in a 100 mL round bottomed flask. 3 g (16.5 mol) of acenaphthenequinone was added slowly to it and was stirred overnight. The reaction mixture was filtered, washed several times with methanol. The solid mass was recrystallized from chloroform-hexane mixture. Yield = 2.5 g

^{1}HNMR. 7.9 (d, 2, naphthyl), 7.4 (t, 2, naphthyl), 7.25 (s, 6, H aryl), 6.15 (d, 2, naphthyl), 3.05 (septet, 4, C**H**$(Me)_2$), 1.25 (d, 12, CH(C**H**$_3)_2$, 1.0 (d, 12, CH(C**H**$_3)_2$)

3.4.2. Synthesis of (1,2-dimethoxyethane)nickel(II)bromide

In a 100 mL round bottomed flask, 2 g of nickel(II)bromide and 20 mL of anhydrous ethanol were added. The homogenous green solution was stirred under reflux for 2 hours. The solution was evaporated to the stage of incipient crystallization at the boiling point and diluted with 15 mL of 1,2-dimethoxyethane (dried over lithium aluminium hydride). A pink colored precipitate formed, was collected and washed successively with anhydrous 1,2-dimethoxyethane and dried under vacuum. Yield = 1.5 g

3.4.3. Synthesis of the catalyst

0.750 g (1.5 mmol) of the ligand and 0.440 g (1.43 mmol) of $NiBr_2$(DME) were weighed into a flame-dried Schlenk flask inside a dry box. 20 mL of dichloromethane was added to this mixture. An orange colored solution was formed, which was stirred for 18 hours to obtain a reddish brown suspension. The reaction mixture was allowed to settle and some amount of dichloromethane was removed by means of a cannula. To the resulting mass, dichloromethane was added, stirred for sometime and filtered through a

cannula. Thus the product was washed with dichloromethane and the reddish brown complex was dried in vacuum. Yield was 700 mg (65 %)

Elemental analysis calculated for $C_{36}H_{40}N_2NiBr_2$: C, 60.12; H, 5.61; N, 3.89. Found C, 59.73; H, 5.35; N, 3.66.

3.5. POLYMERIZATION TECHNIQUES

3.5.1. Homopolymerization of propylene using $MgCl_2$-$TiCl_4$/TEAL catalyst system

Polymerization of propylene was carried out using Büchi miniclave reactor (**Figure 3.1**). The reactor was kept in oven at 130 ^oC over night and cooled under nitrogen. Toluene (20 mL) was introduced into the reactor using a hypodermic syringe and saturated with propylene. Toluene solution of TIBAL was added. Polymerization was initiated by the addition of the catalyst ($MgCl_2$-$TiCl_4$) [Source: Union Carbide, USA. Mg, 17-19 wt %; Ti, 2.9-3.3 wt %] dissolved in a toluene. The polymerization temperature was maintained using oil bath. The reaction was terminated by the addition of 1:3 mixture of HCl:methanol. The polymer was washed 3 times with methanol and dried under vacuum.

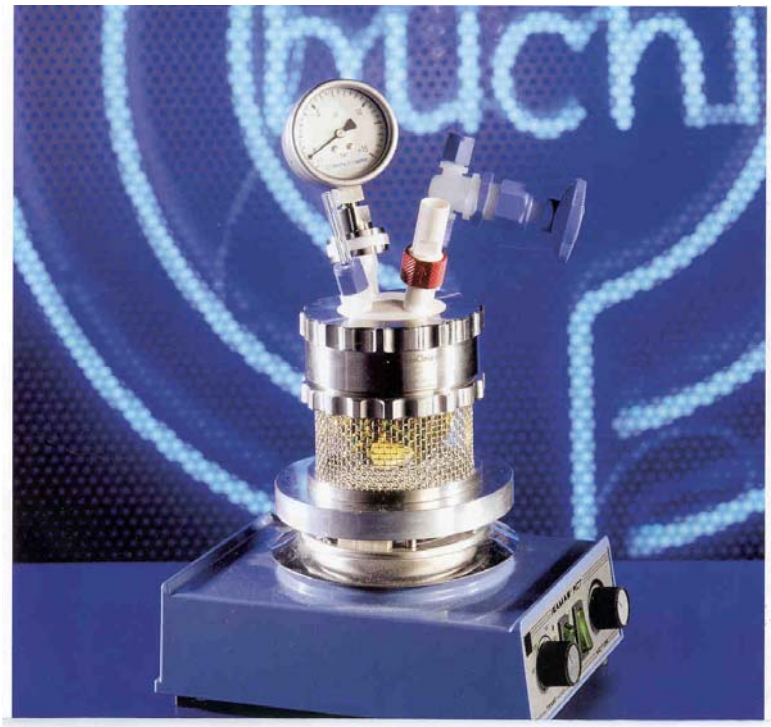

Figure 3.1. Büchi Miniclave

3.5.2. Homopolymerization of hexene-1 using Cp_2ZrCl_2/MAO and rac-$Et(Ind)_2ZrCl_2$/MAO

Homopolymerization of hexene-1 (Chapter 4, **Table 4.1**, entry 2) was performed using a bench-top single-neck glass reactor (**Figure 3.2**) (100 mL) connected to a 3-way stop-cock with septum-adaptor and provided with a magnectic stirring bar. The reactor was charged with the 20 mL of toluene. Freshly distilled hexene-1 (3 mL) was transferred using a hypodermic syringe. Required amount of MAO solution (1.7 mL) was transferred to the flask through a hypodermic syringe. The solution was stirred for 1 h. Reaction was initiated by the addition of catalyst solution (4.8×10^{-3} M) to the reactor using a hypodermic syringe. Polymerization temperature (35 ^{o}C) was maintained using an oil bath. The reaction was terminated by the addition of 1:3 mixture of HCl:methanol. After termination the oligomer was found to separate from the unreacted monomer and methanol mixture. The supernatant liquid was separated and dried under vacuum for 24 h. The obtained oligomer was 0.32 g (conversion, 16 %).

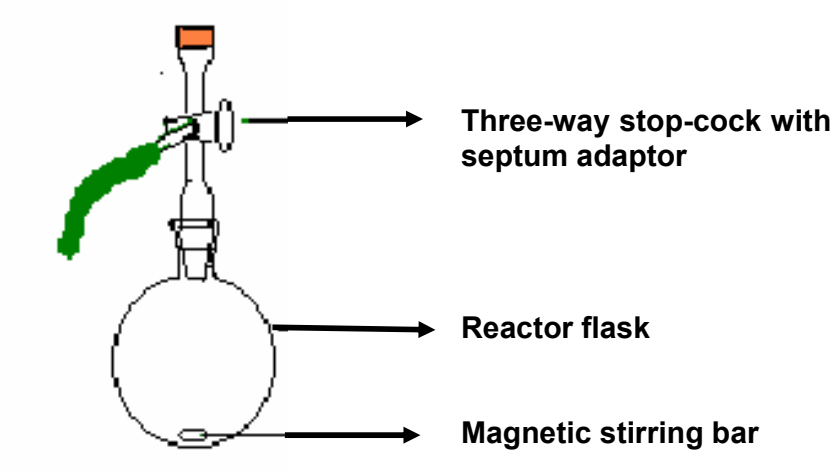

Figure 3.2. Bench-top reactor for α-olefin polymerization

3.5.3. Homopolymerization of octadecene-1 using Cp_2ZrCl_2/MAO

Homopolymerization of octadecene-1 (Chapter 4, **Table 4.1**, entry 9) was performed using a bench-top single-neck glass reactor (**Figure 3.2**) (100 mL) connected to a 3-way stop-cock with septum-adaptor and provided with a magnectic stirring bar. The reactor was charged with the 20 mL of toluene. Freshly distilled octadecene-1 (6 mL) was transferred using a hypodermic syringe. Required amount of MAO solution

(1.7 mL) was transferred to the flask through a hypodermic syringe. Reaction was initiated by the addition of catalyst solution (4.8×10^{-3} M) to the reactor using a hypodermic syringe. The solution was stirred for 1 h. Polymerization temperature (35 ^{o}C) was maintained using oil bath. The reaction was terminated by the addition of 1:3 mixture of HCl:methanol. The polymer was precipitated by addition of 200 mL of acetone. The resulting polymer was washed 3 times with acetone in order to dissolve unreacted octadecene-1. Polymer was dried under vacuum for 24 h. The obtained polymer was 0.7 g (conversion = 15 %).

3.5.4. Homopolymerization of hexene-1, decene-1, dodecene-1, tetradecene-1, hexadecene-1 and octadecene-1 using [N,N′-diisopropylbenzene)-2,3-(1,8-napthyl)1,4-diazabutadiene] dibromonickel/methylaluminoxane (MAO)

Homopolymerizations of hexene-1, decene-1, dodecene-1, tetradecene-1, hexadecene-1 and octadecene-1 were performed using a bench-top single-neck glass reactor (**Figure 3.2**) connected to a 3-way stop-cock with septum-adaptor and provided with a magnectic stirring bar, which contained the required amount of catalyst and solvent (toluene). Freshly distilled monomer was transferred using a hypodermic syringe. Required amount of cocatalyst solution was transferred to the flask through hypodermic syringe. The solution was stirred for 1 h. Polymerization was quenched with a mixture of acetone and dilute hydrochloric acid and the precipitated polymer was separated by filtration. The resulting polymer was washed three times with acetone and dried under vacuum.

3.6. CHARACTERIZATION TECHNIQUES

3.6.1 Gas chromatography (GC)

Monomer conversion was determined by GC (Perkin Elmer, Model no. 2011, detector: FID) and cyclohexane was used as internal standard. The column used was BP-1 (non-polar), and the oven, injector and detector temperatures were maintained at 60, 150 and 180 ^{o}C respectively.

3.6.2. Gel permeation chromatography (GPC)

The molar masses of the poly(α-olefin)s were measured by GPC in 1,2,4-trichlorobenzene at 135 ^{o}C. For these measurements, a Polymer Laboratories 220 high temperature GPC was used. This instrument is equipped with polystyrene gel columns (PL Gel - 3 x Mixed B, Particle size - 10 μ) along with refractive index, viscosity and light scattering triple detector system. The mass and viscosity constants for of RI and viscosity detector were determined using a 0.08 wt % solution (in 1,2,4-TCB) of polystyrene standard of $\bar{M}_n$ = 1,86,000 supplied by Polymer Laboratory. The absolute molecular masses of poly(hexene-1)s were calculated using Trisec Triple Detector GPC software supplied by Viscotek. The dn/dC values for poly(hexene-1)s were calculated from the mass constant (k) of RI detector and the actual weight of the sample injected (C) using the following equation.

$$\text{Area under the peak (RI)} = k.\ dn/dC.\ C$$

Where, area under the concentration trace is directly related to the mass [concentration, (1.79 mg/mL) x injection volume (200 μL)] of the sample injected. Mass constant (k) = 2128 mg and Sample concentration, C = 1.79 mg/mL.

Poly(hexene-1)s synthesized using nickel(α-diimine)/MAO catalyst (Chapter 6, **Table 6.2**, entry 4) was analysed for GPC. The dn/dc was found to be 0.094 mL/g. There is only one other reference to a dn/dC value for poly(hexene-1)s in the literature[3]. Deffieux and coworkers determined the dn/dC value in THF at 25 ^{o}C as 0.068 cm^3/g using GPC/MALLS. The absolute $\bar{M}_n$, $\bar{M}_w$ and MWD were estimated to be 97,200; 114,700 and 1.18 respectively.

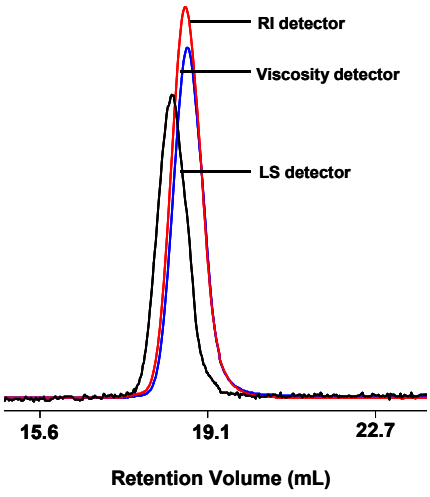

Figure. 3.3. GPC trace of poly(hexene-1)s synthesized using nickel(α-diimine)/MAO catalyst system (Chapter 6, **Table 6.2**, entry 4)

3.6.3. Nuclear magnetic resonance spectroscopy (NMR) techniques

High resolution ^{1}H NMR spectra were recorded on a Brüker DRX 500 MHz NMR spectrometer in $CDCl_3$ at room temperature (25 ^{o}C) using a 45 ^{o} flip angle and a relaxation delay of 3 sec. 125.77 MHz ^{13}C NMR spectra were also obtained on the same spectrometer either in $CDCl_3$ at ambient temperature or in ODCB containing 3% (v/v) C_6D_6 at 120 ^{o}C. Typically, 10 % (w/v) solutions of the polymers were used for high temperature measurements. The high temperature measurements were carried out on a dedicated 10 mm high temperature probe. The measurement conditions for quantitative ^{13}C measurements are as follows: using 45^{o} pulse, spectral width of 20.66 kHz, a relaxation delay of 10 s, an acquisition time of 1.59 s. Spectra are referenced to the highest field solvent resonance at 127.9 ppm. The ^{1}H-^{1}H 2D J resolution, ^{13}C HMQC and HMBC (Gradient accelerated) experiments were performed on a broad-band 5 mm inverse probe in $CDCl_3$ at room temperature. For HMQC and HMBC, a delay of 3.4 ms was used for the INEPT and a delay of 50 ms was employed for the HMBC experiment for the evolution due to long-range couplings.

3.6.4. Differential scanning calorimetry (DSC)

Melting and crystallization behavior of poly(α-olefin)s were performed using Perkin-Elmer DSC-7. Following steps are used to perform thermal scanning; (1) hold for 1 min. at -40 ^{o}C (2) heat from -40 to 150 °C at 10 ^{o}C/min. (3) cool from 150 ^{o}C to 60 at 90 ^{o}C/min. (4) hold for 20 min. at 60 ^{o}C (5) cool from 60 to 50 ^{o}C at 10 ^{o}C/min. (6) hold for 20 min. at 50 ^{o}C (7) cool from 50 to 40 ^{o}C at 10 ^{o}C/min. (8) hold for 20 min. at 40 ^{o}C (9) cool from 40 to 30 ^{o}C at 10 ^{o}C/min. (10) hold for 20 min. at 30 ^{o}C (11) cool from 30 to -40 ^{o}C at 70 ^{o}C/min. (12) hold for 1 min. at -40 ^{o}C (13) heat from -40 to 150 ^{o}C at 10 ^{o}C/min. Second heating scan i.e. step 12 was used to calculate meting and crystallization temperatures of poly(olefin)s.

3.6.5. Dynamic mechanical thermal analysis (DMTA)

The dynamic mechanical tests were performed using Rheometrics solids analyzer RSA II at 1 Hz and a heating rate 5 ^{o}C/min using tensile geometry and applying

a strain 0.2 %. The storage (E′) and loss moduli (E″) and the loss tangent [tan (δ)] are measured from -150 to 60 ^{o}C. The maximum of loss tangent curve is used to determine glass transition temperature (T_g). To measure accuracy of T_g determined by means of DMA, the same sample is measured three times.

3.6.6. Film preparation

Poly(α-olefin) films were prepared using a Carver press Monarch series, model 3710 ASTM. The required amount of polymers were placed between Teflon sheets and preheated for 10 min at 110 ^{o}C between the press plates without pressure and then pressed by 10 min at 3 kgf/cm^2 at the same temperature. Subsequently the films were cooled down to room temperature.

3.7. REFERENCES

(1) Armarego, W. L. F.; Perrin, D. D.; Heinemann, B. "*Purification of laboratory chemicals*", *4th Edn*. **1996**.

(2) Johnson, L. K.; Killian, C. M.; Brookhart, M. S. *J. Am. Chem. Soc*. **1995**, *117*, 6414.

(3) Peruch, F.; Cramail, H.; Deffieux, A. *Macromolecules* **1999**, *32*, 7977.

CHAPTER 4

A STUDY OF THE STRUCUTER OF POLY(HEXENE-1)S PREPARED BY NICKEL(-DIIMINE) / MAO CATALYST USING HIGH-RESOLUTION NUCLEAR MAGNETIC RESONACE (NMR) SPECTROSCOPY

4.1. INTRODUCTION

Late transition metal catalyst such as nickel(II) and palladium(II) α-diimine produce poly(α-olefin)s, which exhibits different structural properties than those prepared by Ziegler-Natta or metallocene catalysts[1-6]. The differences in their structural properties are attributed to the formation of various unconventional branches and insertion of many methylene units in the backbone and side chain. The unique feature of these catalysts is their ability to form highly branched and chain-straightened poly(α-olefin)s during the homopolymerization of an α-olefin.

Fink and Möhring reported the oligomerization of propylene and higher α-olefins using an (aminobisphosphorane)nickel catalyst[7,8] systems previously described by Keim[9]. They shown the existence of chain running in poly(α-olefin)s synthesized by nickel catalysts[8]. The proposed mechanism predicts that 1,2-insertion of α-olefins is followed by chain migration prior to insertion of an additional monomer unit. Therefore, only methyl branched oligomers result from this system. Poly(hexene-1)s can be polymerized in three primary tactic forms-isotactic, syndiotactic and atactic as well as many combinations of these. A variety of Ziegler-Natta catalysts and metallocene catalysts yield stereoirregular atactic poly(hexene-1)s. Most of the efforts with metallocene catalysts is directed toward the preparation of isotactic poly(hexene-1)s. Formation of isolated methyl, different configurations of regioirregular head-to-head methyl branches and ethylene sequence in hexene-1 polymerization have not been observed so far. Brookhart and coworkers[2-4] reported that nickel(α-diimine) catalyst polymerizes ethylene and other α-olefins to high molecular weight polymers with unconventional microstructures. Poly(α-olefin)s made with these catalysts had fewer branches than those expected for the 1,2-insertion. McCord and coworkers[10] have recently reported the microstructure analysis of polypropylenes synthesized using nickel(α-diimine) catalyst system. These poly(propylene)s showed additional features not seen in any previously known poly(propylene)s, including long branches, branches on branches, isobutyl branches, intermediate and highly variable levels of 1,3-enchainments, and runs of methylenes in the backbone of many different well-defined lengths. The extent of 1,3-enchainments ranges from 9 to 55 %. These features are found to vary with polymerization conditions. The proposed mechanism for the

behavior of the catalyst involves the migration of the metal followed by β-hydride elimination during polymerization. According to literature[1a] α-olefins, other than propylene, cannot insert into metal-secondary carbon[10].

NMR spectroscopy, especially, ^{13}C NMR, has been frequently used for the microstructure determination of a number of poly(olefin)s and their copolymers[11,12]. The assignment of NMR signals of poly(propylene) (PP) to various tactic sequences and regioirregular defects was investigated by a number of groups[13-25]. Many catalyst systems are known to be nonregiospecific[26] and invariably lead to the formation of head-to-head structures to some extent. In addition, it is interesting to note that the property of elasticity is conferred on PP by the presence of many inverted units. The regioselectivity of propene insertion in terms of 1,2- or 2,1-insertion can be determined by the presence of regioirregular monomer placement[27]. Zambelli and coworkers[28] reported the formation of regioirregular methyl branches in poly(propylene) synthesized using VCl_4-$Al(CH_3)_3$. Asakura and his coworkers[29] discussed the ^{13}C NMR chemical shifts of regioirregular polypropylene on the basis of the ^{13}C NMR γ-effect and application of the rotational isomeric state model. In another report the ^{13}C NMR spectrum of regioirregular polypropylene containing upto 40 % inverted 1,3 units were assigned using the 2D INADEQUATE and INEPT techniques[30].

In the present study, we report a detailed investigation of the polymerization of hexene-1 using late transition [*N*,*N*′-diisopropyl benzene)-2,3-(1,8-napthyl)1,4-diazabutadiene]dibromonickel (**catalyst 1**)/methylaluminoxane (MAO). High-resolution ^1H and ^{13}C NMR spectroscopy has been used to obtain information about the microstructure of poly(hexene-1)s. A plausible mechanistic description has been proposed to explain the observed microstructures. The complete assignment of all the peaks and the effect of polymerization temperature on the microstructure of poly(hexene-1)s are discussed. A comparison of the structural features of poly(hexene-1)s is made with those of poly(octene-1)s, poly(decene-1)s and poly(tetradecene-1)s prepared using the same catalyst.

4.2. EXPERIMENTAL

4.2.1. Materials

This is described in the Chapter 3 under section 3.3.

4.2.2. Synthesis of catalyst

The **catalyst 1** was synthesized according to literature procedure[2]. **Catalyst 4** was prepared according to reported procedure[31].

4.2.3. Synthesis of poly(α-olefin)s

The detailed polymerization procedure and work up is given in Chapter 3.

4.2.4. ^{1}H and ^{13}C NMR spectroscopy

Details are given in Chapter 3.

4.2.5. Nomenclature

The ^{13}C NMR chemical shift assignments of different carbons are labeled according to the literature[10].

4.3. RESULTS AND DISCUSSION

The detailed microstructure of poly(hexene-1)s, poly(octene-1)s, poly(decene-1)s and poly(tetradecene-1)s synthesized using late transition nickel(α-diimine)/MAO (**1**) was studied by NMR spectroscopy using ^{1}H, ^{13}C and HMQC, HMBC experiments. For the purposes of comparison atactic, isotactic poly(hexene-1)s and polypropylene, ethylene-propylene copolymer were synthesized using Cp_2ZrCl_2/MAO (**2**), *rac*-$C_2H_5(Ind)_2ZrCl_2$/MAO (**3**) and supported $MgCl_2$-$TiCl_4$/TEAL (**4**), respectively. Details of polymerization conditions are shown in **Table 4.1**.

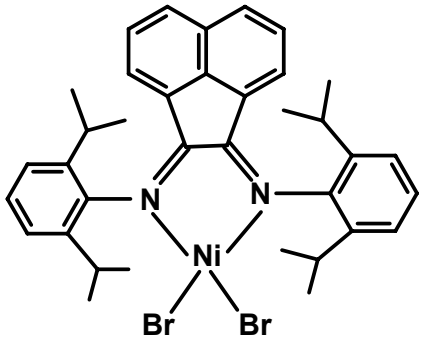

Catalyst 1: *N,N′*-diisopropyl benzene)-2,3-(1,8-napthyl) 1,4-diazabutadiene] dibromonickel

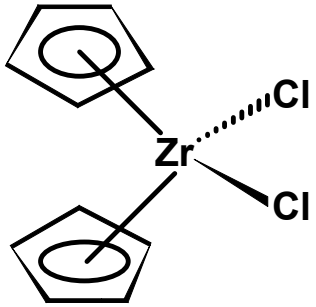

Catalyst 2:
bis(cyclopentadienyl)zirconium dichloride

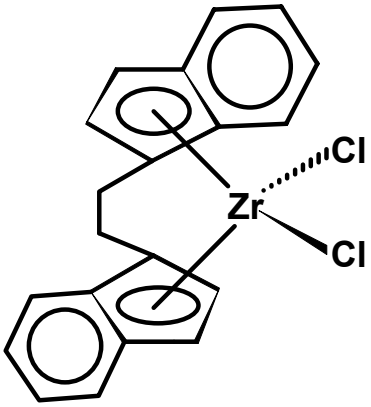

Catalyst 3:
rac-Ethylene bis(indenyl)zirconium dichloride

Table 4.1. Homopolymerization of α-olefins using $NiBr_2$(*α*-diimine) (**1**)/MAO, Cp_2ZrCl_2 (**2**)/MAO, *rac*-$C_2H_5(Ind)_2ZrCl_2$ (**3**)/MAO and $MgCl_2$-$TiCl_4$/TEAL(**4**)[a]

Entry	Polymer	Catalyst	[Catalyst].10^3 (M)	[Al/ catalyst]	T (^oC)
1	Poly(propylene)	4	0.15	100	35
2	Poly(hexene-1)	2	4.8	1000	35
3	Poly(hexene-1)	3	4.8	1000	35
4	Poly(hexene-1)	1	0.34	150	5
5	Poly(hexene-1)	1	0.34	150	70
6	Poly(octene-1)	1	0.34	150	70
7	Poly(decene-1)	1	0.34	150	70
8	Poly(tetradecene-1)	1	0.34	150	70
9	Poly(octadecene-1)	2	4.8	1000	35

[a]Polymerization conditions: Propylene = 1 bar, monomer (hexene-1, octene-1, decene-1, tetradecene-1 and octadecene-1) = 0.5 M, toluene = 20 mL, time = 1 h.

4.3.1. ^{1}H NMR

^{1}H NMR spectrum of poly(hexene-1)s synthesized using early transition metal catalysts is entirely different from that synthesized using **1**. It shows more signals than one would expect from poly(hexene-1)s synthesized using **2**. 500 MHz ^{1}H NMR spectra of poly(hexene-1)s synthesized using **2** and **1** are shown in **Figure 4.1** along with that of polypropylene synthesized using **4**. The peak at 0.82 ppm, which appears as a doublet, is clearly assignable to the methyl branches similar to that in polypropylene (**Figure 4.1a**). A comparison of the spectra in **Figure 4.1** also unambiguously shows that the signal at 0.88 ppm (triplet) is due to the terminal methyl groups of butyl/long branches (**Figure 4.1b, c** and **d**). It is interesting to note that **Figure 4.1d** shows an additional triplet in this region arising probably due to additional terminal methyl group of long chain branches. The spectrum of poly(hexene-1)s synthesized using **1** (**Figure 4.1d**) clearly indicated the presence of signal at 1.24 ppm, the relative intensity of which depends on the reaction conditions (**Figure 4.1c, d**). This signal is typical of long chain methylene groups, $(CH_2)_n$, and can arise from branches as well as backbone. The signals at 0.73 and 0.75 ppm do not appear in the poly(hexene-1)s sample synthesized using **2** (**Figure 4.1b**) and are present only in poly(hexene-1)s prepared using **1**. A detailed NMR investigation was necessary to trace the origin of this observation. The 2D proton J-resolution spectrum of the poly(hexene-1)s (**Figure 4.2**) prepared using **1** clearly showed that these signals possess a doublet nature, i.e. they are coupled to a single proton, i.e. a (CH) group. Hence, it is obvious that they can only be a part of the methyl branches of polypropylene moieties. The observed chemical shift could not be explained only on the basis of tacticity effects. To obtain more insight further investigations using ^{13}C NMR spectroscopy was undertaken.

4.3.2. ^{13}C NMR

In **Figure 4.3** the ^{13}C NMR spectra of poly(propylene) (**a**) synthesized using **4** and poly(hexene-1)s (**b**, **c** and **d**) prepared using **3**, **2** and **1**, respectively are compared. These spectra are obtained in $CDCl_3$ at ambient temperature. The methyl, methylene and methine carbons are differentiated with the help of DEPT spectra. The signal at 14.16 ppm is assigned to the methyl carbon of butyl or long chain branches. The 19.73 ppm

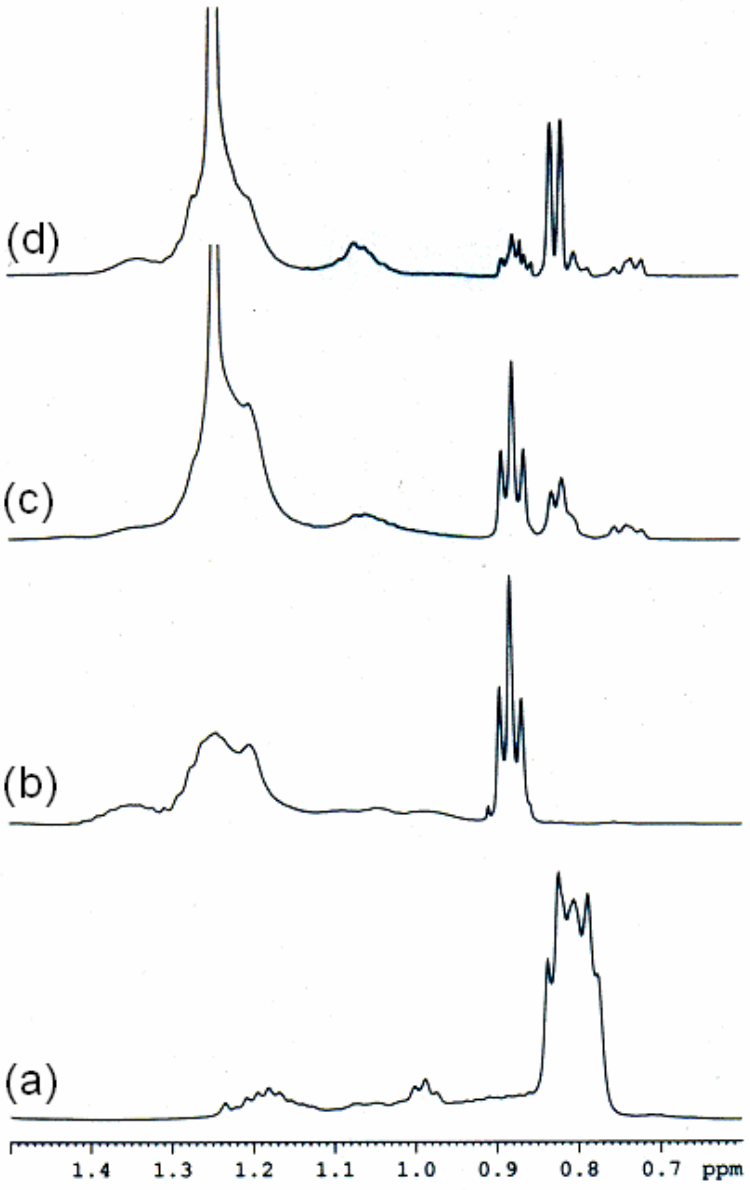

Figure 4.1. Comparison of the room temperature (25 ^{o}C) 500 MH_z ^{1}H NMR spectra in $CDCl_3$ of an atactic polypropylene synthesized using **4** (a), atactic poly(hexene-1) synthesized using **2** (b), and poly(hexene-1)s synthesized using **1** at 5 ^{o}C (c) and at 70 ^{o}C (d).

signal arises exclusively from the methyl branches in polypropylene and the observed multiplicity can be explained in terms of tacticity effects. For poly(hexene-1) prepared using **1** (**Figure 4.3d**) the methyl signals are observed in the region of 14.00-17.00 ppm. It is likely that these correspond to the methyl proton signals observed at 0.82 and 0.73 ppm in the ^{1}H NMR (**Figure 4.1d**). This was unambiguously verified by an HMQC experiment (**Figure 4.4a**) for this sample. It is known that head-to-head polymerization

of propylene leads to the formation of regio- irregular centers (**Chart 4.1a, b**) and these methyl groups can show characteristic chemical shifts which are different from that observed from the one originating from the normal head-to-tail polymerization. The values observed here closely matches with the reported value for regio-irregular polypropylene[13-25]. Other correlations such as the one between the methyl protons at 0.82 ppm and 0.88 ppm with carbons at 20.00 ppm and 14.16 ppm, respectively are also clearly visible in the HMQC spectrum.

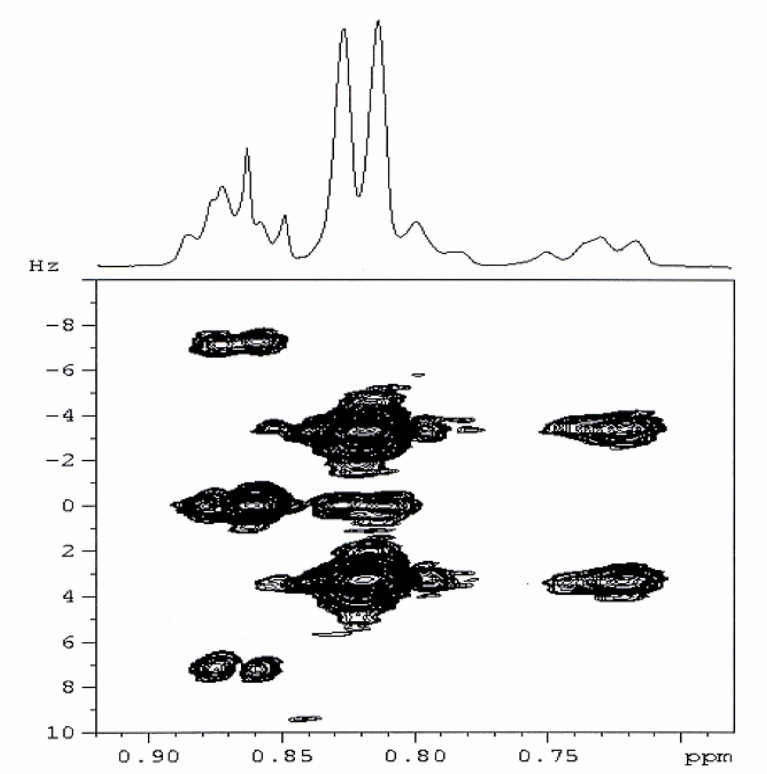

Figure 4.2. 500 MHz 2D ^{1}H-^{1}H J-resolution spectrum of poly(hexene-1) synthesized using **1**/MAO

The (ω-1)CH_2 carbons of the branches appear at 22.70-23.18 ppm. Multiplicity can also be seen in the case of poly(hexene-1)s (**Figure 4.3c**), which can be attributed to tacticity effects. The isotactic poly(hexene-1)s gives only one signal at 23.18 ppm (**Figure 4.3b**). It is interesting to note that the 30.08 ppm signal, which is typical of polyethylene type of carbons, is seen only in the case of poly(hexene-1)s synthesized using **1**. Another important feature that is borne out from the ^{13}C spectra of poly(hexene-1)s prepared by **1** is the appearance of CH carbons at 42.30 and 37.46-37.60 ppm which

should be associated with the branches in the polymer. It is observed that they do not appear either in poly(hexene-1)s prepared by **2** or in the regio-regular poly(propylene)s. Hence, in accordance with the other evidences seen from the proton and the HMQC spectra, they can be assigned to the CH carbons associated with the regio-irregular centers with methyl branches.

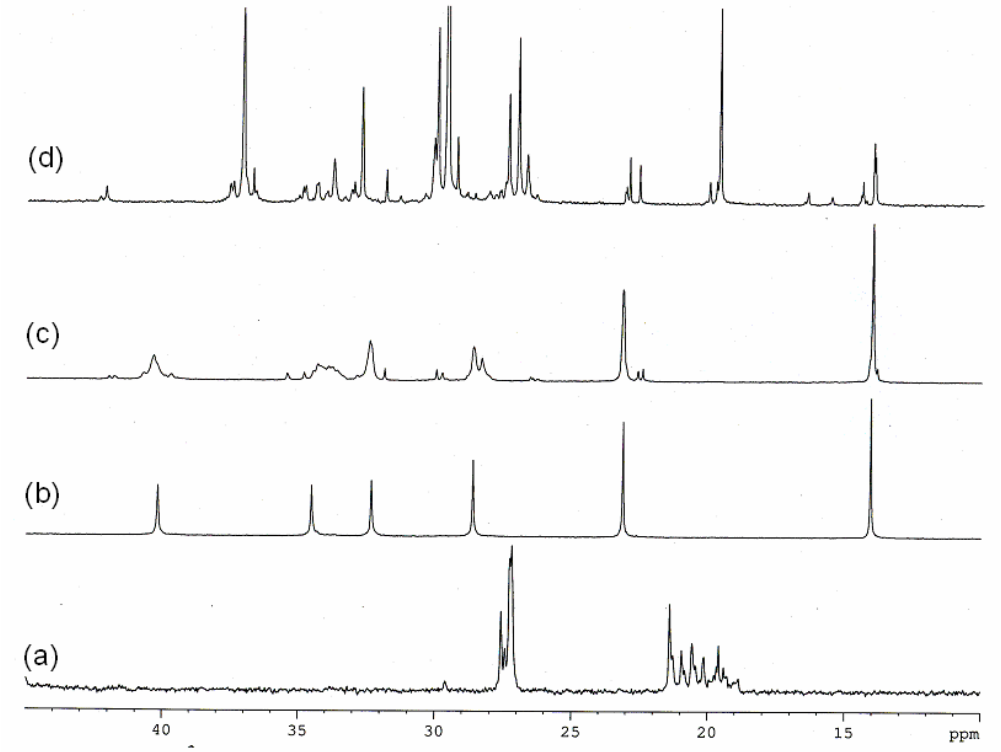

Figure 4.3. Comparison of the 125.77 MHz ^{13}C NMR spectra obtained in $CDCl_3$ at ambient temperature for an atactic polypropylene synthesized using **4** (a), isotactic (b) and atactic (c) poly(hexene-1)s synthesized using **3** and **2**, respectively and (d) poly(hexene-1)s synthesized using **1** at 70 ^{o}C.

The ^{13}C HMBC spectrum, which shows correlation between proton/s and carbon/s that are two/three bonds away from it/them, given in **Figure 4.4b**, proves this point beyond any doubt. One can clearly see the correlation of the 42.30 ppm signal with the regio-irregular methyl at 16.50 ppm and the 37.50 ppm CH carbon with the methyl signal at 14.45 ppm. Thus, an unequivocal assignment of the regio-irregular carbons in these polymers can be made from a combination of 1D ^{13}C, HMBC and HMQC spectra. To our knowledge, this is the first report wherein a clear-cut assignment is made for the protons and ^{13}C signals of the regio-irregular centers.

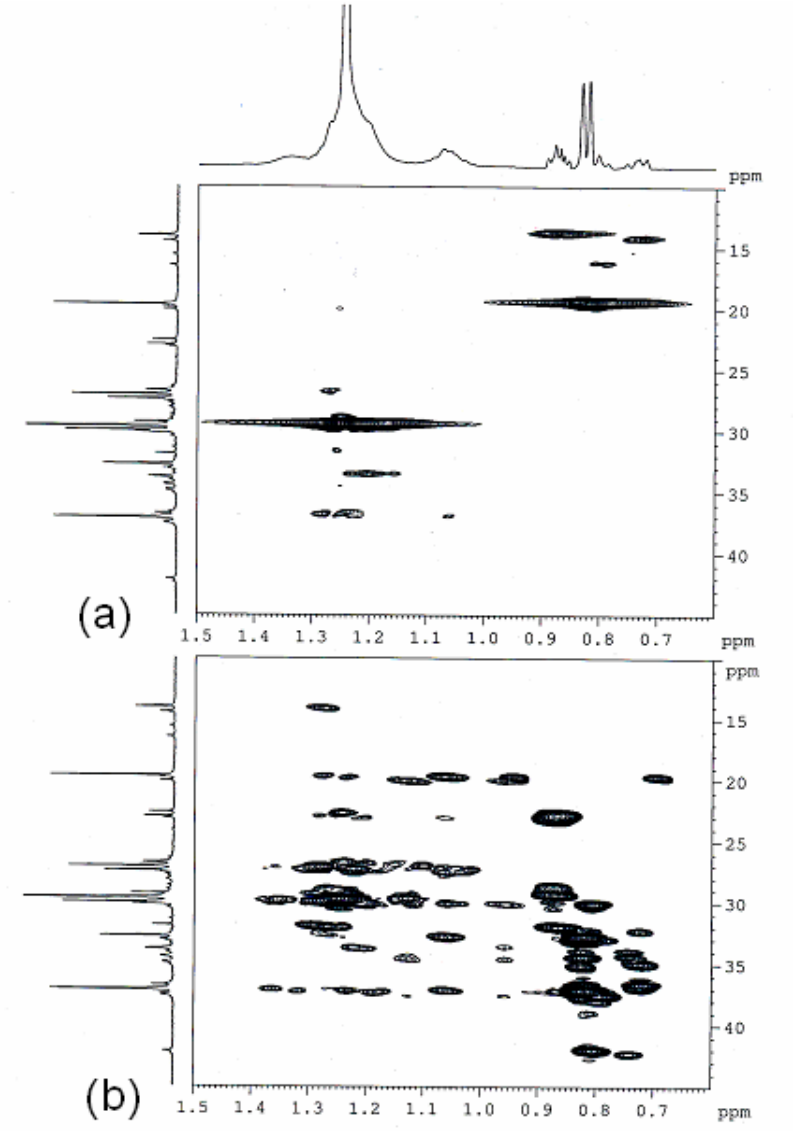

Figure 4.4. 125.77 MHz ^{13}C HMQC (a) and HMBC (b) spectra of poly(hexene-1) prepared using **1** at 70 ^{o}C. The spectra were recorded in $CDCl_3$ at ambient temperature. The experimental conditions for the HMQC spectrum is: 48 scans, 256 experiments and 1.8 Sec. relaxation delay. For the HMBC spectrum 64 scans, 300 number of experiments and 2 Sec relaxation delay were employed. The 2D data was collected as 1Kx1K matrix and the raw data was apodized with appropriate window functions in the F1 (sine squared bell) and F2 (Gaussian) domains prior to Fourier Transformations in both dimensions.

It is evident from the forgoing discussions that the poly(hexene-1)s prepared by **1** can, in principle, be considered as a combination of polymeric structures with regions containing methyl, butyl and higher branches along with polyethylene. Thus, the presence of following constituents for these polymeric structures can be envisaged.

(i) Ethylene-propylene copolymer, (ii) *meso* and *racemic* configurations of regio-irregular head-to-head methyl branches, (iii) poly(hexene-1)s, (iv) poly(α-olefin)s with longer branches and (v) polyethylene. Therefore, it was thought worthwhile to compare the ^{13}C chemical shifts observed for the poly (hexene-1) of interest with those of the individual polymeric constituents. Since most of the values reported in the literature are obtained at higher temperature in ODCB or TCB, the ^{13}C spectra of all the polymers were recorded in ODCB at 120 ^{o}C. Quantitative ^{13}C and DEPT spectra of poly(hexene-1)s synthesized using **1** are given in **Figure 4.5**.

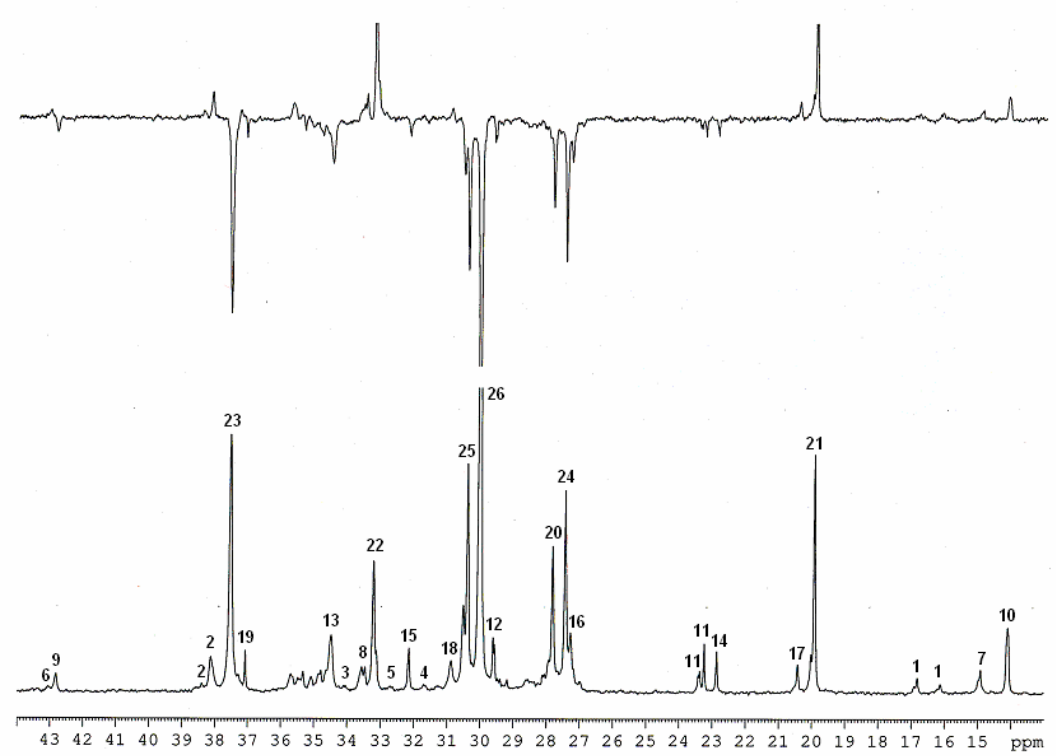

Figure 4.5. Quantitative 125.77 MHz ^{13}C and DEPT spectra of poly(hexene-1) synthesized using **1**/MAO at 70 ^{o}C in ODCB at 120 ^{o}C.

In **Figure 4.6**, we compare the ^{13}C spectra of poly(hexene-1)s (**1**) with those of atactic poly(hexene-1)s, and an EP copolymer prepared by **3**. The salient features that arise out of this comparison, in the context of the structure of poly (hexene-1)s prepared by **1**, can be summarized as follows.

(i) Presence of poly(hexene-1)s units which are similar to the one obtained with **2**. This type of structure could arise via a head-to-tail polymerization of hexene-1. These

units are found to be atactic in nature as is evident from the multiplicities obtained for the (ω-1) methylene carbon (22.85-23.38 ppm).

(ii) Presence of EP copolymer units. One can easily notice that most of the signals seen in the EP copolymer (**Figure 4.6a**) also appear in the poly(hexene-1) prepared by **1** (**Figure 4.6d**) and proves the presence of the poly(ethylene) structural units in the proximity of methyl branches.

(iii) Presence of longer branches arising due to chain running. We find unequivocal evidence for the presence of branches greater than four carbons as evidenced from the appearance of the (ω-1) methylene carbon at the characteristic position of 22.85 ppm. In this figure we have presented the ^{13}C spectrum of poly(octadecene-1)s prepared using **2** as a typical long chain branch (**Figure 4.6c**) for comparison.

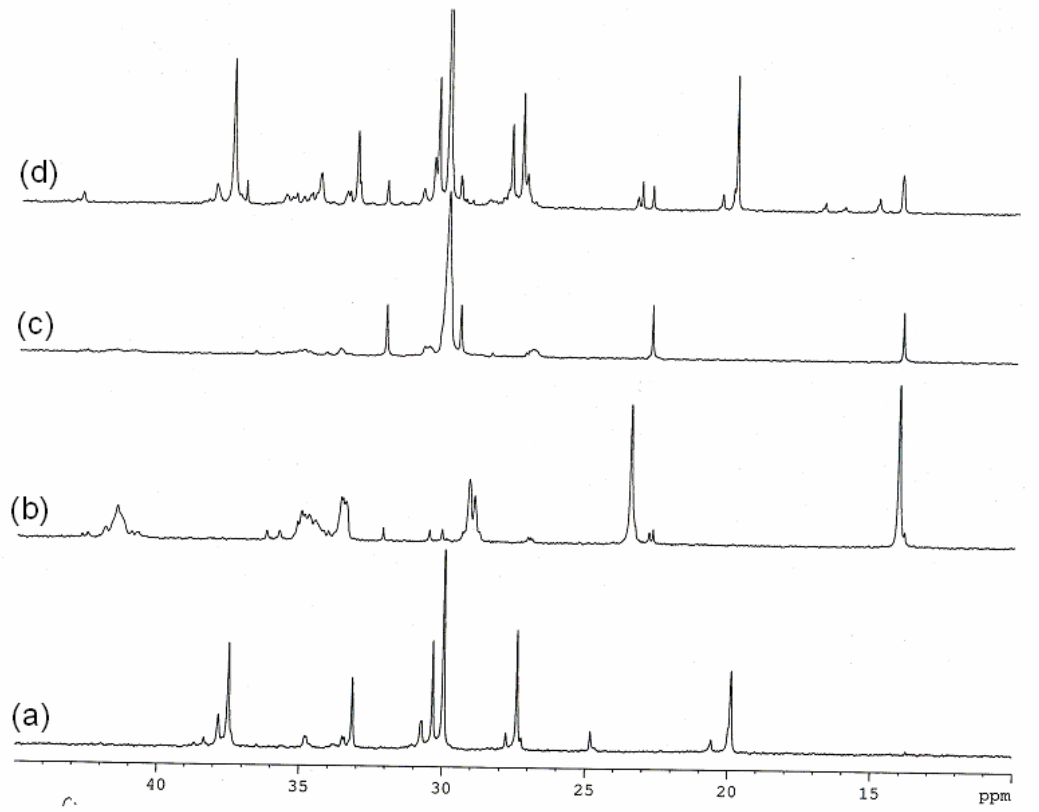

Figure 4.6. Comparison of the quantitative 125.77 MHz ^{13}C NMR spectra of an ethylene-propylene copolymer synthesized using **4** (a), atactic poly(hexene-1)s (b), poly(octadecene-1)s (c) synthesized using **2** and poly(hexene-1)s synthesized using **1** at 70 ^{o}C (d) in ODCB at 120 ^{o}C.

In order to obtain a better perspective, we present separately the ^{13}C spectra of the (ω-1) methylene region (22 to 24.5 ppm) for poly(hexene-1)s samples with other relevant systems in **Figure 4.7**. The effect of tacticity on (ω-1) methylene carbon of a C_4 branches is also visible.

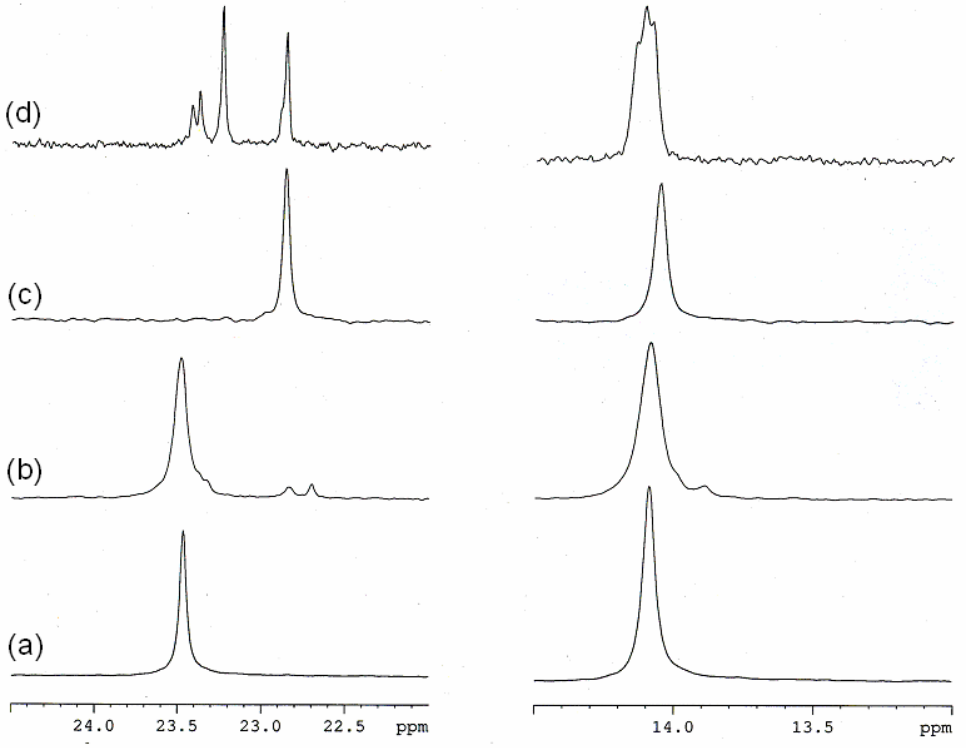

Figure 4.7. Comparison of the ω (right hand side traces), (ω-1) region of the 125.77 MHz ^{13}C NMR spectra of isotactic poly(hexene-1)s synthesized using **3** (a), atactic poly(hexene-1)s (b) and poly(octadecene-1) (c) synthesized using **2** and poly(hexene-1)s synthesized using **1** at 70 ^{o}C (d) in ODCB at 120 ^{o}C.

Though highly atactic poly(hexene-1)s can give rise to a relatively weak signal near to 22.85 ppm, it does not interfere with the conclusions made herein based on the signal at 22.85 ppm since poly(hexene-1)s prepared using **1** hardly show any atactic behavior (evident from the absence of multiple peaks in the region 42.00-41.00 ppm, see **Figure 4.3c,d**). Such fine details are not clearly seen in the ^{13}C spectra of the "ω" methyl region.

(iv) Presence of poly(ethylene) type of structural units. This type of carbon, via, $-(CH_2-CH_2)_n-$ with $n \geq 4$ resonates at the characteristic chemical shift of 30.01 ppm. The

observed intensity of this signal is more than that is seen for the EP co-polymer system (**Figure 4.6a**), and proves the existence of $-(CH_2-CH_2)_n-$ with n > 4 units.

(v) Presence of regio-irregular methyl branches (14.50-15.00 ppm and 16.00-17.00 ppm). These do not appear in any of the other three structural units mentioned so far.

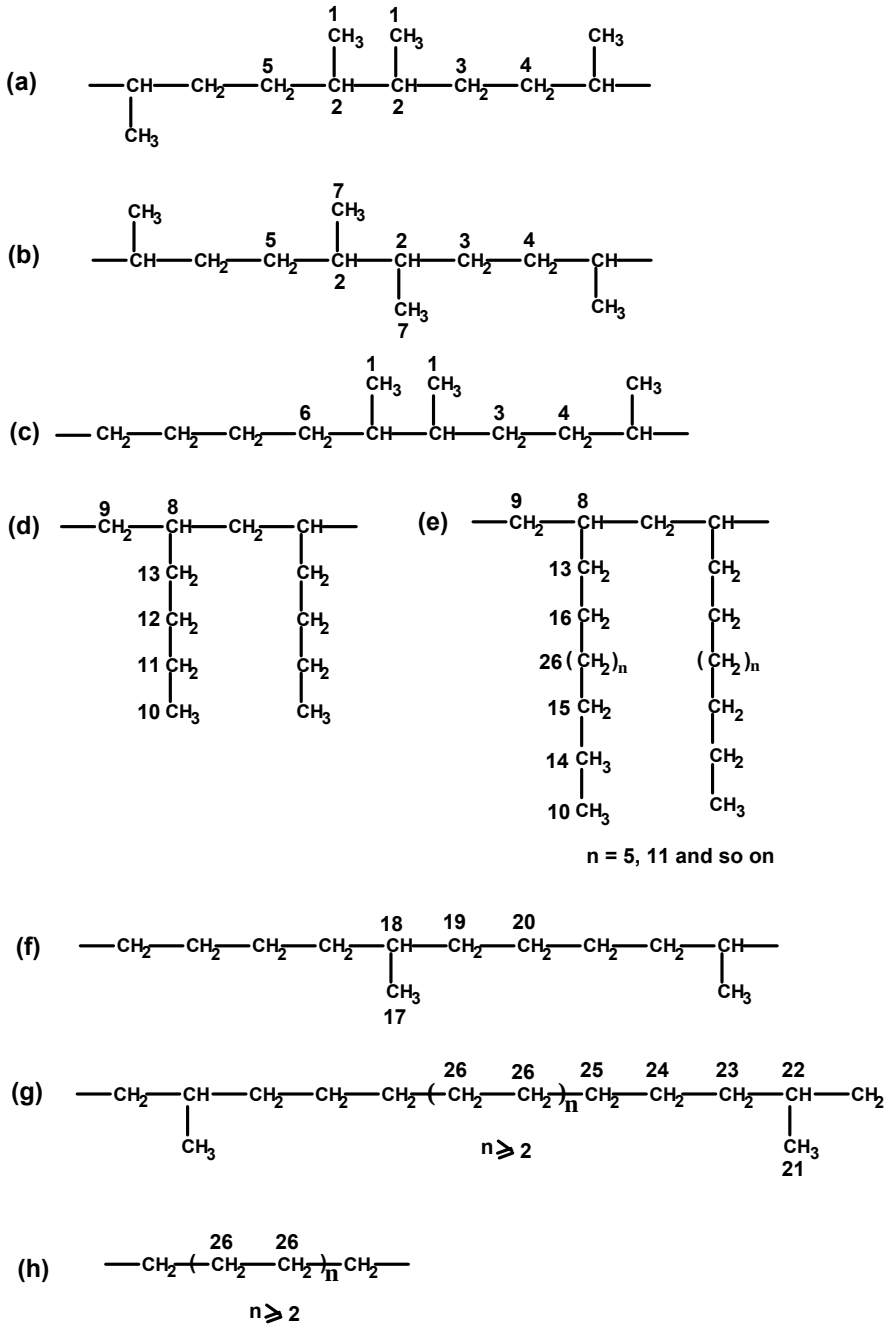

Chart 4.1. Presence of variable subunits in poly(hexene-1)s (**1**)

We have already discussed the unambiguous assignments of the signals arising from the regio-irregular methyl centers and other types of branches. The assignments of various resonances of poly(hexene-1) (**1**), which are named according to the usual procedure followed in literature (**Chart 4.1**), are presented in **Table 4.2**. Comparing the observed chemical shifts with that reported in the literature for various sub-units enables complete assignments of the peaks.

Table 4.2. Chemical shift assignments of poly(hexene-1)s (**1**)

Peak no.	Chemical shift (ppm)	Assignment
1	16.12-16.90	*m*-$P_{\delta\alpha\gamma\delta}$
2	38.12-38.14	$T_{\delta\alpha\gamma\delta}$
3	34.10	$S_{\beta\alpha\beta\gamma}$
4	31.69	$S_{\gamma\beta\alpha\beta}$
5	32.72	$S_{\beta\alpha\beta}$
6	43.05	$T_{\delta}^{+}{}_{\alpha\delta}$
7	14.6-14.92	*r*-$P_{\delta\alpha\gamma\delta}$
8	33.46-33.56	Br B_4
9	42.81	αB_4
10	14.10	$1B_4$, $1B_{10}$
11	23.23-23.38	$2B_4$
12	29.60	$3B_4$
13	34.48	$4B_4$
14	22.85	$2B_{10}$
15	32.14	$3B_{10}$
16	27.27	$9B_{10}$/$15B_{16}$
17	20.42	$P_{\alpha\delta}^{+}$
18	30.87	$T_{\delta}^{+}{}_{\delta}^{+}$
19	37.07	$S_{\alpha\delta}$
20	27.81	$S_{\beta\gamma}$
21	19.92	$P_{\alpha\delta}^{+}$
22	33.20	$T_{\delta}^{+}{}_{\delta}^{+}$
23	37.52	$S_{\delta}^{+}{}_{\alpha}$
24	27.43	$S_{\delta}^{+}{}_{\beta}$
25	30.37-30.50	$S_{\delta}^{+}{}_{\gamma}$
26	30	$S_{\delta}^{+}{}_{\delta}^{+}$

4.3.3. Mechanistic Explanation

The proposed mechanism for the formation of unusual structures in poly(hexene-1) synthesized using **1**/MAO is explained as follows.

4.3.3.1. Butyl branches

Insertion of hexene-1 in 1,2-fahsion between nickel-carbon, species (2) results. The alkyl olefin species '2' can insert hexene-1 either in a 1,2- or 2,1-fashion. If '2' inserts hexene-1 with 1,2-fashion results in species '3'. Insertion by an additional equivalent of hexene-1 to the species 3 introduces a butyl branch along the backbone (**Scheme 4.1**). The characteristic peaks of these type branches are the terminal methyl at 14.10 ppm and (ω-1) methylene peak at 23.23-23.38 ppm

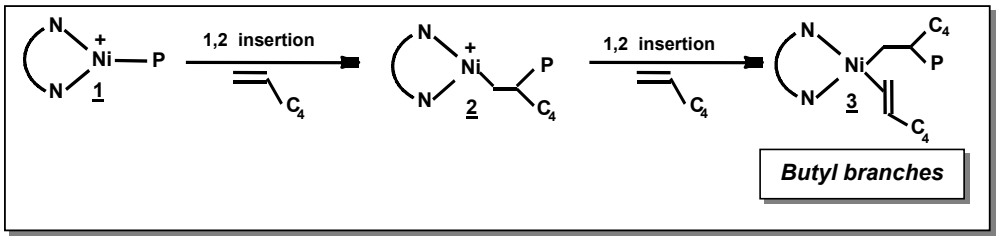

Scheme 4.1. **Formation of butyl branches**

4.3.3.2. Methyl branches

In species 2, the nickel center can first migrate by a series of β-hydride elimination till terminal ("ω") carbon gives species 4. This followed by hexene-1 insertion introduces a methyl branch in the growing polymer chain (signals from 19.9-20.5 ppm range) (**Scheme 4.2**). Here, the multiplicity can arise either due to tacticity or the EP type of arrangement. In the present case the multiplicity more likely arises form EP environments rather than tacticity. This is quiet clear from spectra presented in **Figure 4.3a**,**d** and **Figure 4.6a**,**d**.

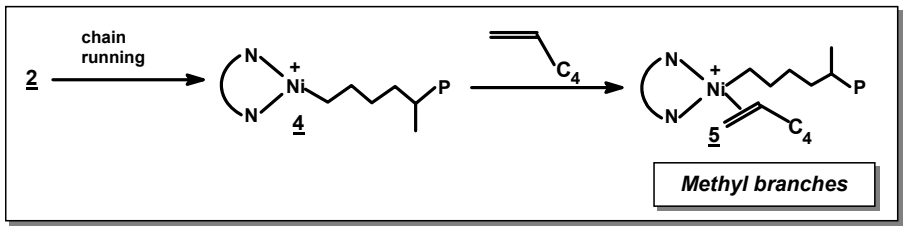

Scheme 4.2. Formation of methyl branches

4.3.3.3. Regio-irregular methyl branches

^{13}C NMR of poly(hexene-1) clearly shows presence of *meso* and *racemic* configuration of head-to-head methyl branches. The respective peaks are observed in the range of 16.00 to 17.00 ppm and 14.50 to 15.00 ppm. From the integrated area of ^{13}C spectrum we found that the regio-irregular adjacent methyls are formed in the proportion of 45 % *meso*, 55 % *racemic*. This is the first report wherein the formation of regio-irregular head-to-head methyls is seen in hexene-1 polymerization. The assignments of these different configurations compare with those reported in the literature for poly(propylene)s and model compounds[22,24,29,32-34]. Formation of these types of structures depends also on polymerization temperature. Depending on the extent of chain running different types of regio-irregular units are formed (species 12-15 in **Scheme 4.3**).

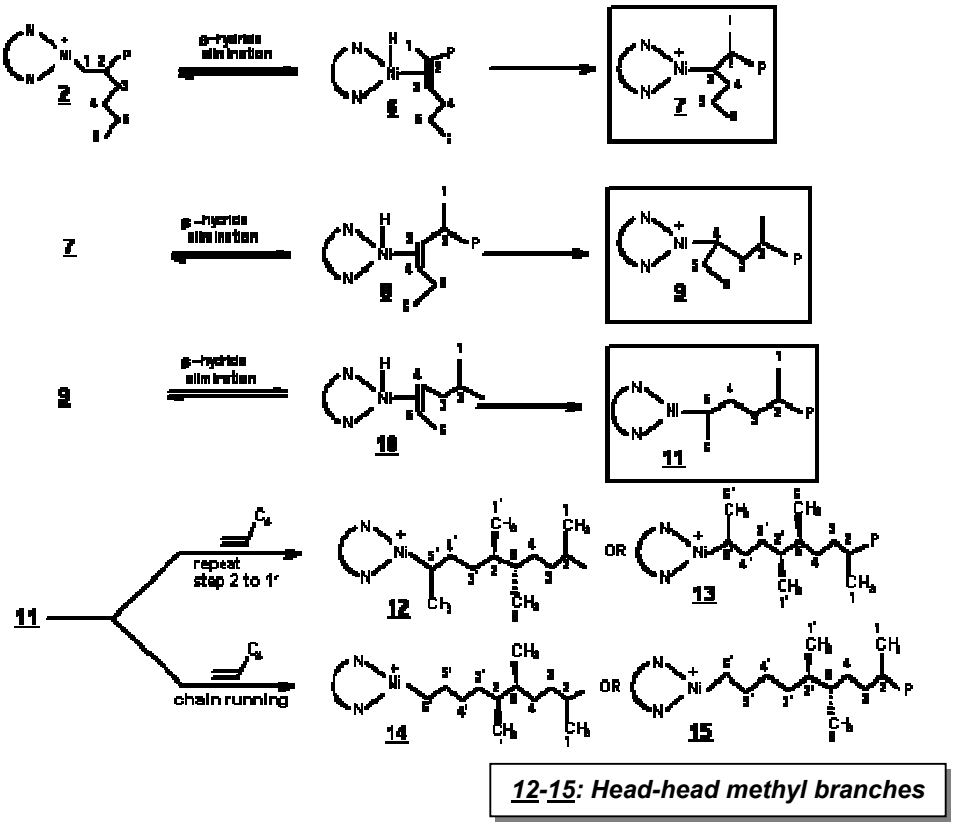

Scheme 4.3. Formation of regioirregular head-to-head (*meso* and *rac*-) methyl branches

It should be mentioned here that the signal at 43.05 ppm arising from one of the CH carbons of regio-irregular units in the ^{13}C NMR spectra of poly(hexene-1)s could be rationalized only in terms of the presence of number of adjacent methylenes near the regio-irregular methyl branch (species 14, 15) rather than species 12 and 13. The CH carbons observed at 38.12 ppm result from latter type of moieties, which are very similar to the one reported for regio-irregular part of polypropylene.

The formation of species 12, 13 and 14, 15 can be explained in the following sequential manner. (i) An insertion in 1,2-fashion, (ii) migration of nickel center upto (ω-1) carbon (species 11), (iii) 1,2-insertion of hexene-1 in species 11, repetition the steps from 2 to 11 results the species 12, 13 and 1,2-insertion of hexene-1 in species 11, metal migration upto ω carbon gives species 14, 15.

4.3.3.4. Insertion at a secondary carbon adjacent to metal

From this study it was observed that the formation of regio-irregular head-to-head methyl branch (12, 13 and 14, 15) is possible only when there is a 1,2-insertion of hexene-1 into a metal to secondary carbon bond. The reports available for polymerization of (α-olefin)s[1a] other than propylene[10] by nickel(II) and palladium(II)-α-diimine catalyst system does not consider the possibility of monomer insertion at the metal to secondary carbon center during propagation. We have seen that the extent of this type of insertion is less (~ 20 %) compared to the insertions at a primary metal to carbon center. An insertion at a metal to secondary carbon has been invoked to explain the formation of regio-irregular head-to-head methyl branches in polypropylene synthesized by the same catalyst[10].

Metal migration can, in principle, take place either in a sequential manner (β-hydride elimination) or in a fashion that involves cyclic intermediates. Intermediacy of a four-membered cyclic intermediate can lead to the formation ethyl braches while a five and six membered intermediates can lead to the formation of methyl branch and 1,6-enchainment, respectively. During the sequential metal migration, formation of all the branches i.e. propyl, ethyl and methyl can be envisaged apart from the 1,6-enchainment as the chain running can also take place to (ω-2) and (ω-3) carbons (**Scheme 4.4**). However, formation of ethyl and propyl branches could not be found in the ^{13}C spectra. It has been reported that the metal migration proceeds sequentially in a manner that is

very facile compared to monomer insertion[35]. The fact that ethyl and propyl branches are not observed suggest that the metal either does not migrate or it prefers to migrate either to (ω-1) or to ω carbon. In other words, the monomer insertion is possible whenever the metal reaches (ω-1) or ω position by migration or when it doesn't undergo any migration. The monomer gets inserted to the intermediate only when the latter imparts certain stability. Thus, our observations seem to indicate that the intermediates formed when metal is at C-1, C-5 and C-6 positions in hexene-1 is stable enough to allow monomer insertion and whenever the metal is in C-3 (species 7) and C-4 (species 17) positions it prefer to migrate. More detailed investigations are required to support this explanation.

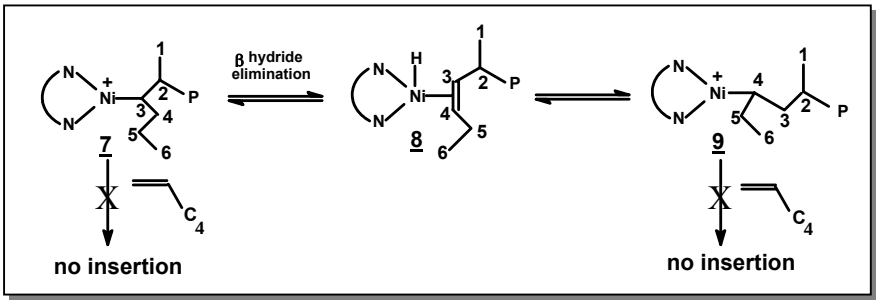

Scheme 4.4. Monomer insertion at nickel-adjacent secondary carbon

In order to obtain further insight of the nature of metal migration, we studied the polymerization of octene-1, decene-1 and tetradecene-1 using **1**/MAO. In **Figure 4.8** we show the comparative ^{13}C spectra of these polymers with that of poly(hexene-1)s. It is evident from this that for these higher α-olefins also only methyl and higher branches is observed with complete chain running. As in the case of hexene-1, the absence of other branches, especially propyl and ethyl are noticeable. This study also rules out the possibility of the existence of four, five or six memberd cyclic intermediates, as we do not observe the presence of butyl, propyl and ethyl branches for the poly(octene-1)s. The extent of chain running tends to decreases with increase in the length of the side chain of the α-olefin.

4.3.3.5. Long side chain branches

From species 4, after a 2,1-insertion of the monomer (18), the migration of nickel center down the polymer chain past the butyl branch can give rise to the formation

of (19), a C_{10} branch. Repetition of these processes after trapping and insertion of an additional equivalent of monomer gives branches longer than C_{10} (a C_{16} branch here) etc (**Scheme 4.5**).

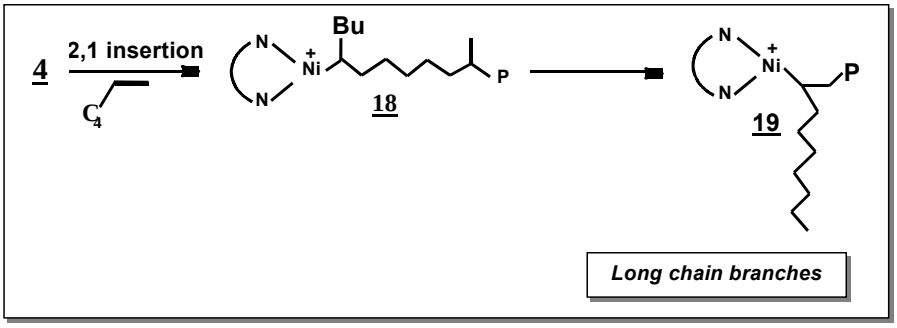

Scheme 4.5. Formation of long chain branches

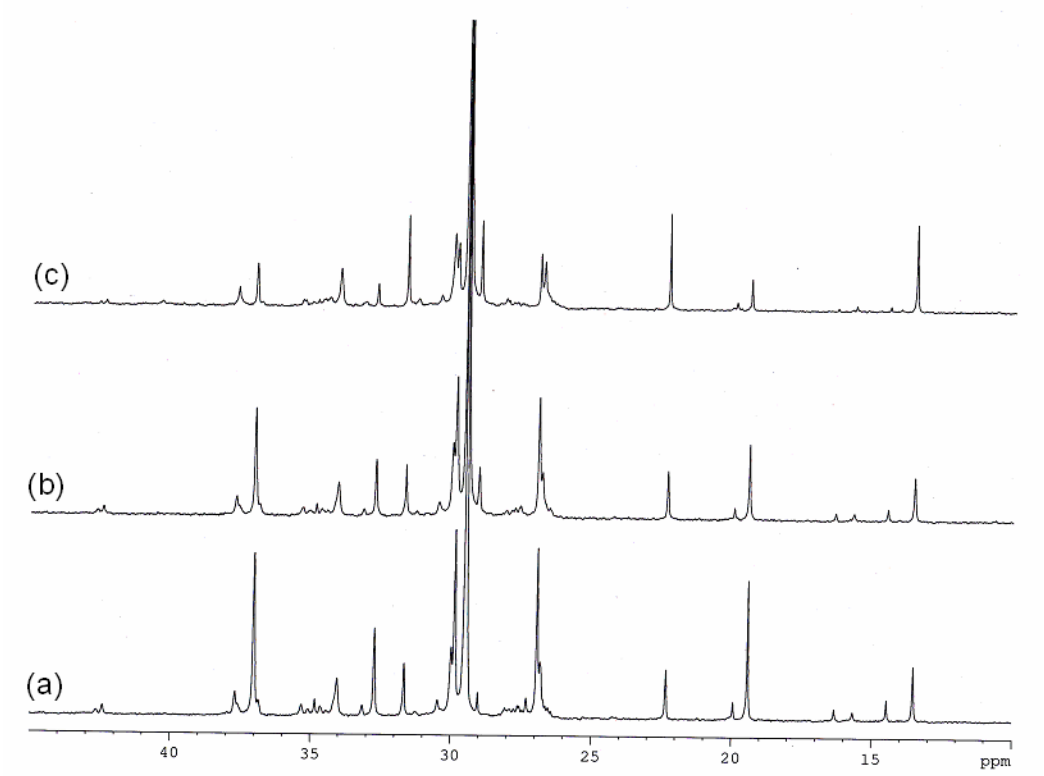

Figure 4.8. Quantitative 125.77 MHz ^{13}C NMR spectra of poly(octene-1)s (a), poly(decene-1)s (b) and poly(tetradecene-1)s (c) synthesized using catalyst **1** at 70 ^{o}C in ODCB at 120 ^{o}C.

The proof for the formation of branches longer than butyl can be seen in the ^{13}C NMR of poly(hexene-1)s (**1**). The methyl peak corresponds to butyl and longer branches

overlap in the region of 14.10 ppm in the spectra recorded at 120 ^{o}C in ODCB. However, the presence of at least two environments can be observed in the spectra recorded in $CDCl_3$ at ambient temperature **Figure 4.9**. Nevertheless, as we have discussed, a clear distinction is possible from the (ω-1) methylene carbon that appears at 22.85 ppm. The presence of this resonance unambiguously shows the formation of long chain branches. The length of the side chain must be 4, 10, 16 and so on depending on the number of 2,1-insertions followed by 1,6-enchainment. Presence of only butyl (2) and butyl and longer branches (1) are clearly seen in **Figure 4.7**. The detailed assignments are given in **Table 4.1**.

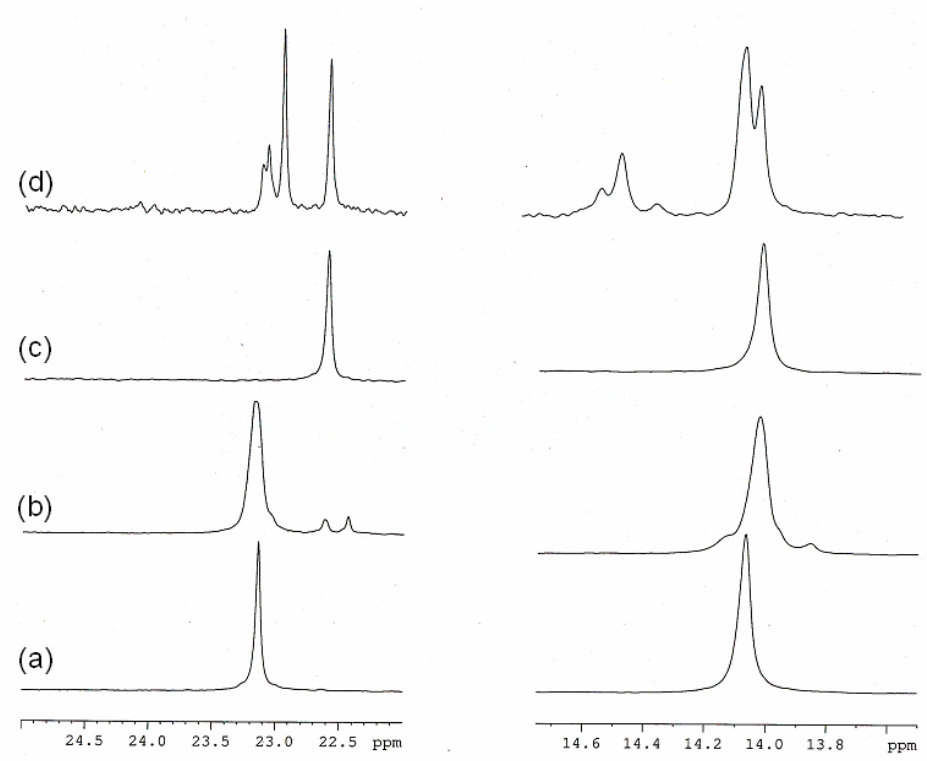

Figure 4.9. 125.77 MHz ^{13}C NMR spectra of ω (14-14.2 ppm, right hand side), (ω-1) carbon region (22.5-23.4 ppm, left hand side) of (a) isotactic poly(hexene-1)s synthesized using **3**, (b) atactic poly(hexene-1)s synthesized using **2**, (c) poly(octadecene-1)s synthesized using **2**, (d) poly(hexene-1)s synthesized using **1** (Entry 1, **Table 4.3**), in $CDCl_3$ at room temperature.

4.3.3.6. Ethylene-propylene copolymer units

Evidence for the formation of significant amount of ethylene-propylene sequences is clearly manifested in the ^{13}C NMR of poly(hexene-1)s prepared by **1**/MAO

(**Figure 4.6d**). The EP type environments can arise in the system from the species 5 by 1,2-insertion followed by chain running (upto ω carbon) and repetition of the same. This type of propagation gives four methylene units in between two methyl branches. An insertion of 2,1- type followed by 1,6-enchainment (full chain running) will lead to the incorporation of larger number of methylene units in the backbone and isolated methyl branches. Structure and assignments of these types of carbons are shown in **Chart 4.1** (structure f and g) and **Table 4.2**, respectively.

4.3.3.7. Ethylene units

Whenever hexene-1 inserts in 2,1-fashion, there will be full chain running with the resultant formation of methylene units (**Scheme 4.6**). One such full chain running leads to the insertion of six methylene units in the polymer backbone. Such enchainment in the branches will give rise to longer branches as discussed before. The carbons belonging to both these types of methylene units resonate at 30.01 ppm if the number of methylene groups is grater that four ($(CH_2)_n$, $n \geq 4$). Thus, the sequence at 30.01 ppm corresponds to the one in the backbone as well as in the side chain.

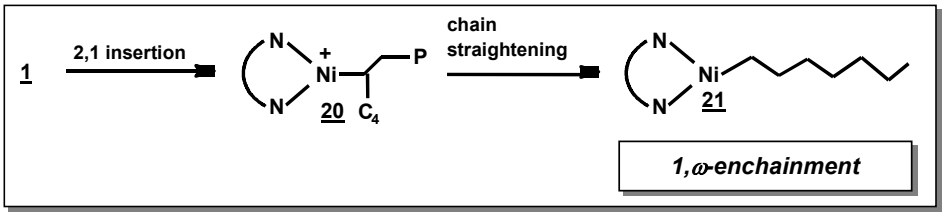

Scheme 4.6. Formation of 1,ω-enchainment

4.3.4. Effect of Polymerization Conditions on Poly(hexene-1)s Microstructure

The unusual microstructures of poly(hexene-1)s is likely to depend on reaction conditions, especially, the temperature and monomer concentration. Consequently, the microstructural features of the polymer were monitored by ^{13}C NMR spectroscopy as a function of temperature and monomer concentrations.

4.3.4.1.1. Effect of Polymerization Temperature

It was found that temperature has a more profound influence on the microstructure of poly(hexene-1)s. The results of this investigation are presented in

Table 4.3 and **Table 4.4** and the ^{1}H and ^{13}C spectra are depicted in **Figure 4.10** and **4.11** respectively. The maximum turn over frequency (TOF) is obtained at 35 ^{o}C. Consequences of nickel migration on the microstructure of poly(hexene-1)s at different temperatures is of interest to study.

Table 4.3. Homopolymerization of hexene-1 using **1**/MAO

Entry	Polymerization Temperature (^{o}C)	Yield (g)	TOF[a] (per h)
1	- 7	0.5	50
2	5	0.5	50
3	35	1.0	100
4	60	0.9	90
5	70	0.5	50

Reaction conditions: [hexene-1] = 0.25 M, (hexene-1+toluene) = 25 mL, catalyst = $3.4x10^{-4}$ M, MAO = $3.4x10^{-2}$ M, time = 1h.
[a] TOF = mol of polymer/mol of catalyst

Table 4.4. Effect of polymerization temperature on microstructure of poly(hexene-1)s synthesized using **1**/MAO[a]

Entry	T (^{o}C)	DB[b]	Branch Distribution[c] (mol %)				n_E [d] (mol %)	% 1,6-enchain-ment[e] (mol %)
			Methyl	Regio-irregular methyl	Butyl	> Butyl		
1	70	114	64	16	14	8	12	42
2	60	117	65	15	15	7	12	39
3	35	122	58	15	21	6	11	36
4	5	127	30	9	60	3	8	27
5	-7	130	26	8	65	2	7	25

[a] all the estimations are made from quantitative ^{13}C NMR spectra recorded in ODCB at 120 ^{o}C, [b] total methyl per 1000 carbon atoms, [c] branch distribution calculated using eq. 1-3, [d] n_E (number of ethylene's) calculated based on 30 ppm peak in ^{13}C NMR spectra, [e] calculated using eq. 5.

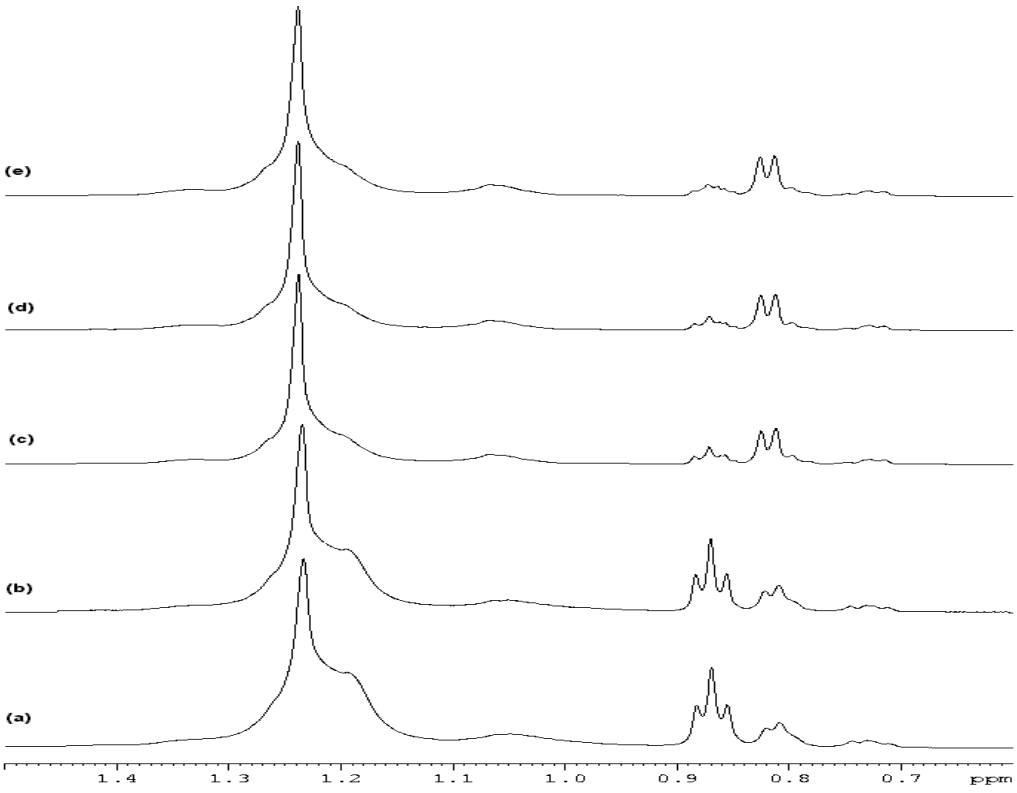

Figure 4.10. ^{1}H NMR spectra of poly(hexene-1)s (a, b, c, d and e are entry 5, 4, 3, 2 and 1 respectively in **Table 4.4**) synthesized using **1**/MAO.

The following inferences can be arrived from these data. Both 1,2- and 2,1-insertions of hexene-1 are possible during polymerization with **catalyst 1**. It has already been shown in the proposed mechanism (**Scheme 4.1** and **4.5**) that the origin for the formation of methyl (**Scheme 4.2**) and butyl (**Scheme 4.1**) branches is due to insertion of hexene-1 in a 1,2-fashion during the polymerization. The predominance of the methyl and butyl branches clearly indicates the dominance of 1,2-insertion over 2,1-insertion. Structure (d), (e) and (f) in **Chart 4.1** arise from the 1,2-insertion of hexene-1. The percentage of each type of branching with respect to the total branching can be obtained from the following relationships:

I_M (%) $= [I_M / (I_M + I_{RM} + I_B + I_L)] \times 100$ ---------- **Eq. 1**

I_{RM} (%) $= [I_{RM} / (I_M + I_{RM} + I_B + I_L)] \times 100$ ---------- **Eq. 2**

I_B (%) $= [I_B / (I_M + I_{RM} + I_B + I_L)] \times 100$ ---------- **Eq. 3**

I_L (%) $= [I_L / (I_M + I_{RM} + I_B + I_L)] \times 100$ ---------- **Eq. 4**

where, I_M, I_{RM}, I_B, and I_L are integrated area of methyl, regio-irregular methyl, butyl and longer branches. Similarly, the extent of chain running can also be evaluated from the number of methyl groups present and the total number of carbons.

% 1,6-enchainment = $\{[167 - (I_X - I_Y)] / 167\} \times 100$ ---------- **Eq. 5**

where, 167 is the theoretical number of branches per 1000 carbon atoms, 'I_X' is the intensity of total methyl branches (14.5-15 ppm, 16-17 ppm and 19.9-20.5 ppm) and methyl of butyl branches per 1000 carbons; 'Y' is the total methyl braches arising from branches longer than butyl branches (considering one 1,6-enchainment of hexene-1 in side chain) per 1000 carbons.

The latter gives the value for Y. It was found that the percentage of hexene-1 units that are undergoing full chain running (1,6-enchainment) falls within the range of 25-42 (**Table 4.4**). The following inferences can be arrived at from the details presented in **Table 4.4.**

(i) In general, 1,2-insertion of hexene-1, which leads to the formation of methyl and butyl branches, is the predominant mode of addition rather than 2,1-insertion, which leads to 1,6-enchainments. It is evident that this mode of insertion ranges from 65 to 15 % as the reaction temperature increases.

Since the methyl signals of the butyl and longer branches resonate inseparably close to each other at 14.10 ppm, these could not be used for calculation. Instead, the intrinsic chemical shift dispersion observed (**Figure 4.7**) for the (ω-1) methylene carbon of the butyl (23.23-23.38 ppm) and longer branches (22.85 ppm) were made use of to separate the contribution from these branches.

(ii) 1,2-insertion of hexene-1 followed by nickel migration is high at higher reaction temperatures. This results in the formation of more ethylene-propylene type copolymer units in the polymer backbone. This can clearly be seen from the change in the intensity of the signal at 27.43 ppm, which is arising from one of the methylene carbon (peak 20, **Figure 4.5**, **Table 4.4**)

(iii) From the area of the regio-irregular methyl groups, it was found that the formation of regio-irregular methyl decreases with decreasing the temperature.

(iv) Extent of full chain running and, thus, the formation of polyethylene type of units (30.01 ppm signal) is high at higher reaction temperature. This shows that the 2,1-addtion of hexene-1 is low at low temperature. The backbone and branch structure of the polymer can also be analyzed in terms of the number of adjacent methylenes. That is, the number of methylenes that are four or more carbon removed from a branch site per 1000 methylenes (these methylenes can be in the backbone or in the side chain, as long as they are least four carbons removed from the end of the branch). The existence of δ^+ carbons depends on the probability of an insertion of at least one hexene-1 unit with 1,6-enchainment.

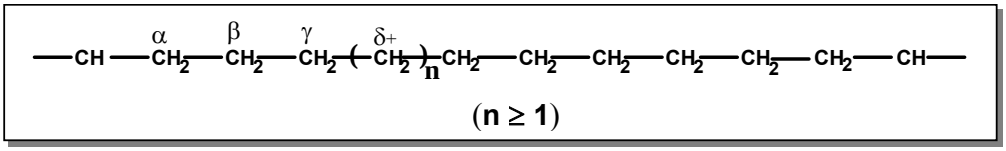

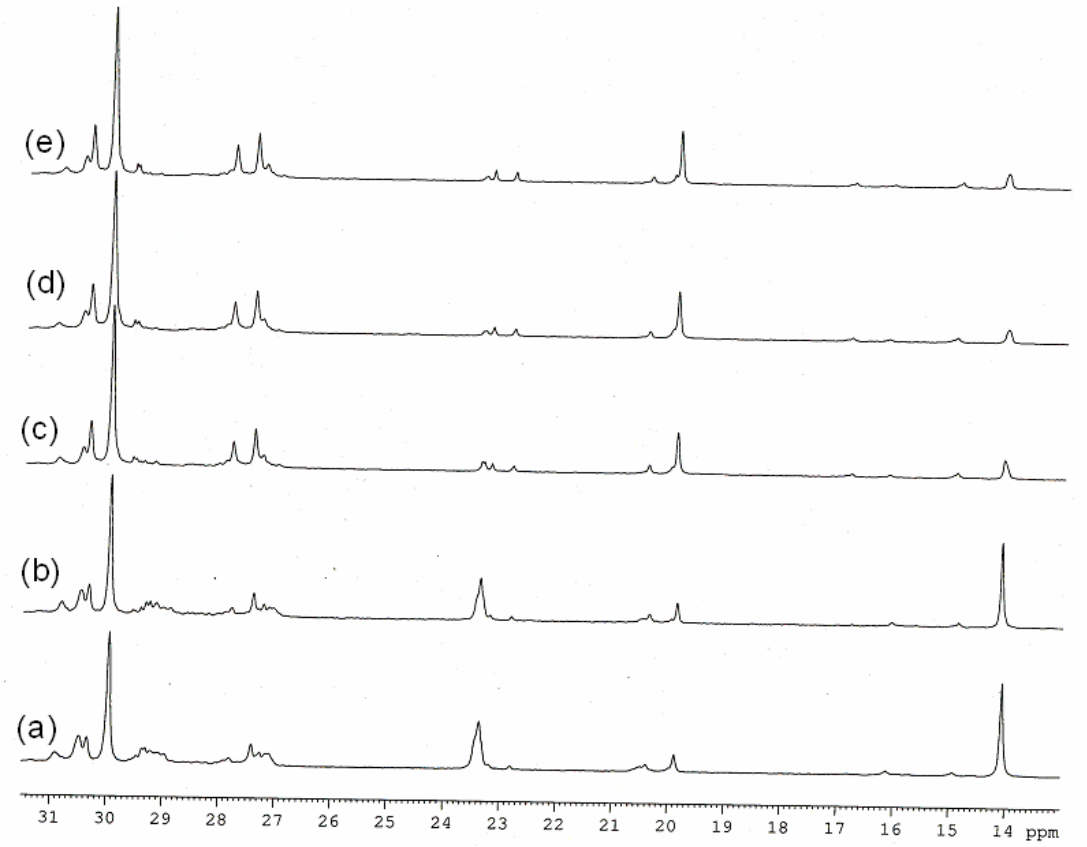

Figure 4.11. 125.77 MHz ^{13}C quantitative NMR spectra of poly(hexene-1)s synthesized using **1**/MAO at -7 (a), 5 (b), 35 (c), 60 (d) and 70 ^{o}C (e) in ODCB at 120 ^{o}C

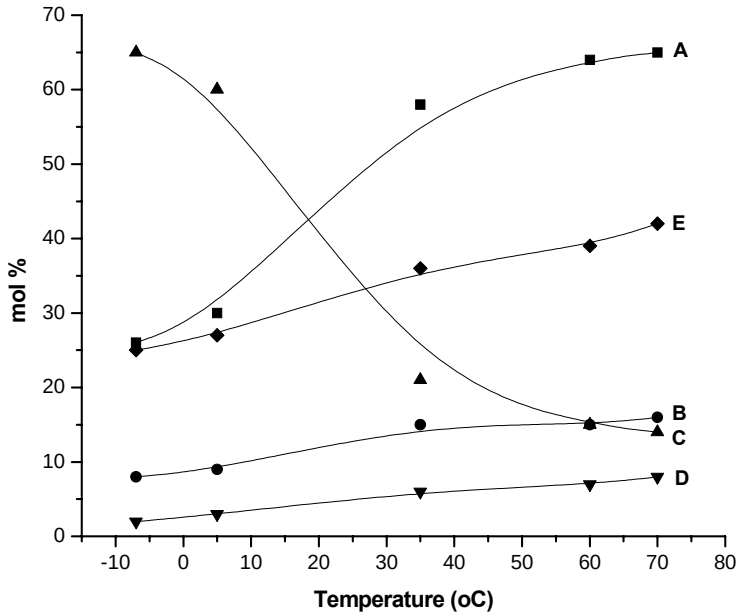

Figure 4.12. Reaction temperature vs microstructure of poly(hexene-1)s. The mol percentages are calculated using equation (1)-(5) in the text from the quantitative ^{13}C spectra. A: Methyl branches, B: regio-irregular methyl branches, C: butyl branches, D: longer branches and E: 1,6-enchainment

4.3.4.2. Effect of Monomer Concentration

Poly(hexene-1)s were prepared using **1**/MAO at variable monomer concentrations. The results are shown in **Table 4.5**. TOF (per h) increases with increasing monomer concentration and levels off beyond 1.0 M. This can be attributed to reduced monomer diffusion on account of increased solution viscosity. Extent of chain running is not affected by hexene-1 concentration. The relative mol % of different branches with different hexene-1 concentration is shown in **Table 4.6**.

Table 4.5. Homopolymerization of hexene-1 using **catalyst 1**/MAO

Entry	H-1 (M)	[M/catalyst]	Yield (g)	TOF[a] (per h)
1	0.20	590	0.34	480
2	0.30	880	0.50	700
3	0.40	1180	0.65	910
4	0.50	1470	0.73	1020
5	0.70	2060	0.93	1300
6	1.00	2940	1.33	1860
7	1.50	4410	1.10	1540

Reaction conditions: (hexene-1+toluene) = 25 mL, catalyst = 3.4×10^{-4} M, MAO = 3.4×10^{-2} M, time = 1 h. [a] TOF = mol of polymer/mol of catalyst

Table 4.6. Characterization of poly(hexene-1)s using ^{13}C NMR

Entry	Hexene-1 (M)	Total methyl (mol %)	Branch Distribution (mol %)				% 1,6-Enchain-ment[e] (mol %)
			Methyl	Regio-irregular methyl	Butyl	> Butyl	
1	0.20	111	64	17	11	8	38
2	0.30	112	64	16	12	8	38
3	0.40	111	64	16	14	7	38
4	0.50	109	63	16	16	7	39

4.4. CONCLUSIONS

Poly(hexene-1)s synthesized using $NiBr_2$(α-diimine) (**1**)/MAO possess a complex microstructure consisting of sub units of ethylene-propylene copolymer, polypropylene, poly(hexene-1), poly(α-olefin)s with longer branches and polyethylene. The following conclusions can be drawn from the present study.

(i) During polymerization, both 1,2 and 2,1-insertion of hexene-1 is observed with former dominating over the latter.

(ii) 1,2-insertion of hexene-1 followed by full chain running results in methyl branches, whereas, two consecutive 1,2-insertions results in butyl branches. Formation of ethyl, propyl branches are not observed.

(iii) The insertions are found to occur on the metal to secondary carbon centers. Whenever insertion of hexene-1 occurs at the secondary carbon, regio-irregular methyl branches are formed.

(iv) 2,1-insertion of hexene-1 results in 1,6-enchainment. The number of ethylene sequences depends on the frequency of adjacent 2,1-insertions. Long chain branches results if the nickel center runs down the polymer chain past a branch followed by a 2,1-insertion of an additional equivalent of hexene-1.

(v) The extent of occurrence of these unusual structures in poly(hexene-1) is dependent on the reaction temperature.

In the case of poly(octene-1)s, poly(decene-1)s and poly(tetradecene-1), only methyl and higher branches can be seen apart from the full chain running which decreases with the length of the α-olefin. No intermediate branches are observed.

4.5. REFERENCES

(1) (a) Ittel, S. D.; Johnson, L. K.; Brookhart, M. *Chem. Rev*. **2000,** *100*, 1169. (b) Britovsek, G. J. P.; Gibson, V. C.; Wass, D. F. *Angew. Chem., Int. Ed. Engl.* **1999**, *38*, 428.

(2) Johnson, L. K.; Killian, C. M.; Brookhart, M. *J. Am. Chem. Soc*. **1995**, *117*, 6414.

(3) Johnson, L. K.; Killian, C. M.; Arthur, S. D.; Feldman, J.; McCord, E. F.; McLain, S. J.; Kreutzer, K. A.; Bennett, A. M. A.; Coughlin, E. B.; Ittel, S. D.; Parathasarathy, A.; Tempel, D. J.; Brookhart, M. S. *Pat. Appl WO 9623-10*,**1996**.

(4) Killian, C. M.; Tempel, D. J.; Johnson, L. K.; Brookhart, M. *J. Am. Chem. Soc.* **1996**, *118*, 11664.

(5) Mecking, S. *Angew. Chem., Int. Ed*. **2001**, *40*, 534.

(6) Mader, D.; Heinemann, J.; Mulhaupt, R. *Macromolecules* **2000**, *33*, 1254.

(7) Schubbe, R.; Angermund, K.; Fink, G.; Goddard, R. *Macromol. Chem. Phys*. **1995**, *196*, 467.

(8) M**ö**hring, V. M.; Fink, G. *Angew. Chem., Ind. Ed. Eng.* **1985**, *24*, 1001.

(9) Keim, W.; Appel, R.; Storeck, A.; Kruger, C.; Goddard, R. *Angew. Chem., Int. Ed. Eng*. **1981**, *20*, 116.

(10) McCord, E. F.; McLain, S. J.; Nelson, L. T. J.; Arthur, S. D.; Coughlin, E. B.; Ittel, S. D.; Johnson, L. K.; Tempel, D.; Killian, C. M.; Brookhart, M. *Macromolecules* **2001**, *34*, 362.

(11) Antoni, J.; Nancy, W. E.; Eric, T. H. *Macromolecules* **1999**, *32*, 5471.

(12) Busico, V.; Cipullo, R.; Chadwick, J. C.; Modder, J. F.; Sudmeijer, O. *Macromolecules* **1994**, *27*, 7538.

(13) Zambelli, A.; Locatelli, P.; Provasoli, A.; Ferro, D. R. *Macromolecules* **1980**, *13*, 267.

(14) Zambelli, A.; Locatelli, P.; Zannoni, G.; Bovey, F. A. *Macromolecules* **1978**, *11*, 923.

(15) Asakura, T.; Nakayama, N.; Demura, M.; Asano, A. *Macromolecules* **1992**, *25*, 4876.

(16) Schilling, F. C.; Tonelli, A. E. *Macromolecules* **1980**, *13*, 270.

(17) Zambelli, A.; Locatelli, P.; Bajo, G.; Bovey, F. A. *Macromolecules* **1975**, *8*, 687.

(18) Asakura, T.; Nishiyama, Y.; Doi, Y. *Macromolecules* **1987**, *20*, 616.

(19) Asakura, T.; Ando, I.; Nishioka, A.; Doi, Y.; Keii, T. *Makromol. Chem*. **1977**, *178*, 791.

(20) Doi, Y. *Macromolecules* **1979**, *12*, 248.

(21) Doi, Y. *Macromolecules* **1979**, *180*, 2447.

(22) Cheng, H. N. *Polym. Bull*. **1985**, *14*, 347.

(23) Zambelli, A.; Gatti, G. *Macromolecules* **1978**, *11*, 1485.

(24) Zambelli, A.; Bajo, G.; Rigamonti, E. *Makromol. Chem*. **1978**, *179*, 1249.

(25) Grassi, A.; Zambelli, A.; Resconi, L.; Albizzati, E.; Mazzocchi, R. *Macromolecules* **1988**, *21*, 617.

(26) Zambelli, A.; Tosi, C. *Adv. Polym. Sci*. **1974**, *15*, 31.

(27) Grassi, A.; Zambelli, A.; Resconi, L.; Albizzati, E.; Mazzocchi, R. *Macromolecules* **1988**, *21*, 617.

(28) Zambelli, A.; Locatelli, P.; Rigamonti, E. *Macromolecules* **1979**, *12*, 156.

(29) Asakura, T.; Nishiyama, Y.; Doi, Y. *Macromolecules* **1987**, *20*, 616.

(30) Asakura, T.; Nakayama, N.; Demura, M.; Asano, M. *Macromolecules* **1992**, *25*, 4876.

(31) Robert, J. C. *US Pat. 4535068*, **1985**.

(32) Lindeman, L. P.; Adams, J. Q. *Analytical Chemistry* **1971**, *43*, 1245.

(33) Carman, C. J.; Tarpley, A. R.; Goldstein, J. H. *Macromolecules* **1973**, *6*, 719.

(34) Randall, J. C. *J. Polym. Sci., Polym. Phy. Ed*. **1973**, *11*, 275.

(35) Gottfried, A. C.; Brookhart, M. *Macromolecules* **2003**, *36*, 3085.

CHAPTER 5

SNTHESIS AND CHARACTERIZATION OF POLY(OCTADECENE-1)S USING $NiBr_2$(-DIIMINE) / MAO CATALYST: EFFECT OF CHAIN RUNNING ON PROPERTIES

5.1. INTRODUCTION

In 1985, Fink and coworkers[1] explored the concept of chain running during α-olefin polymerization using a late transition nickel based catalyst. Homopolymerization of α-olefins using this catalyst gives oligomers containing methyl branches. This mechanism states that the 1,2-insertion of α-olefin followed by 2,ω-enchainment of α-olefin leads to the formation of methyl branches in polymer chain. The variation of extent of nickel migration with reaction conditions was also reported.

Brookhart and coworkers[2] reported the synthesis of a new generation of nickel(α-diimine) catalysts, which gives a novel microstructure for the resulting poly(α-olefin)s. The concept of chain running i.e., consecutive β-hydride elimination subsequent metal migration followed by olefin insertion with opposite regiochemistry is a distinguishing mechanistic feature of these catalysts. Occurrence of variable enchainments during polymerization results in different frequency levels of methylenes in the polymers. Poly(propylene)s[3] made by these catalysts contain stereo and regio specific methyl branches, isolated methyl, longer than methyl branches and variable levels of 1,3-enchainments. Recently Landis and coworkers[4] reported the formation of rare secondary Zr-polymer bond in propylene polymerization and observed the accumulation of catalyst as dormant secondary sites. Later Busico and coworkers[5] confirmed the poor reactivity of secondary metal-polymer bond towards propylene and ascribed this to the formation of dormant chains in propylene polymerization.

The consequences of chain running on melting, crystallization behavior and dynamic mechanical properties of poly(α-olefin)s are of great interest to understand the structure-property relationship of these novel poly(α-olefin)s. Mechanism of chain running in α-olefin polymerization introduces variable levels of methylene sequences in the main as well as side chain of the polymer[3]. Mauler et al[6] reported that the melting and crystallization behavior of branched polyethylene is dependent on several factors. Arnold and coworkers[7] synthesized poly(α-olefin)s such as, poly(decene-1), poly(tetradecene-1), poly(hexadecene-1) and poly(octadecene-1) using various metallocene-based catalysts and examined their thermal behaviour. The studies revealed that side chain crystallization occurs when the length of the side chain exceeds eight carbon atoms. This side chain crystallization is of great interest in ethylene copolymers.

Presence of short chain branches like methyl, ethyl in the polyethylene backbone disturbs the crystallinity and cause lowering of lamella thickness[8-11]. Sequence length of methylene plays a major role on the polymer properties in the case branched polyethylene[12-14]. Poly(ethylene-*co*-eicosene-1)[15] containing 5.9 mol % of comonomer showed an additional melting peak, which arises from the side chain crystallization of methylenes in the side chain. Waymouth *et al* reported[16] the influence of ethylene sequence on the melting behavior of ethylene copolymers using DSC. The multiple melting endotherms obtained in the case of ethylene-α-olefin copolymers is due to the distribution of ethylene sequences or chain segments that can participate in the crystallization. Guerra et al[17] reported the influence of regio- and stereoregular, irregular of propene insertion on crystallization behavior of ethylene/alkene-1 copolymers. The disturbances in crystallinity of these copolymers are more on account of regioirregularity of propene insertion than streoirregularity.

Mulhaupt and coworkers[18] reported the influence of α-olefin insertion into copolymers with different stereo and regio chemistry on melting and crystallization behavior. In case of branched polyethylene prepared by early and late transition metal catalysts, the T_g is dependent on number of short chain branches as well as on the branch length[8].

In this chapter, we report the homopolymerization of octadecene-1 using [*N,N´*-diisopropylbenzene)-2,3-(1,8-napthyl)-1,4-diazabutadiene]dibromonickel (**catalyst 1**)/ MAO. The main focus of this work is to study the effect of chain running on microstructure of poly(octadecene-1)s the using high-resolution NMR spectroscopy.

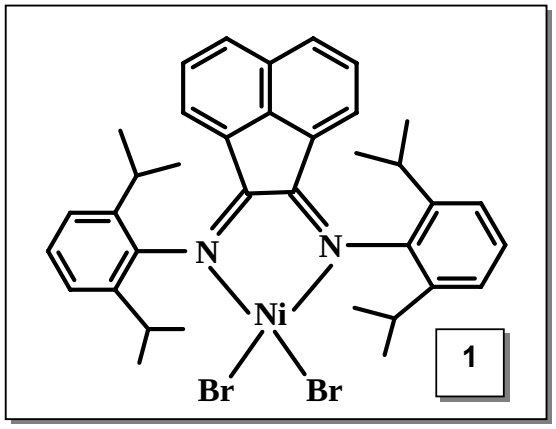

Consequences of chain running on melting, crystallization and mechanical properties of poly(octadecene-1)s are examined using differential scanning calorimetry (DSC) and dynamic mechanical thermal analysis (DMTA). Similarly, extent of nickel migration with decene-1, dodecene-1, tetradecene-1 and hexadecene-1 was correlated with the properties of the corresponding polymers.

5.2. EXPERIMENTAL

5.2.1. Materials

This is described in the Chapter 3 under section 3.3.

5.2.2. Synthesis of catalyst

The **catalyst 1** was synthesized according to reported procedure[19].

5.2.3. Synthesis of poly(α-olefin)s

Detailed polymerization procedures and work up are given in Chapter 3.

5.2.4. ^{1}H and ^{13}C NMR spectroscopy

Details are given in Chapter 3.

5.2.5. Nomenclature

^{13}C NMR chemical shifts assignments of different carbons are labeled according to reference[3].

5.2.6. Gel permeation chromatography (GPC)

Details are given in Chapter 3.

5.2.7. Film preparation

Details are given in Chapter 3.

5.2.8. Differential scanning calorimetry (DSC)

Details are given in Chapter 3.

5.2.9. Dynamic mechanical thermal analysis (DMTA)

Details are given in Chapter 3.

5.3. RESULTS AND DISCUSSION

5.3.1. Effect of Polymerization Temperature on Poly(octadecene-1)s Properties

The turnover frequency (TOF) and molecular weight data of poly(octadecene-1)s prepared by **catalyst 1**/MAO at different temperatures are shown in **Table 5.1**. For the purpose of comparison among monomer, catalyst and cocatalyst concentrations were kept same. All reactions were carried out using glass ampoule reactor and the accurate polymerization temperature was maintained using a constant temperature circulating bath.

Table 5.1. Synthesis and characterization of poly(octadecene-1)s prepared by **1**/MAO using GPC

Entry	T (^oC)	Yield (g)	TOF[a] (per h)	GPC			
				$\overline{M}_n$	$\overline{M}_w$	MWD	R_g[b] (nm)
1	- 10	0.15	35	26,620	37,800	1.42	6.96
2	0	0.64	150	51,500	73,300	1.42	11.04
3	10	0.96	225	48,100	85,100	1.77	12.24
4	20	1.25	290	55,200	109,600	1.99	13.86
5	30	1.35	315	100,700	156,600	1.55	17.16
6	45	1.88	440	175,500	232,500	1.33	20.21
7	60	1.50	350	111,600	196,000	1.76	20.33
8	70	1.06	250	91,100	185,700	2.04	22.82

Reaction conditions: [octadecene-1] = 0.25 M, (octadecene-1+toluene) = 50 mL, catalyst 1 = $3.4x10^{-4}$ M, MAO = $3.4x10^{-2}$ M, time = 1h
[a] TOF = mol of polymer/mol of catalyst, [b] R_g = Radius of gyration

5.3.1.1. TOF (per h) and GPC

Upon addition of MAO solution, the reaction mixture (catalyst + monomer + toluene) turns purple from orange color and remains same throughout the polymerization at temperatures upto 45 ^oC. At higher polymerization temperature the color further turned blue, which indicates the deactivation of catalyst species. Yield is increases with polymerization temperature from -10 to 45 ^oC and tends to decrease at higher

polymerization temperatures. This may be due to increase in rate of chain transfer reactions as evidenced by a decrease of number average molecular weight ($\overline{M}_n$) at higher polymerization temperatures. GPC traces of poly(octadecene-1)s synthesized at -10, 0, 30 and 60 ^oC are depicted in **Figure 5.1**. The radius of gyration (R_g) is high (22.82 nm) for poly(octadecene-1)s (**Table 5.1**, entry 8) synthesized at 70 ^oC. R_g decreases from 20.33 nm to 6.96 nm when the polymerization temperature is lowered from 60 ^oC to -10 ^oC. This clearly indicates that the topology of polymer is dependent on the polymerization temperature. To further understand the structure of the polymer, detailed microstructure analysis of poly(octadecene-1)s was undertaken.

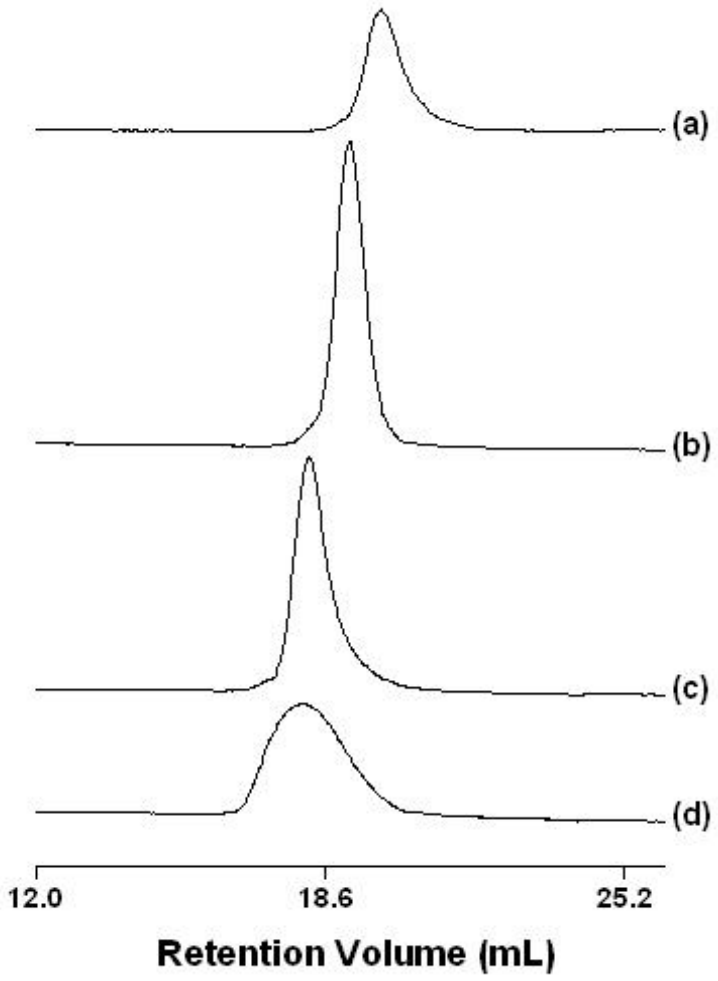

Figure 5.1. GPC of poly(octadecene-1)s prepared by **1**/MAO. (a) T = -10 ^oC, (b) T = 0 ^oC, (c) T = 30 ^oC and (d) T = 60 ^oC.

5.3.1.2. ^{1}H NMR

500 MHz ^{1}H NMR spectra of poly(octadecene-1)s prepared by **1**/MAO is shown in **Figure 5.2(c)** and **(d)**. The observed chemical shifts are different from those of poly(octadecene-1)s prepared by early transition metal catalysts[7,20-22]. The peak observed at 0.88 ppm is assigned to CH_3 protons of hexadecyl (C_{16}) branches of poly(octadecene-1) (**Figure 5.2 (b)**) prepared by Cp_2ZrCl_2/MAO (**2**). Additional two peaks are noticed at 0.82 and 0.74 ppm (doublets), which arise exclusively from methyl (C_1) branches. These peaks are similar to that observed for poly(propylene)s, which is depicted in **Figure 5.2(a)**.

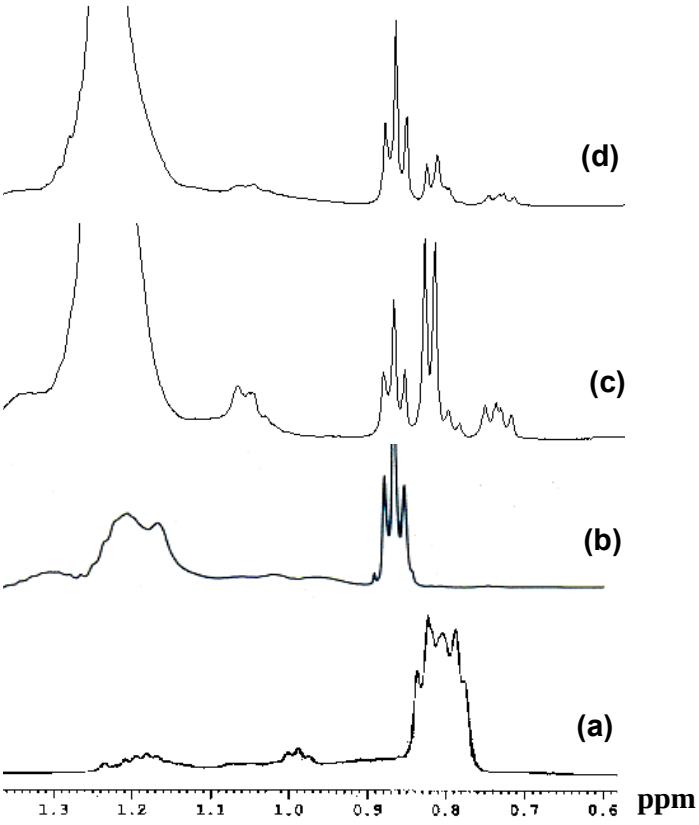

Figure 5.2. ^{1}H NMR, (a) poly(propylene) synthesized using **2**/MAO, (b) poly(octadecene-1) synthesized using **2**/MAO, (c) and (d) poly(octadecene-1)s synthesized using **1**/MAO at T = 60 ^{o}C and T = 0 ^{o}C.

Poly(octadecene-1)s synthesized using **1**/MAO at different temperatures showed similar total number of branches and is lower than poly(octadecene-1)s synthesized using conventional Ziegler-Natta or metallocene catalysts. However, percent

mole ratio of C_{16} and C_1 protons of methyl branches varied (total mol % is same) with polymerization temperature. Lower number branches observed compared to that predicted by theory is due to nickel migration followed by variable enchainments during polymerization. It is observed that mol % of protons of C_{16} branches are higher at lower polymerization temperatures (**Figure 5.2d**), which tend to decrease with increasing temperature (**Figure 5.2c**). The mol % protons of C_1 branches are high at higher polymerization temperatures (**Figure 5.2c**). The details of polymerization conditions and ^{1}H NMR chemical shifts of polypropylene and poly(octadecene-1)s prepared by **2** and catalyst **2**, **1**, respectively, is shown in **Table 5.2**.

Table 5.2. Chemical shifts of ^{1}H NMR for poly(propylene) and poly(octadecene-1)s prepared by **2**/MAO and **1**/MAO

Entry	Polymer	Catalyst	[Catalyst].10^3 (M)	[Al/ catalyst]	T (^{o}C)	^{1}H NMR chemical shift (ppm)	
						Hexadecyl branches (a)	Methyl branches (b)
1	Poly(propylene)	2	0.15	1000	35	NIL	0.82
2	Poly(octadecene-1)	2	4.80	1000	35	0.88	NIL
3	Poly(octadecene-1)	1	0.34	150	0	0.88	0.82 and 0.74
4	Poly(octadecene-1)	1	0.34	150	60	0.88	0.82 and 0.74

5.3.1.3. ^{13}C NMR

^{13}C NMR spectra of poly(octadecene-1)s prepared by **catalyst 1**/MAO at different polymerization temperatures (60 and 0 ^{o}C) are shown in **Figure 5.3** (**c** and **d**). The total number of branches per 1000 carbons is lesser than what is predicted by theory. Additional peaks are observed with ^{13}C NMR of poly(octadecene-1)s prepared by **1**/MAO, which is not observed in poly(octadecene-1)s prepared by Cp_2ZrCl_2 and other metallocene catalysts[7]. Additional peaks observed in the region from 15-17 ppm and at 20 ppm are attributed to the methyl branches of polypropylene[23,24] A detailed study was performed to assign the chemical shifts of poly(octadecene-1) (1).

For the purpose of comparison polypropylene and poly(octadecene-1)s prepared by **2**/MAO are also shown in **Figure 5.3** (**a** and **b**). In **Figure 5.3** (**c** and **d**) peak at 14 ppm is due to methyl of hexadecyl branches, which exactly match with the methyls of C_{16} branches of pure poly(octadecene-1) (**2**). The peak at 20 ppm exclusively arises from isolated methyl branches. This peak is similar to that observed with the methyl branches of poly(propylene)s. The peaks in the range 15-17 ppm correspond to the regioirregular methyl branches. A similar observation has also been made in the case of poly(hexene-1)s (**Chapter 4**, section 4.3.2). The microstructure of poly(octadecene-1)s was also investigated using HMQC and HMBC.

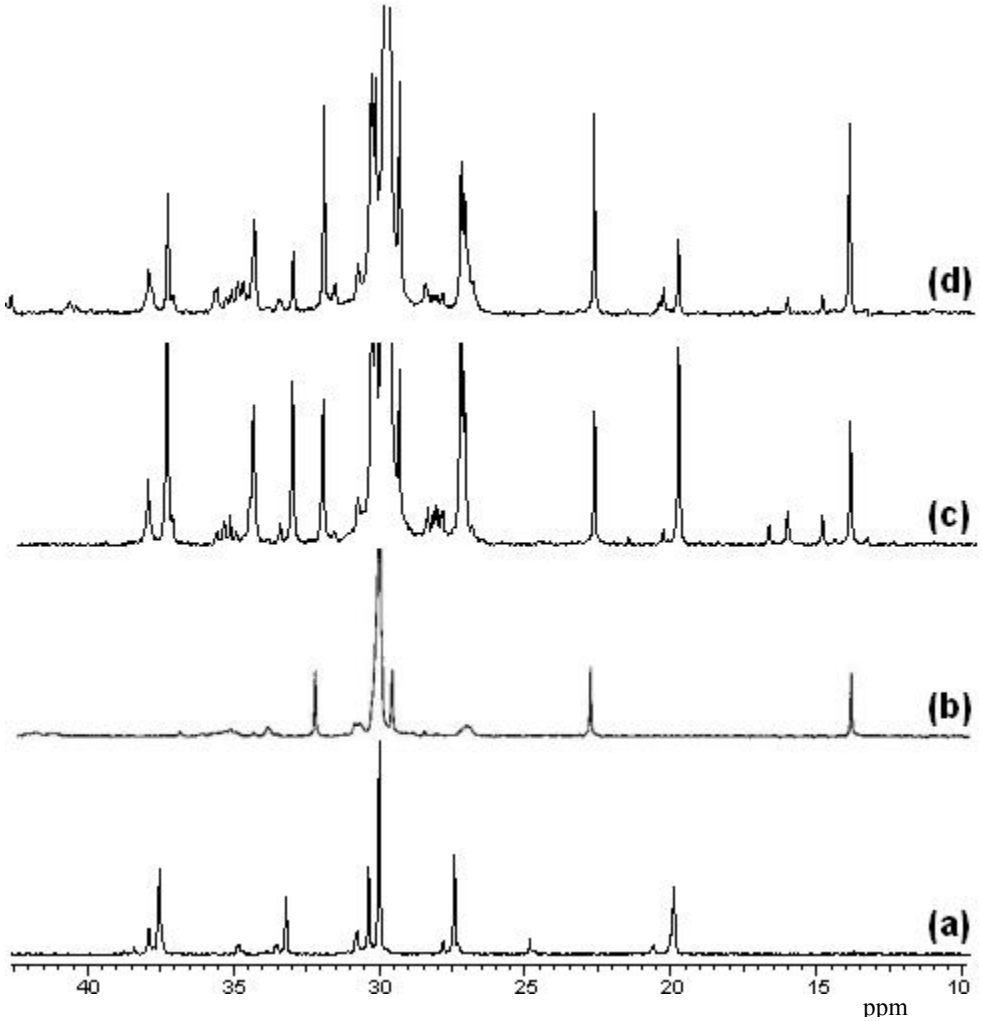

Figure 5.3. Quantitative 125.77 MHz ^{13}C NMR of **(a)** EP synthesized using **2**/MAO, **(b)** poly(octadecene-1) synthesized using **2**/MAO, **(c)** and **(d)** poly(octadecene-1)s synthesized using **1**/MAO at T = 60 ^{o}C and T = 0 ^{o}C.

5.3.1.3.1. HMQC and HMBC

HMQC reveals that protons directly attached to carbon atoms. HMQC of poly(octadecene-1)s prepared by **1**/MAO is shown in **Figure 5.4**. The following salient features are observed. (i) In ^{1}H NMR, the chemical shifts values of 0.88 ppm is directly correlated to the 14 ppm peak in the ^{13}C NMR. This is indicative of the presence of hexadecyl branches. (ii) Protons observed in the region 0.72-0.88 ppm are correlated to carbons of methyl branches, i.e. 15-17 ppm region in ^{13}C NMR The peaks in the region 15-17 ppm are exclusively arising from regio-irregular head-to-head of *meso* and *rac*-type of methyl branches. The observed chemical shift values exactly correspond to reported values of polyolefins[25-30]. (iii) methylene protons arising at 1.2 ppm are correlated with carbon at 30 ppm region.

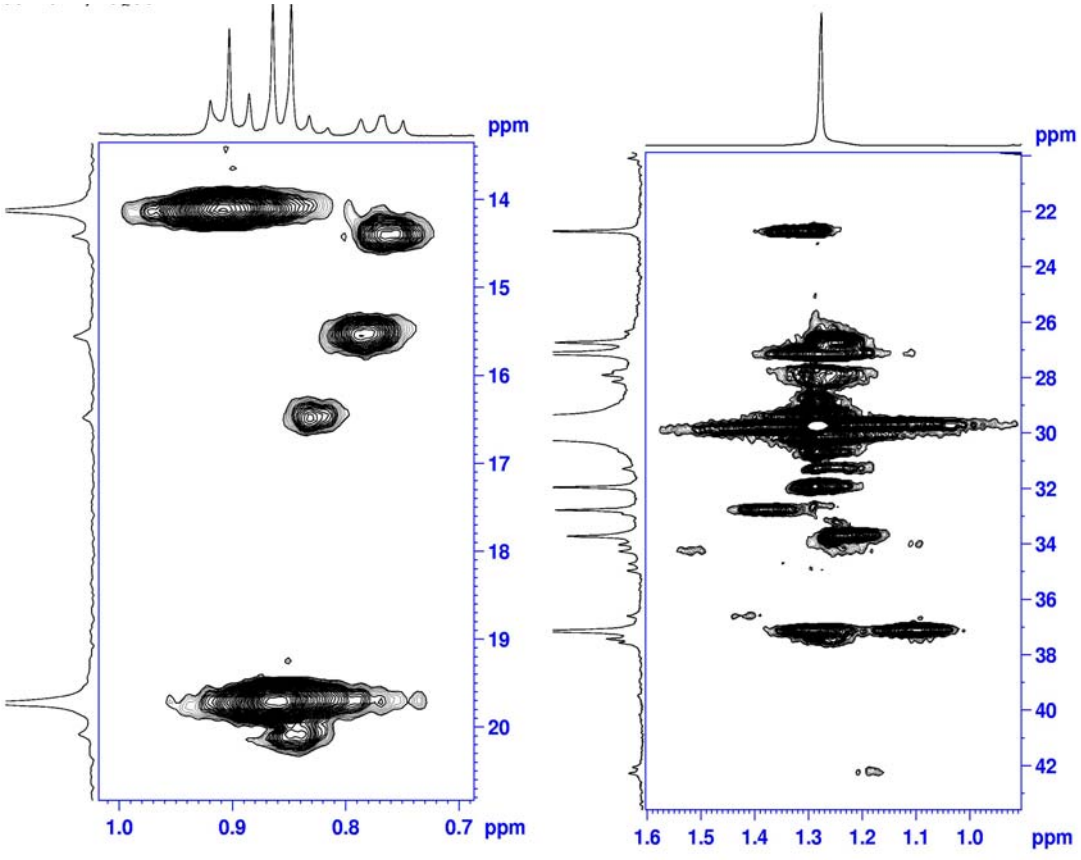

Figure 5.4. Quantitative 125.77 MHz ^{13}C HMQC spectrum of poly(octadecene-1)s synthesized using **1**/MAO

In order to assign the adjacent protons and carbons that are two or three bonds away an HMBC study was performed. From **Figure 5.5**, one can clearly see the correlation of the 42.30 ppm signal with the regio-irregular methyl at 16.50 ppm and the 37.50 ppm CH carbon with the methyl signal at 14.45 ppm.

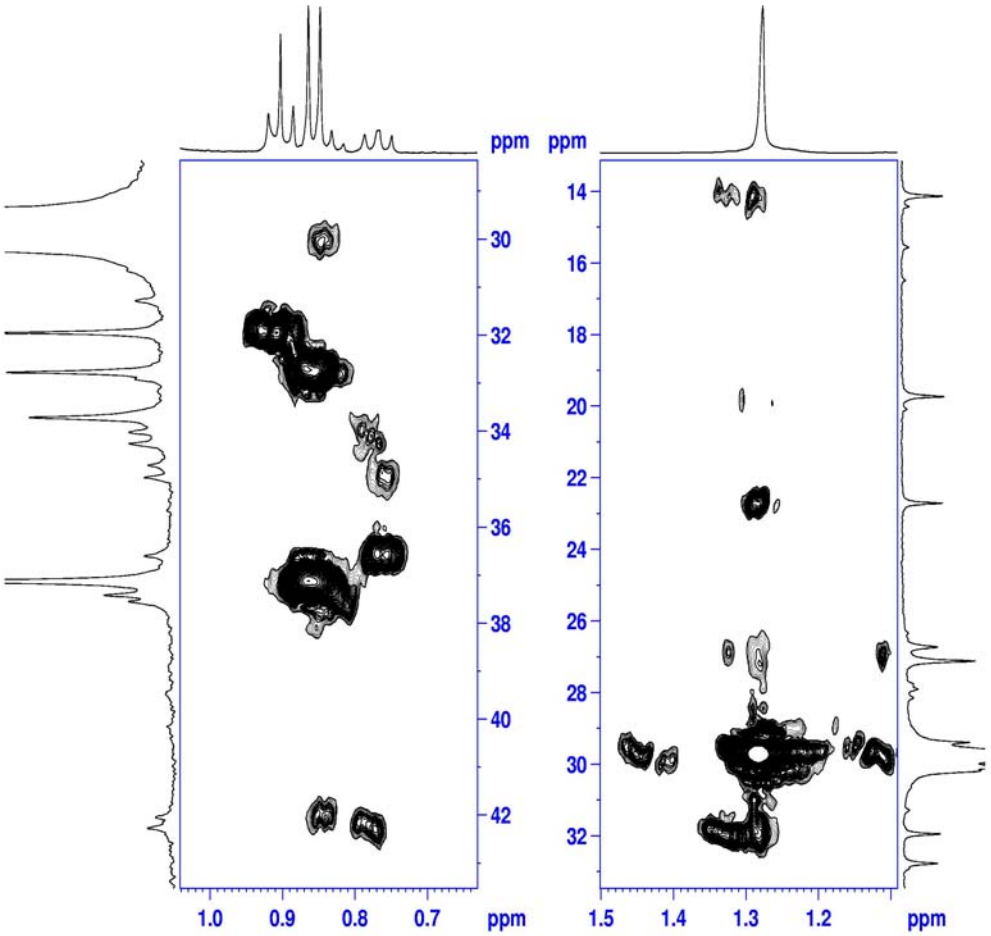

Figure 5.5. Quantitative 125.77 MHz ^{13}C HMBC spectrum of poly(octadecene-1)s synthesized using **1**/MAO

^{13}C NMR and DEPT of poly(octadecene-1) is shown in **Figure 5.6**. The detailed chemical shifts of all peaks have been assigned and are shown in **Table 5.3**. Based on correlation spectroscopic techniques, poly(octadecene-1)s prepared by **1**/MAO contain the following subunits. (i) Poly(octadecene-1), (ii) methyl branches with long methylene sequences in between branches, (iii) *meso* and *racemic* configurations of regio-irregular head-to-head methyl branches and (iv) polyethylene. The possible structural units in the poly(octadecene-1)s are shown in **Chart 5.1**.

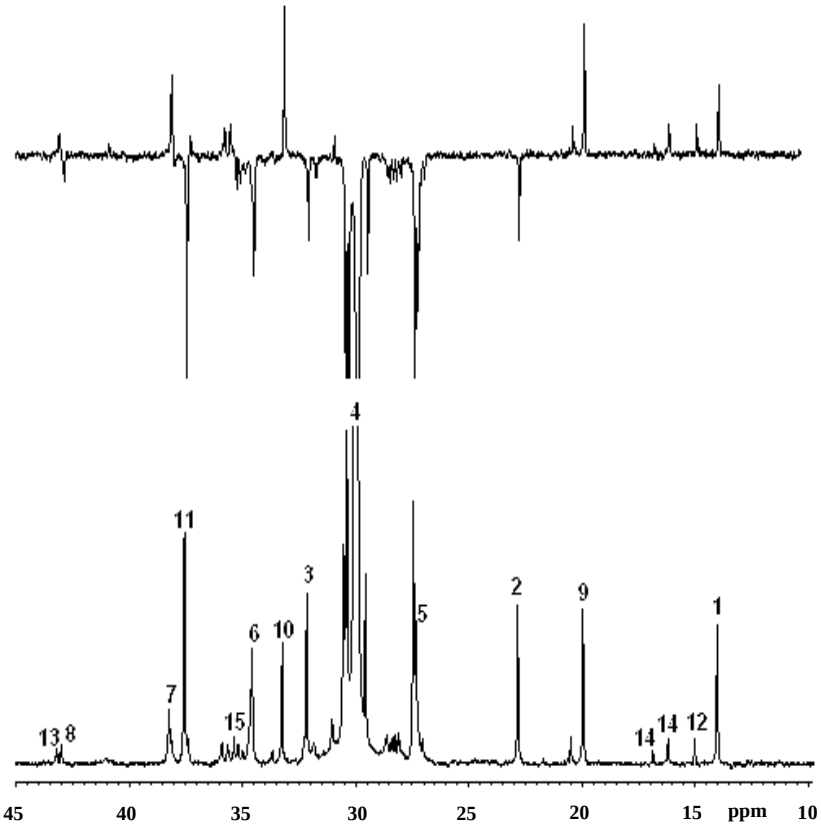

Figure 5.6. Quantitative 125.77 MHz ^{13}C and DEPT spectra of poly(octadecene-1)s synthesized using **1**/MAO

Chart 5.1. Structures of different subunits in poly(octadecene-1)s (**1**)

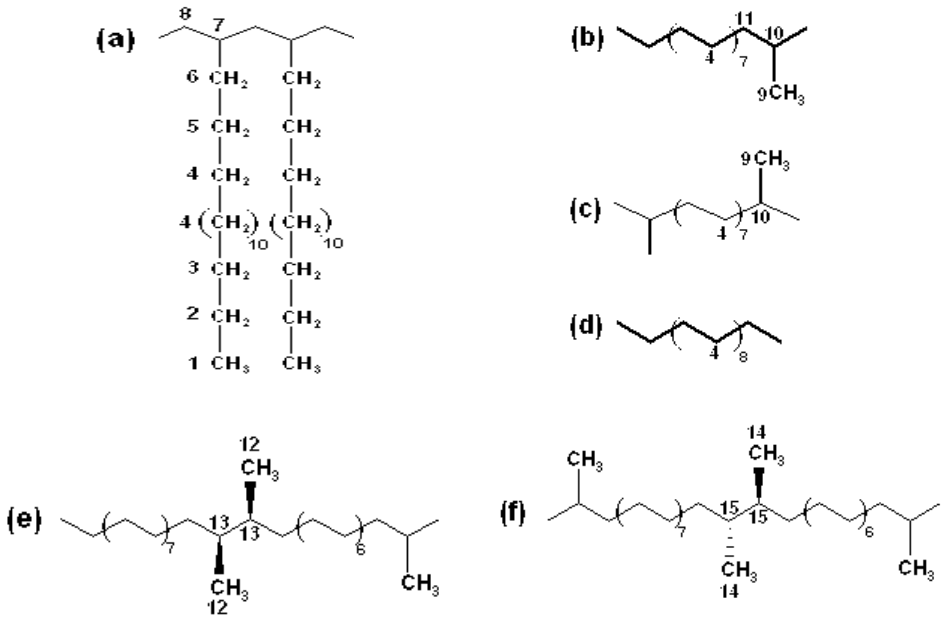

Table 5.3. Chemical shift assignments of poly(octadecene-1)s (**1**)

Peak No.	Chemical shift (ppm)	Assignment
1	14.04	$1B_{16}$
2	22.85	$2B_{16}$
3	32.17	$3B_{16}$
4	30.00	$S\delta^+$
5	27.32	$15B_{16}$
6	34.56	$16B_{16}$
7	38.21	Br_{16}
8	42.96	$\alpha B16$
9	19.96	$P\alpha^+\delta$
10	33.23	$T\delta^+$
11	37.54	$S\delta^+\alpha$
12	15.00	$r\text{-}P_{\delta\alpha\gamma\delta}$
13	43.16	$T\delta\alpha\gamma\delta$
14	16.21, 16.86	$m\text{-}P_{\delta\alpha\gamma\delta}$
15	36.21	$T_{\delta\alpha\gamma\delta}$

Quantitative ^{13}C NMR spectra of poly(octadecene-1)s prepared by **1**/MAO at different polymerization temperature are shown in **Figure 5.7**. The total number of branches per 1000 carbon atoms is 39, which is less than that predicted by theory, namely, 55. During polymerization β-hydride elimination followed by nickel migration leads to different types of enchainments[31-33], which is called "chain running" (or) "chain walking" (or) "chain straightening" behavior. Effect of polymerization temperature on chain running behavior during octadecene-1 polymerization using **1**/MAO and microstructure details is shown in **Table 5.4**. The mol % of hexadecyl branches and 2,ω-enchainment with polymerization temperature is depicted in **Figure 5.7**

Table 5.4. Branching distribution of poly(octadecene-1)s (**1**) using ^{13}C NMR

Entry	T (^oC)	DB[a]	1,2-insertion (mol %)			2,1-inserstion (mol %) [1,ω-enchainment]
			C_{16} branches	Isolated C_1 branches [2,ω-enchainment]	Regio-irregular C_1 branches [2,(ω-1)-enchainment]	
1	- 10	39	87	10	4	30
2	0	40	68	23	9	29
3	10	38	60	33	8	32
4	20	40	46	40	14	29
5	30	40	38	46	16	29
6	45	39	33	51	17	30
7	60	40	31	49	20	29

[a] Degree of branching per 1000 carbons

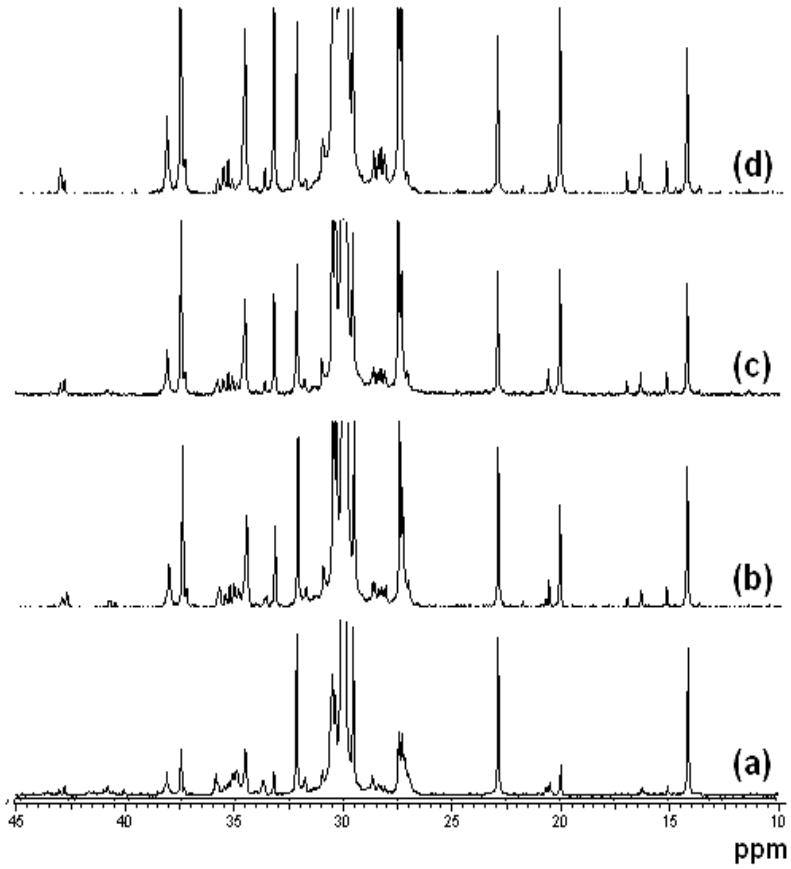

Figure 5.7. Quantitative 125.77 MHz quantitative ^{13}C NMR spectra of poly(octadecene-1)s synthesized using **1**/MAO at –10 ^oC (a), 0 ^oC (b), 30 ^oC (c) and 60 ^oC (d) in ODCB at 120 ^oC.

5.3.1.4. MECHANISTIC EXPLANATION

During polymerization insertion (1,2- or 2,1-) of octadecene-1 into nickel cation-carbon (primary or secondary) different type of branches and number of methylenes in the backbone are obtained. Possible mechanism for the formation of different sub units is shown in **Scheme 5.1**.

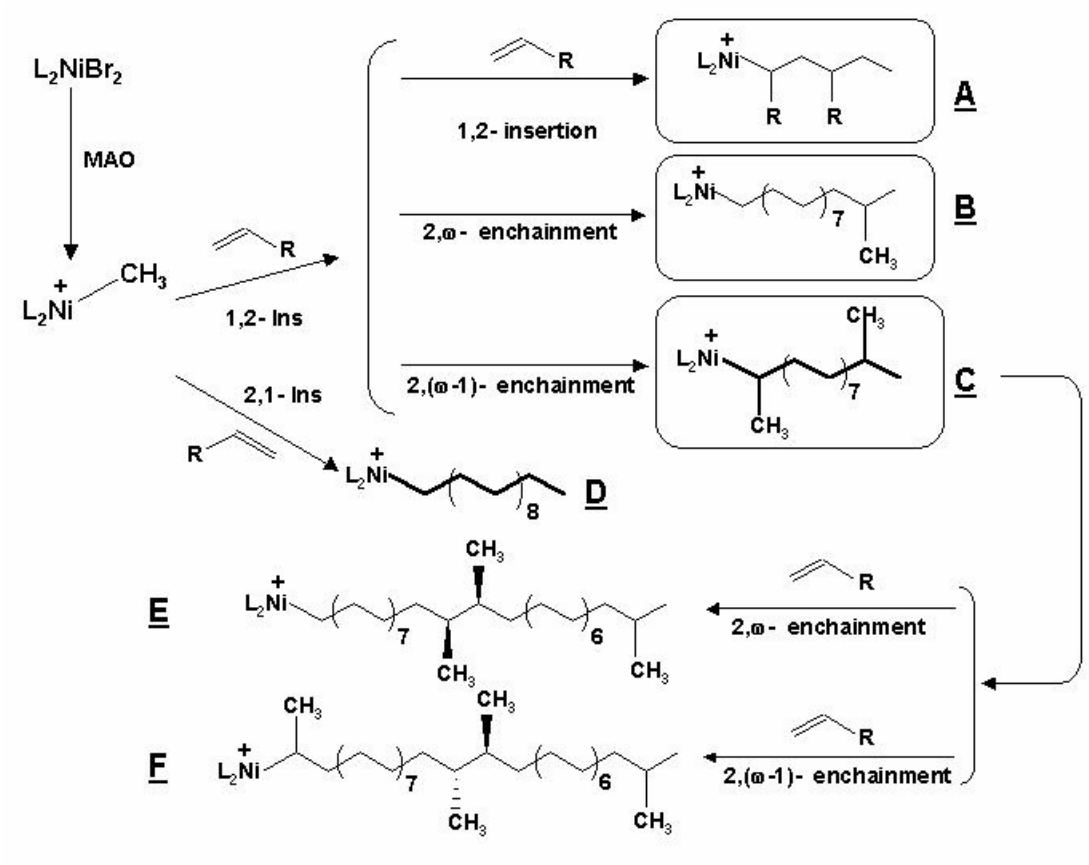

Scheme 5.1. Formation of different subunits with poly(octadecene-1)s

5.3.1.4.1. 1,2-insertion

1,2-insertion of octadecene-1 into nickel cation-carbon is the predominant mode of addition rather than 2,1-insertion. 1,2-insertion followed by with or without chain running leads to two different types of branching units (hexadecyl and isolated methyl) in the polymer chain, the amount of which varies with polymerization temperature.

5.3.1.4.1.1. Hexadecyl branches

1,2-insertion of octadecene-1 into nickel cation-primary carbon followed by similar insertion gives hexadecyl branches in the alternate carbons in the backbone. This leads to hexadecyl branches in the polymer backbone. This type of insertion is well known with other poly(olefin)s synthesized by Group IV transition metal catalysts[20,34,35]. The chemical shift of terminal CH_3 (i.e., 'ω' carbon) is observed at 14 ppm and the corresponding '(ω-1)' carbon of methylene peak arising at 23.23 ppm. In **Scheme 5.1**, route A depicts the formation of hexadecyl branches.

Polymerization temperature profoundly influences the formation of hexadecyl branches. Occurrence of these types of branches is more predominant at lower temperature. This is due to the fact that insertion of octadecene-1 units is much faster than nickel migration at low polymerization temperatures. The mol % of hexadecyl branches varies from 31 to 87 mol % as the temperature is reduced from 60 to -10 ^{o}C.

5.3.1.4.1.2. Methyl branches (2,ω- enchainment)

1,2-insertion of octadecene-1 and subsequent β-hydride elimination followed by nickel migration upto terminal carbon ('ω') gives isolated methyl branches in the polymer chain. This contributes 16 methylenes in the backbone and is classified as 2,ω-enchainment[1,3,36]. **Scheme 5.1**; Route B shows the formation of isolated methyl branches. Repetition of these insertion and 2,ω-enchainment leads to isolated methyl branches with 16 methylenes in the backbone. These units in the polymer chain are similar to ethylene-propylene type of copolymers and characteristic chemical shifts are observed in the range 20-22 ppm.

The probability of this mode of enchainment is faster at higher polymerization temperatures. 2,ω-enchainment varies from 10 to 50 mol % when polymerization temperature is increased from -10 to 60 ^{o}C.

5.3.1.4.1.3. Regio-irregular methyl branches

Insertion of octadecene-1 in a 1,2-fashion followed by series of β-hydride elimination upto (ω-1) carbon generates methyl branch in the polymer chain with metal-secondary carbon bond. Further insertion onto metal-secondary carbon followed by

similar steps gives rise to regio-irregular head-to-head (*meso* and *rac*) methyl branches. Insertion of linear α-olefins into metal cation-carbon (secondary) of early and late transition metal catalysts[34-36] is not favorable due to steric and electronic factors resulting in dormant sites.

The rate of octadecene-1 insertion into metal cation-carbon (secondary) bond is higher at higher polymerization temperature and varies from 4 to 20 mol %. The characteristic chemical shift is observed at 14-17 ppm. The region 14-16 ppm is due to *meso*- and region 16-17 ppm is due to *rac*- head-to-head methyl branch. The observed chemical shift values of regio-irregular head-to-head methyl branches (*meso* and *rac*) exactly correspond to the reported values of regio-irregular head-to-head methyl branches in poly(propylene)s[37,38].

5.3.1.4.2. 2,1-insertion

2,1-insertion of octadecene-1 into nickel cation-carbon bond followed by a series of β-hydride eliminations and subsequent nickel migration upto ω carbon leads to 16 methylenes in the backbone. This process is called 1,ω-enchainment (in present case it is 1,16-enchainment), resulting in less number of branches per 1000 carbon atoms than predicted by theory. Characteristic chemical shift values of these methylenes are observed at 30 ppm. Extent of 1,16-enchainment appears to be independent of polymerization temperature.

5.3.1.5. Melting and crystallization behavior

The melting and crystallization behavior of poly(octadecene-1)s synthesized using **catalyst 1**/MAO was studied using differential scanning calorimetry (DSC). Appearance of multiple melting and crystallization transitions in poly(octadecene-1)s is due to presence of various blocks of crystallizable regions which arise from various subunits i.e., hexadecyl branches, ethylene-propylene copolymers with different levels of methylene sequences as well as presence of regio-irregular head-to-head methyl branches in the polymer chain. The distributions of various blocks of crystallizable methylene regions vary with polymerization temperatures, which are reflected in the thermal properties of polymers. The results are shown in **Table 5.5**. **Figure 5.8** depicts the first and second heating endotherms. During the first heating (from -40 ^{o}C to 120 ^{o}C), the

samples show two distinct broad melting endotherms (1 and 2). During cooling (from 120 ^{o}C to -40 ^{o}C), the samples were annealed at 60, 50, 40 and 30 ^{o}C for 20 min. Upon second heating, the second broad melting endotherm at 60 ^{o}C is split into three melting peaks namely 2a, 2b and 2c (49 ^{o}C, 59 ^{o}C and 70 ^{o}C, respectively). This arises on account of melting of different sequences of methylenes. The following section describes the consequence of chain running behavior on multiple melting endotherms.

Table 5.5. Differential scanning calorimetry of poly(octadecene-1)s (**1**)

Entry	Polymerization Temperature (^{o}C)	Melting temperature[a] (^{o}C)				Crystallization temperature (T_c, ^{o}C)
		Tm_1	Tm_2	Tm_3	Tm_4	
1	- 10	40	47	---	---	20, 38
2	0	37	47	58	---	33, 44
3	10	38	49	59	70	29, 45
4	20	38	48	59	70	29, 47
5	30	40	50	60	70	51
6	45	40	51	61	70	52
7	60	40	50	60	70	54

[a] Second heating endotherms after isothermal crystallization

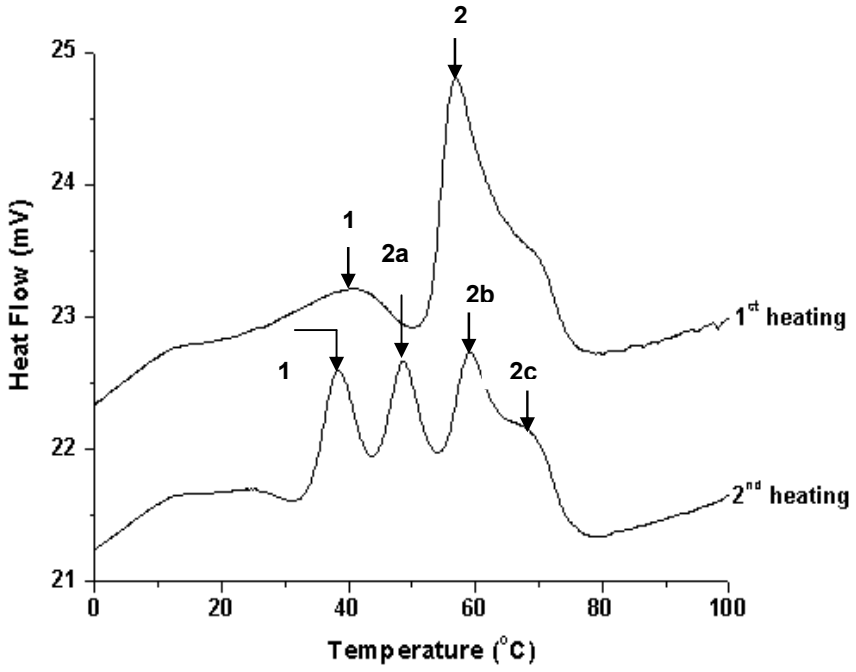

Figure 5.8. DSC of poly(octadecene-1)s [1st and 2nd heating] synthesized by **1**/MAO

5.3.1.5.1. Side chain crystallization

Poly(octadecene-1)s synthesized at lower polymerization temperatures contain high mol % of hexadecyl branches. The T_m of hexadecyl branches is observed at 41 ^oC and during cooling it undergoes crystallization at 35 ^oC. It is noticed from **Figure 5.9** that the heat of fusion (ΔH, J/g) of this particular peak increases as the polymerization temperature decreases. This is indicative of the fact that blocks of hexadecyl branches are more predominant at lower polymerization temperatures. A distinct crystallization peak

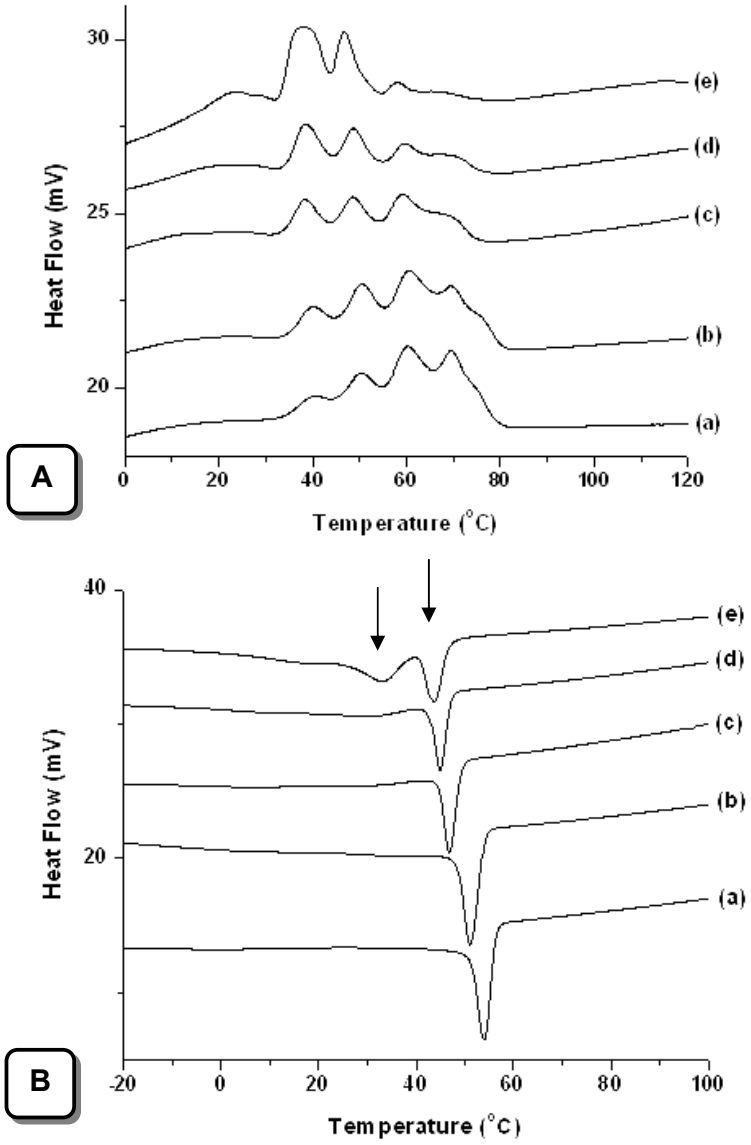

Figure 5.9. DSC of poly(octadecene-1)s (**1**) synthesized at different temperatures, (a) T = 60 ^oC, (b) T = 30 ^oC, (c) T = 20 ^oC, (d) T = 10 ^oC and (e) T = 0 ^oC. [A] melting endotherm (T_m), [B] crystalline transition (T_c).

for hexadecyl branches is observed at 33 ^{o}C in poly(octadecene-1)s containing 68 mol % of hexadecyl branches. This feature implies that the 1,2-insertion of octadecene-1 in nickel-carbon bond is faster than chain running at lower polymerization temperatures. The observed melting and crystallization temperatures are similar to that observed for poly(octadecene-1)s synthesized using Cp_2ZrCl_2 which exhibits a T_m at 40 ^{o}C and crystallizes at 35 ^{o}C. It is generally agreed that side chain crystallization occurs when the length of the side chain exceeds eight-carbon atoms[7]. Poly(ethylene-*co*-eicosene-1) containing more than 5.9 mol % (39 wt %) eicosene-1 showed an additional melting point at 45 ^{o}C which was assigned to side chain crystallinity[15].

5.3.1.5.2. Main chain crystallization

Polymerization of octadecene-1 with different types of enchainments leads to variable methylenes sequences in the backbone. This results in the increase in intrinsic chain rigidity, chain length and concentrations of chemical regio, or stereo defects along the polymer backbone which, in turn, affect the lamellae thickness and has great influence on melting and crystallization behavior. Possibility of different types of crystalline regions is directly dependent on the frequency of methylene sequences. In poly(octadecene-1)s synthesized using **catalyst 1**, the frequency of methylene sequence varies with polymerization temperature. At higher polymerization temperature 2,ω-enchainment is high, which leads large number of methylenes in the backbone.

Presence of different frequency levels of methylene sequences in the backbone influences the multiple melting behavior of polymer. Poly(octadecene-1)s synthesized by **catalyst 1**/MAO showed two broad endotherm. These broad endotherms arise due to melting of different degrees of crystalline portions in the polymer chain, which are resulting from variable sequence lengths of methylene in the backbone as well as the side chain. Similarly, in the case of poly(ethylene-*co*-octene-1) under isothermal crystallization conditions multiple endotherms were observed, which are attributed to the distribution of ethylene sequences or chain segments that can participate in the crystallization and annealing at a particular temperature[39-43]. Therefore a detailed study on the effect of methylene sequence length on melting and crystallization behavior of poly(octadecene-1)s was performed to gain a better understanding of this phenomena.

The melting and crystallization behavior of various poly(octadecene-1) samples were studied by initially heating from -40 to 120 ^{o}C at 10 ^{o}C/min. Two broad distinct melting endotherms are observed starting from 24 to 53 ^{o}C (ΔH = 6 J/g) and 53 to 75 ^{o}C (ΔH = 24 J/g) (Entry 4, **Table 5.5**). Upon cooling from the melt, the crystallization process is characterized by a sharp high temperature exotherm followed immediately by a broad exotherm extending to much lower temperature. The two distinct crystallization peaks are observed at 47 and 29 ^{o}C during the cooling of sample from 120 to -40 ^{o}C at 10 ^{o}C/min. The crystallization peak observed at 47 ^{o}C is very sharp than the one observed at 29 ^{o}C. The first crystallization peak (47 ^{o}C) is exclusively arising from the crystallization of long methylene sequences of polymer backbone. The DSC data of the poly(octadecene-1)s samples support the presence of different microstructures depending on the order of monomer enchainment.

Thus, the higher T_m observed with poly(octadecene-1)s is related to the longer crystallizable sequences of methylene units whereas the lower T_m is associated with the crystallization of hexadecyl branches. To the best of our knowledge, this is first instance, wherein, the melting transitions of both the backbone and side chain crystallizable group is observed. This observation also implies that the side chain hexadecyl branches cannot cocrystallize with the backbone poly(methylene) groups.

5.3.1.6. Dynamic Mechanical Thermal Analysis (DMTA)

Glass transition temperature (T_g) is one of fundamental properties of polymer materials. Influence of comonomer incorporation and stereochemical irregularities on melting temperature (T_m) and crystallization behavior is clear in the literature[18]. However, there is a dearth of scientific information about the influence of branching density and type of branching on T_g. Poly(octadecene-1)s synthesized using **catalyst 1** at different polymerization temperature results in a similar number of branches per 1000 carbon atoms with a distribution of side chain branch length with differing lengths of methylene sequences in the backbone. These different types of crystallization block (i.e., variable levels of methylene sequences in the backbone and hexadecyl branches) and crystalline-amorphous interfacial regions is expected to have an influence on the glass transition temperature.

With a view to study these dependencies in greater detail we examined the β-transition and γ-relaxation behavior of poly(octadecene-1)s synthesized using **catalyst 1** at various temp. using DMTA. These results are shown in **Table 5.6** and in **Figure 5.10**.

Table 5.6. DMTA of poly(octadecene-1)s (**1**)

Entry	Polymerization temperature (°C)	β-relaxation		γ-transition		Modulus (MPa)
		Temp. (°C)	Intensity	Temp. (°C)	Intensity	
1	0	1	0.0730	- 120	0.0474	1.110
2	10	2	0.1049	- 122	0.0584	1.965
3	20	4	0.1217	- 121	0.0442	2.157
4	30	5	0.1328	- 121	0.0480	2.297
5	45	2	0.1453	- 118	0.0506	2.041
6	60	5	0.1300	- 120	0.0433	2.631

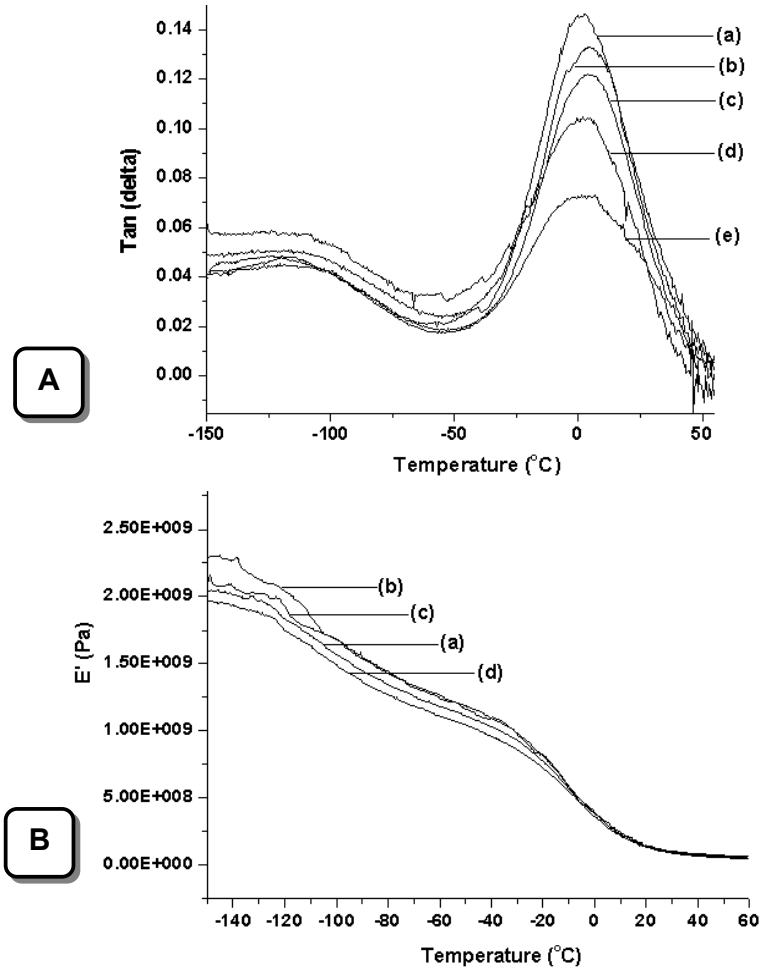

Figure 5.10. DMA of poly(octadecene-1)s (**1**) synthesized at different temperatures: [A] time vs tan (delta), [B] time vs E′ (modulus, MPa). (a) 45 °C, (b) 30 °C, (c) 20 °C, (d) 10 °C and (e) 0 °C

5.3.1.6.1. Branching point vs intensity of β-transition

All poly(octadecene-1)s synthesized using **catalyst 1** has similar *β*-transition (i.e., T_g) at 3 ± 2 °C. As discussed in Section 5.3.1.3, the percent formation of isolated methyl as well as regioirregular head-to-head (*meso* and *rac*-) methyl branches are high at higher polymerization temperatures. *β*-transition has been attributed to segmental motions occurring within the crystal-amorphous interfacial regions. In is observed that poly(octadecene-1) synthesized at lower polymerization temperature has higher intensity of β-transition which tends to decrease with increase of polymerization temperature. As the methine branch points in combination with methyl (C_1) branches rather than C_{16} branches increases the intensity of *β*-transition also increases. Intensity of *β*-transition is strongly influenced by the isolated methyl and regioirregular methyl branches. In the case of ethylene-propylene copolymers[9], higher content of propylene exhibit high values of tan(δ) because there is no residual crystallinity. The intensity of *β*-transition is strongly influenced by the presence of EP of isolated methyl branches and regioirregular methyl branch points in the polymer chain. Mandelkern and coworkers reported that *β*-transition is attributed to the segmental motions occurring within the crystal-amorphous interfacial regions[44]. The trend of tan(*δ*) with respect to methyl branches of EP and regioirregular arrangement is shown in **Figure 5.11**. The intensity of the *β*-transition substantially increases with an increase in methyl (C_1) branches.

To summarize, (i) poly(octadecene-1)s having the same number of total branches per 1000 carbon atoms with variable percentage of C_{16} and C_1 branches has similar T_g. (ii) The intensity of *β*-transition is highly dependent on the type of branches connected to the methine branch point. Methine branch point connected to large number of methyl branches exhibit highest intensity of *β*-transition. We conclude that the branch point consisting of methyl (isolated and regioirregular) branches are the major contributors to the amorphous zones.

Poly(octadecene-1)s synthesized using **1**/MAO at different temperatures has similar *γ*-relaxation at -120 ± 2 °C with negligible change in intensity. This region is independent of changes in the type of branch content. *γ*-relaxation involves the motion of a short segment of amorphous region in addition to the reorientation of loose chain ends within the crystalline and amorphous fraction[45,46]. The modulus increases from 1.110 MPa to

2.631 MPa with increase 2,ω-enchainment from 23 mol % to 49 mol % (**Table 5.6**, entry 1 and 6).

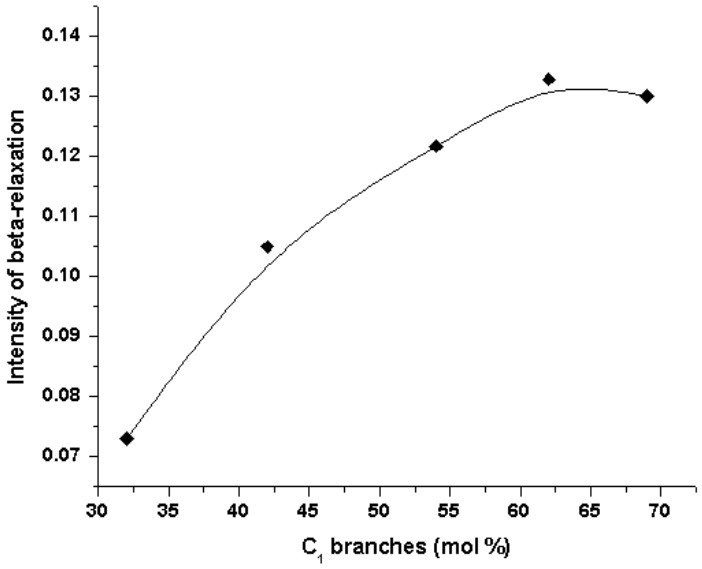

Figure 5.11. Percent C_1 branches (isolated EP + regioirregular methyl) vs intensity of β-relaxation

5.3.2. EFFECT OF MONOMER CONCENTRATION ON STRUCTURE AND PROPERTIES OF POLY(OCTADECENE-1)S (1)

Homopolymerization of octadecene-1 using **1**/MAO was performed at different monomer concentrations. The experimental results are shown in **Table 5.7**. The effect of monomer concentration on nickel migration during polymerization and resulting properties of polymers are discussed using NMR, DSC and DMTA.

Table 5.7. Synthesis and characterization of poly(octadecene-1)s by **1**/MAO using GPC

Entry	Octadecene-1 (M)	Yield (g)	TOF[a] (per h)	GPC		
				M_n	M_w	MWD
1	0.06	0.46	107	48,800	76,500	1.57
2	0.12	0.88	205	110,800	162,000	1.46
3	0.19	1.33	310	154,900	225,300	1.45
4	0.50	1.32	308	198,500	337,700	1.70

Reaction conditions: (octadecene-1+ toluene) = 50 mL, catalyst = 3.4×10^{-4} M, MAO = 3.4×10^{-2} M, temperature = 60 ^{o}C, time = 1h

5.3.2.1. TOF and GPC

Turn over frequency (TOF, per h) increases with increasing monomer concentration and levels off beyond 0.5 M. The molecular weight of poly(octadecene-1) also levels off beyond 0.5 M. Both these observations can be attributed to the reduced monomer diffusion on account of increased solution viscosity. **Figure 5.12** depicts the effect of monomer concentration on number average molecular weight (M_n).

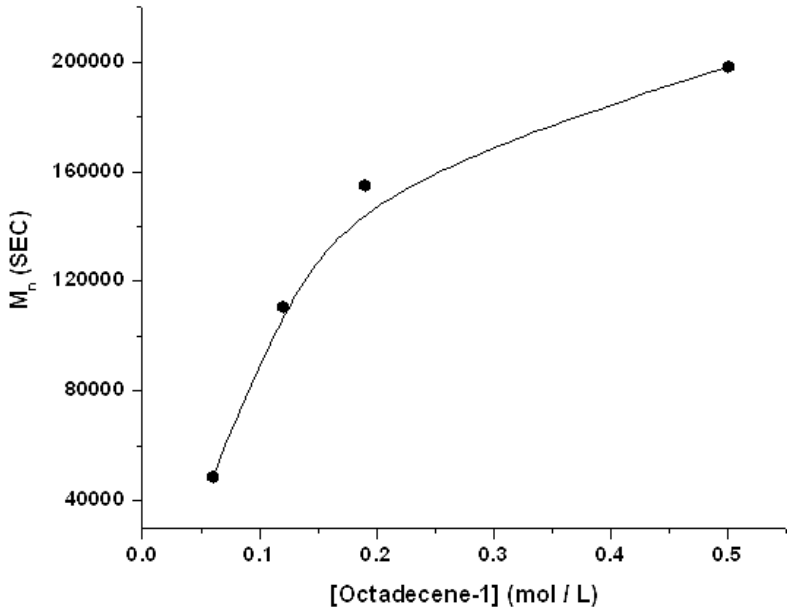

Figure 5.12. Dependence of $\overline{M}n$ on octadecene-1 concentration

5.3.2.2. ^{1}H NMR

^{1}H NMR spectra of poly(octadecene-1)s synthesized using **1**/MAO at different monomer concentrations are similar. Presence of hexadecyl and different types of methyl branches can be seen at 0.88 and 0.77 ppm respectively. These values are similar to what has been discussed in Section 3.4.1 for poly(octadecene-1)s prepared at different temperatures. The relative ratio of hexadecyl and methyl branches is similar for all concentration levels of monomer. The percent 1,ω- and 2,ω-enchainments are also same.

5.3.2.3. ^{13}C NMR

^{13}C NMR spectra of poly(octadecene-1)s prepared at different monomer concentrations are also similar. The percent content of hexadecyl, isolated methyl and

regioirregular head-to-head (*meso* and *rac*-) methyl branches is same for all monomer concentrations. This shows that the relative competition between insertion of monomer units and chain running mechanism is not affected by concentration of monomer. The overall percent chain running i.e., 2,ω- and 1,ω-enchainments do not also have a dependence on monomer concentration. The details of chemical shifts and reaction mechanism during polymerization are discussed in **Table 5.3** and Section 3.4 respectively.

Table 5.8. Branching distribution of poly(octadecene-1)s using ^{13}C NMR

Entry	Octadecene-1 (M)	DB[a]	1,2- insertion (mol %)			2,1- insertion (mol %) [1,ω- enchainment][b]
				2,ω- enchainment		
			C_{16} branches	Isolated C_1 branches	Regio-irregular C_1 branches	
1	0.06	nd	nd	nd	nd	nd
2	0.12	40	32	49	20	29
3	0.19	39	32	49	20	30
4	0.50	39	33	48	19	30

[a] Degree of branching per 1000 carbons; [b] 1,ω- enchainment = 1,16- enchainment = full chain running; nd = not determined

5.3.2.4. DSC

Melting and crystallization behavior of poly(octadecene-1)s synthesized at variable concentration levels using **1**/MAO were investigated using DSC. The results are shown in **Table 5.10**. **Figure 5.13** indicates the second heating endotherm of poly(octadecene-1)s after cooling from 120 ^{o}C to -40 ^{o}C and subsequent annealing at 60 ^{o}C, 50 ^{o}C, 40 ^{o}C and 30 ^{o}C for 20 min. The total enthalpy of fusion was calculated for the second heating melting endotherm.

Multiple melting peaks are observed for all poly(octadecene-1)s. This arising due to different types of crystallizable regions in the polymer chain. Poly(octadecene-1)s synthesized at lower monomer concentrations has higher melting point and crystallizes faster than poly(octadecene-1) prepared at higher monomer concentration. This indicates that the length of methylene sequences is larger for poly(octadecene-1)s synthesized at

lower monomer concentrations. At lower monomer concentrations nickel has a tendency to migrate in either of the following two ways leading to highly crystallizable methylenes sequences in the backbone. (i) Subsequent 2,ω-enchainments leads to long methylene sequences or (ii) repeated 1,ω-enchainments gives 36 methylenes (for 2 repeat enchainments) in the backbone.

Table 5.9. DSC of poly(octadecene-1)s (**1**)

Entry	Octadecene-1 (M)	Melting temperature (^oC)				Crystallization temperature (T_c, ^oC)
		Tm_1	Tm_2	Tm_3	Tm_4	
1	0.06	40	50	59	70	59
2	0.12	39	50	60	70	57
3	0.19	41	52	61	72	56
4	0.50	40	50	62	---	51

5.3.2.5. DMTA

The β, γ-transitions and modulus of poly(octadecene-1)s synthesized at different monomer concentration are shown in **Table 5.10** along with analysis in **Figure 5.14**. The T_g of all poly(octadecene-1)s is same with significant change in intensity of β-relaxation. The intensity is high for poly(octadecene-1) synthesized at lower monomer concentrations than at higher monomer concentrations. Which indicates the blocks of crystallizable long methylene sequences is high. The frequency of crystallizable methylene sequences is less, which reveals in high intensity of β-relaxation of poly(octadecene-1)s prepared at higher monomer concentrations. The γ-transition and modulus of all poly(octadecene-1)s is same.

Table 5.10. DMTA of poly(octadecene-1)s (**1**)

Entry	Octadecene-1 (M)	β-relaxation		γ-transition		Modulus (MPa)
		Temp. (^oC)	Intensity	Temp. (^oC)	Intensity	
1	0.06	4	0.1110	- 120	0.04391	2.004
2	0.12	3	0.1227	- 120	0.05284	2.083
3	0.19	3	0.1251	- 120	0.03929	1.897
4	0.50	7	0.1433	-120	0.04123	1.806

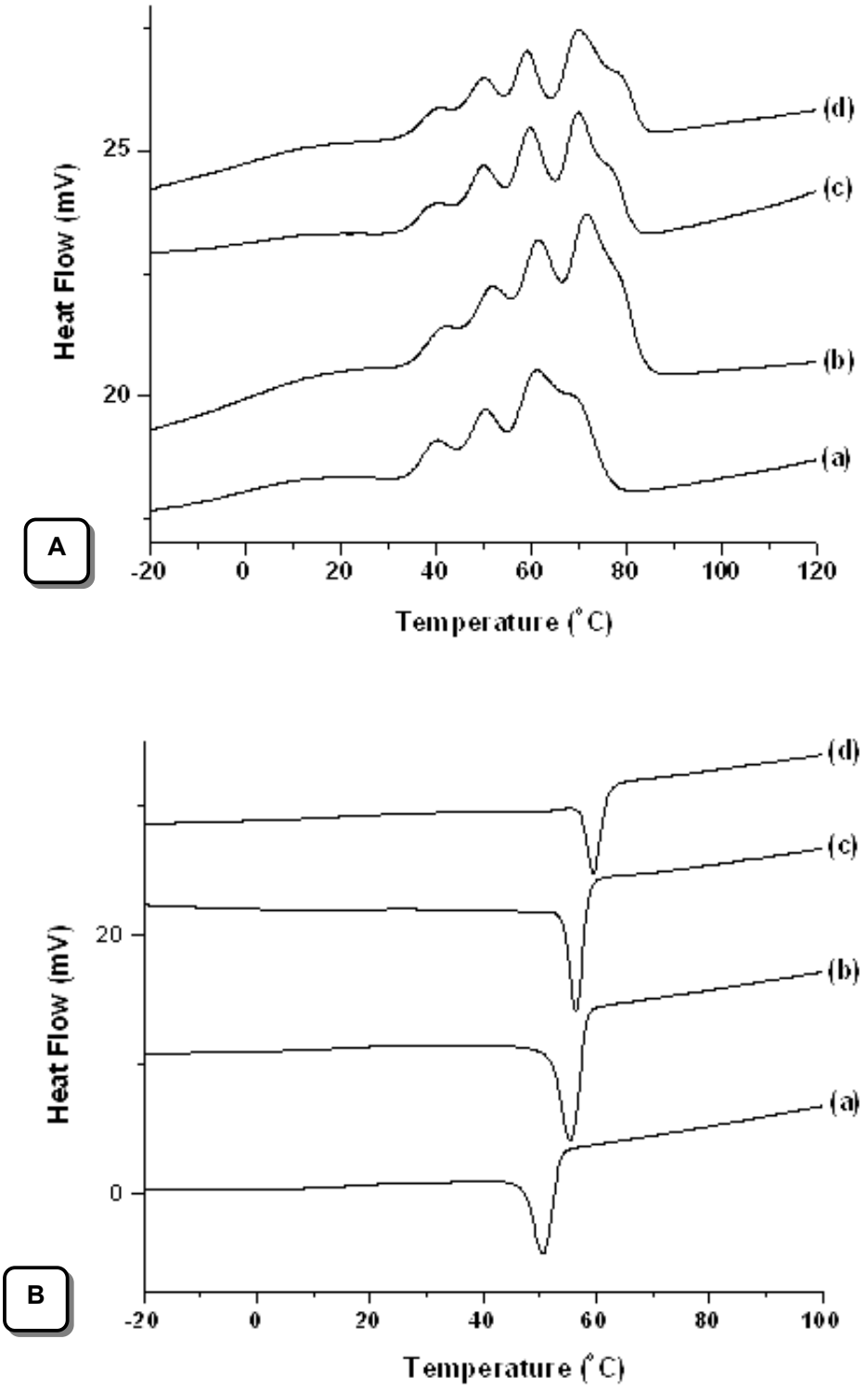

Figure 5.13. DSC of poly(octadecene-1)s (**1**) synthesized at different monomer concentrations, (a) [M] = 0.5 M, (b) [M] = 0.19 M, (c) [M] = 0.12 M and (d) [M] = 0.06 M. [A] melting endotherm (T_m), [B] crystalline transition (T_c).

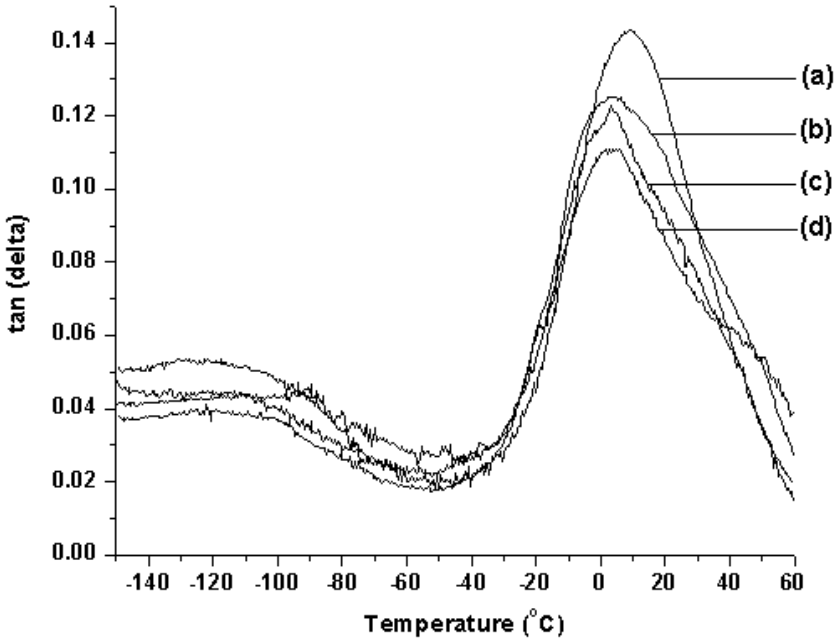

Figure 5.14. tan(delta) curves of poly(octadecene-1)s (**1**) synthesized at different monomer concentrations; (a) [M] = 0.50 M, (b) [M] = 0.19 M, (c) [M] = 0.12 M, (d) [M] = 0.06 M.

5.3.3. Synthesis and Characterization of poly(decene-1)s, poly(dodecene-1)s, poly(tetradecene-1)s, poly(hexadecene-1)s, poly(octadecene-1)s

The objective of this study was to understand the nickel migration during polymerization with different linear α-olefins (i.e., C_nH_{2n}, n = 8, 10, 12, 14 and 16). The consequences of chain running behavior on resulting polymers were examined by ^1H and ^{13}C NMR, GPC, DSC, DMTA. The polymerization data and GPC results are shown in **Table 5.11**.

Table 5.11. Synthesis and characterization of poly(*α*-olefin)s by **1**/MAO using GPC

Entry	*α*-Olefin	Yield (g)	TOF[a] (per h)	GPC		
				M_n	M_w	MWD
1	Decene-1	1.44	605	120,200	178,500	1.48
2	Dodecene-1	1.73	605	136,500	204,400	1.49
3	Tetradecene-1	1.90	570	186,500	282,600	1.51
4	Hexadecene-1	1.70	445	176,100	276,000	1.57
5	Octadecene-1	1.50	350	109,500	196,000	1.79

Reaction conditions: [α-olefin] = 0.25 M, (*α*-olefin+toluene) = 50 mL, catalyst = $3.4x10^{-4}$ M, MAO = $3.4x10^{-2}$ M, temperature = 60 °C, time = 1h

5.3.3.1. TOF and GPC

The TOF and number average molecular weight increases from poly(decene-1)s to poly(tetradecene-1)s and decreases thereafter in case of poly(hexadecene-1)s and poly(octadecene-1)s. This is probably due increasing strong steric hindrance associated with higher α-olefins for active site coordination. Similar trend has been noticed for poly(α-olefin)s synthesized using metallocene catalysts[7]. The molecular weight distribution of all poly(α-olefin)s is approximately same, i.e. 1.5. GPC chromatogram of poly(α-olefin)s are shown in **Figure 5.15**.

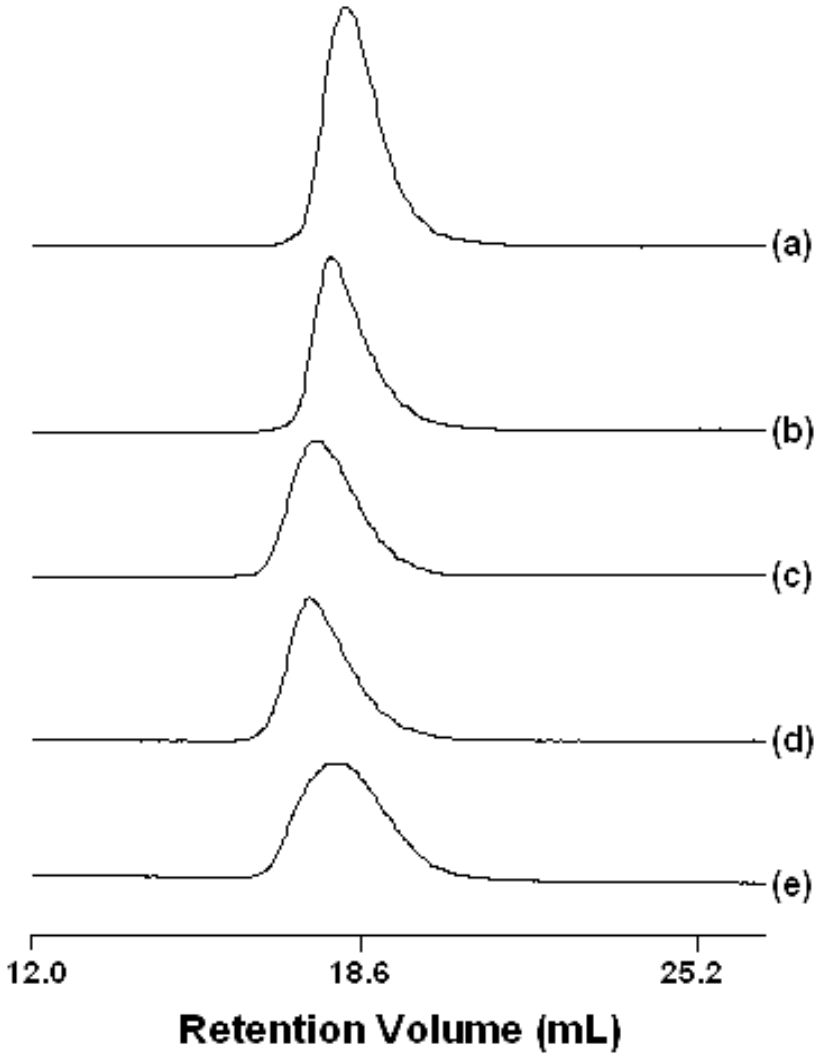

Figure 5.15. GPC of (a) poly(decene-1)s, (b) poly(dodecene-1)s, (c) poly(teredecene-1)s, (d) poly(hexadecene-1)s and (e) poly(octadecene-1)s synthesized by **1**/MAO

5.3.3.2. ^{1}H NMR

^{1}H NMR spectra of poly(decene-1)s, poly(dodecene-1)s, poly(teredecene-1)s, poly(hexadecene-1)s and poly(octadecene-1)s synthesized by **catalyst 1**/MAO is shown in **Figure 5.16**. The chemical shifts observed at 0.88 and 0.74 ppm is due to long chain and methyl branches respectively. The relative ratio of long chain: methyl branches tend to increase from poly(decene-1)s to poly(octadecene-1)s. This signifies that chain running is more predominant with linear α-olefins with smaller carbon numbers.

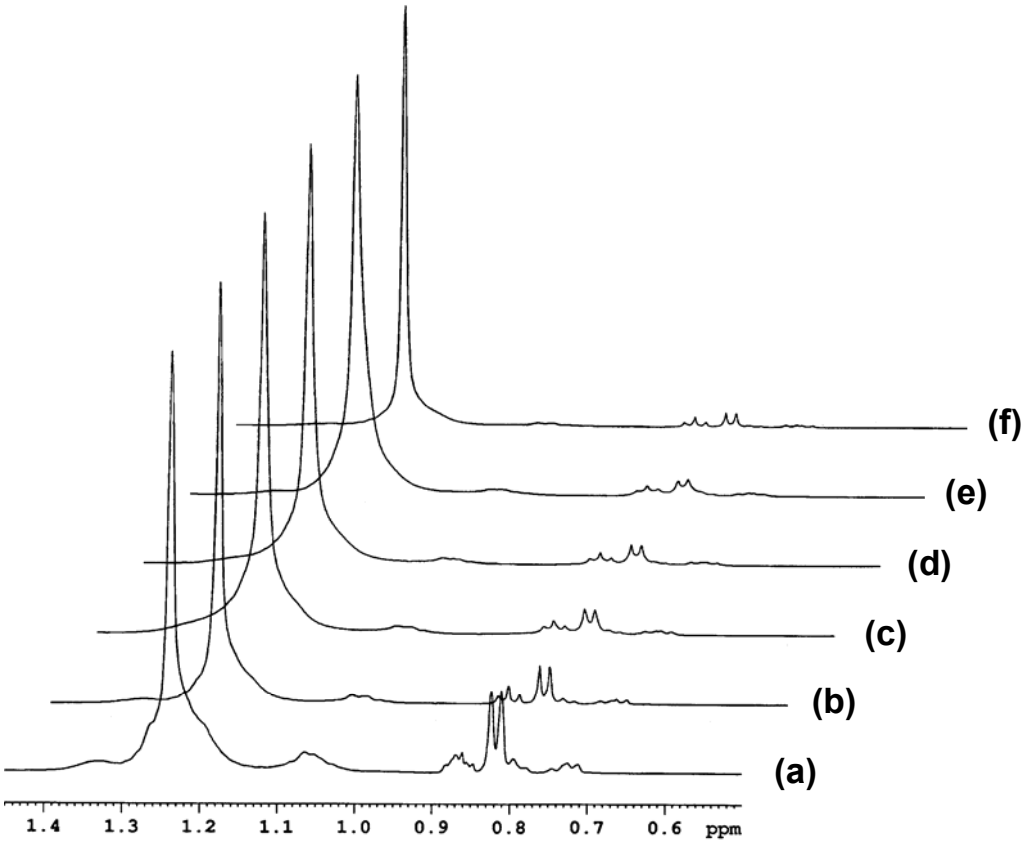

Figure 5.16. ^{1}H NMR spectra of (a) poly(hexene-1)s, (b) poly(decene-1)s, (c) poly(dodecene-1)s, (d) poly(tetradecene-1)s, (e) poly(hexadecene-1)s and (f) poly(octadecene-1)

5.3.3.3. ^{13}C NMR

Quantitative ^{13}C NMR spectra of poly(decene-1)s, poly(dodecene-1)s, poly(tetradecene-1)s, poly(hexadecene-1)s and poly(octadecene-1)s are shown in **Figure 5.17**. Frequency of 1,ω- and 2,ω-enchainments during different α-olefin polymerization and resulting microstructure analysis is also shown in **Table 5.12**.

Table 5.12. Branching distribution of poly(α-olefin)s (**1**)

Entry	Polymer	DB[a]	1,2-insertion (mol %)			2,1-inserstion (mol %) [1,ω-enchainment]
				2,ω-enchainment		
			C_n branches	Isolated C_1 branches	Regio-irregular C_1 branches	
1	Poly(hexene-1)	117	22	65	15	39
2	Poly(decene-1)	67	26	57	17	33
3	Poly(tetradecene-1)	49	31	51	18	31
4	Poly(hexadecene-1)	44	32	51	18	30
5	Poly(octadecene-1)	40	31	49	20	29

[a] Degree of branches per 1000 carbons

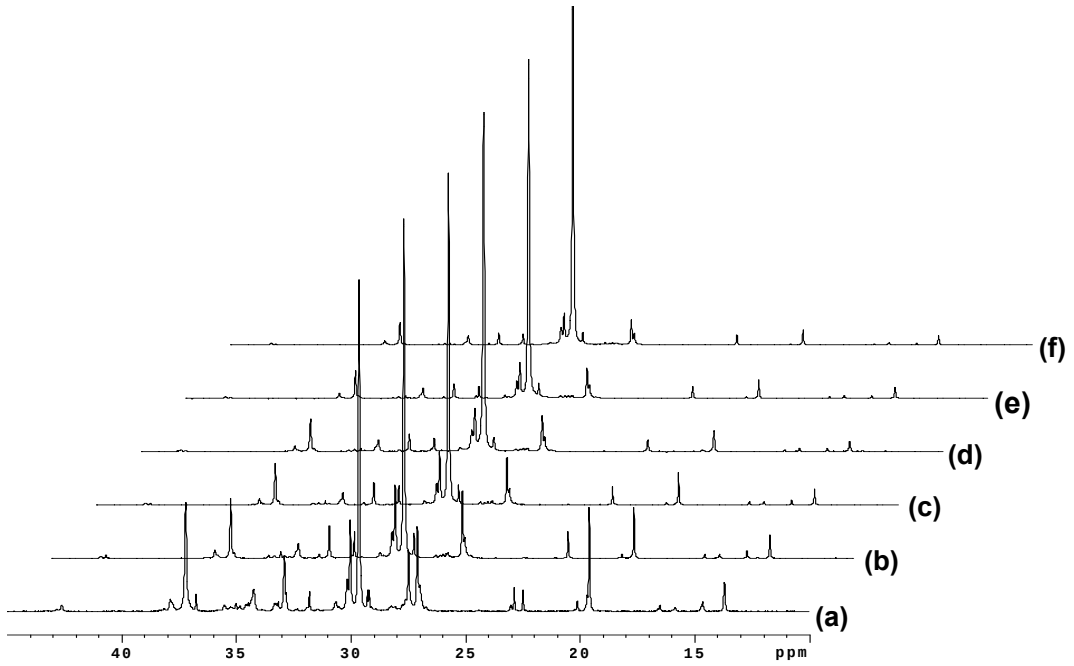

Figure 5.17. ^{13}C NMR spectra of poly(hexene-1)s (a), poly(decene-1)s (b), poly(dodecene-1)s (c), poly(tetradecene-1)s (d), poly(hexadecene-1)s (e) and poly(octadecene-1)s (f)

5.3.3.4. 1,2- and 2,1- insertion

During polymerization, the extent of 1,2- and 2,1-insertion into nickel cation-carbon (primary/secondary) and subsequence nickel migration depends on the carbon number of α-olefin. 1,2-insertion is the predominant mode of addition for all α-olefins.

Microstructure of poly(α-olefin)s prepared by **1**/MAO has additional features not seen in similar polymers prepared using early transition metal catalysts[7].

The consequence of chain running on different poly(α-olefin)s microstructure is as follows, (i) 1,2-insertion is a more favorable mode of addition compared to 2,1-insertion. (ii) 1,2-insertion of α-olefin into nickel-carbon bond followed by 2,ω-enchainment leads to isolated methyl branches. (iii) rate of nickel migration is relatively faster than the insertion of α-olefin to the nickel cation-carbon bond. (iv) 2,ω-enchainment increases as follows: poly(hexene-1) > poly(decene-1) > poly(dodecene-1) > poly(tetradecene-1) > poly(hexadecene-1) > poly(octadecene-1) and (v) 2,1-insertion followed by nickel migration upto to the terminal carbon leads to 1,ω-enchainment which is an unique feature of **catalyst 1**. Extent of 1,ω-enchainment is high (Table 5.13, entry 1) in the case of hexene-1 polymerization. However, 1,ω-enchainment decreases with an increase in the side chain length of α-olefin. 1,ω-enchainment increases in the order: poly(hexene-1) > poly(decene-1) > poly(dodecene-1) > poly(tetradecene-1) > poly(hexadecene-1) > poly(octadecene-1). **Figure 5.18** indicates the relationship of side chain length of α-olefin to 2,ω- and 1,ω-enchainment.

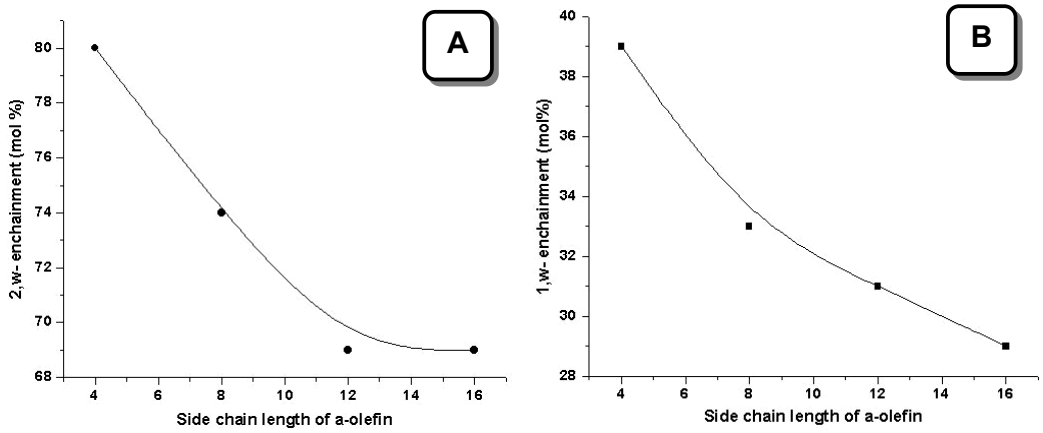

Figure 5.18. Side chain length of α-olefin vs 2,ω- (A) and 1,ω-enchainment (B)

5.3.3.4.1. Insertion of α-olefin into nickel-secondary carbon

The length of the side chain of α-olefin has a significant influence on the occurrence of regioirregular head-to-head methyl branches (*meso* and *rac*-). The tendency of decene-1 insertion into nickel cation-carbon (secondary) is high as compared

to octadecene-1. As the side chain length of α-olefin increases, increased steric hindrance retards the rate of insertion into nickel cation-carbon (secondary) bond. In the case of propylene, occasionally 2,1 units isomerize to 3,1 units, which is indicative of the dormant nature of 2,1-insertion product[25,47]. Regioirregular methyl branches are found to be higher in poly(decene-1) and lower for poly(octadecene-1)s. To the best of our knowledge, there has been no prior report in the literature of the observation of regioirregular methyl branches in case of higher α-olefins.

5.3.3.5. DSC

Poly(α-olefin)s having carbon numbers 10 to 18 prepared by using **1**/MAO were examined by DSC. The consequence of 2,ω- and 1,ω- enchainments on melting and crystallization temperatures are shown in **Table 5.13**. The number of methylene sequences in the backbone as well as the side chain varies with chain running. The resulting melting and crystallization behavior of poly(α-olefin)s are therefore dependent on chain running.

Table 5.13. DSC of poly(α-olefin)s (**1**)

Entry	Poly(α-olefin)	Melting temperature (^{o}C)			Crystallization temperature (T_c, ^{o}C)
		Tm_1	Tm_2	Tm_3	
1	Poly(decene-1)	25	42	---	27
2	Poly(dodecene-1	40	51	---	36
3	Poly(tetradecene-1)	40	50	60	nd
4	Poly(hexadecene-1)	40	50	61	49
5	Poly(octadecene-1)	40	50	62	51

5.3.3.5.1. Effect of chain running on melting and crystallization behavior of poly(α-olefin)s (1)

Chain running leads to different types of branches with different frequency levels of methylene sequences. This, in turn, leads to variable blocks of methylene sequences causing multiple melting behaviors in these polymers. The length of crystallizable methylene sequences is not uniform due to the diversity of chain branches and the distribution of crystal thickness. This causes a broadening of the melting peak. In higher α-olefins polymerization, namely, dodecene-1, tetradecene-1, hexadecene-1 and

octadecene-1, one observes the presence of larger number of methylenes in the backbone and side chain when compared to lower α-olefins (decene-1). Consequently, poly(octadecene-1) shows a high T_m. Decrease in side chain length of α-olefin results in progressively lower T_m. Similar behavior is also observed on crystallization temperature of poly(olefin)s which varies as follows: poly(octadecene-1)s > poly(hexadecene-1)s > poly(tetradecene-1)s > poly(dodecene-1)s > poly(decene-1)s. **Figure 5.19** depicts the effect of side chain length of α-olefin on the crystallization temperature of poly(α-olefin)s.

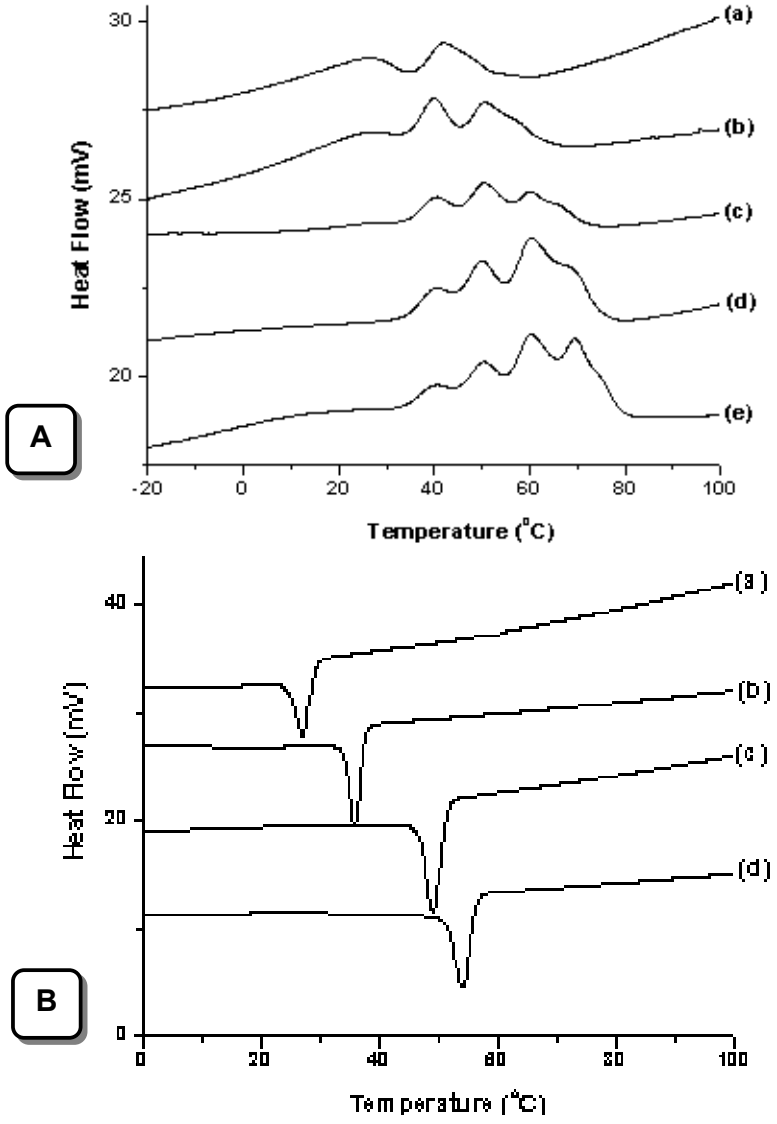

Figure 5.19. DSC of (a) poly(decene-1)s, (b) poly(dodecene-1)s, (c) poly(tetradecene-1)s, (d) poly(hexadecene-1)s and poly(octadecene-1)s synthesized using **1**/MAO, [A] melting temperature (T_m), [B] crystallization temperature (T_c)

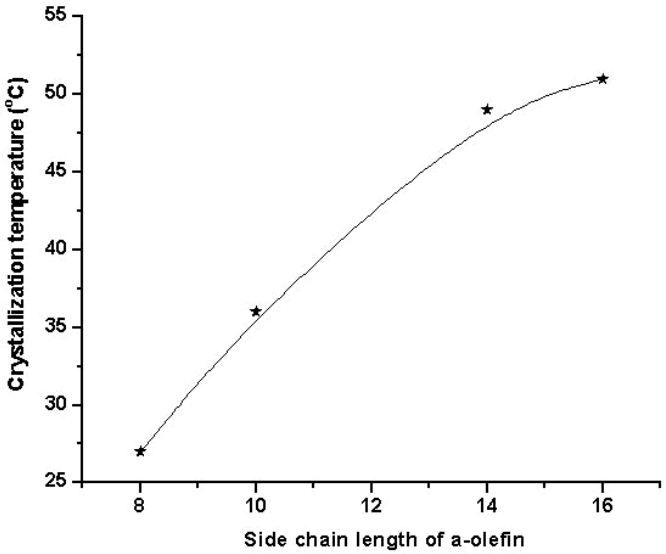

Figure 5.20. Effect of side chain length of α-olefin upon crystallization temperature (T_c)

5.3.3.6. DMTA

Polymer chains precipitate from solution at a given temperature as a function of the length of their longest methylene sequences. The understating of interchain compositional heterogeneity has been shown to be of extreme importance to explain the mechanical behavior of polymers. During α-olefin polymerization β-hydride elimination followed by nickel migration leads to less number of branches than expected. The glass transition temperature is mainly dependent on the length of the n-alkyl branches[8]. DMTA analysis of various poly(α-olefin)s is depicted in **Figure 5.21**.

Table 5.14. Dynamic mechanical thermal analysis of poly(α-olefin)s (**1**)

Entry	Polymer	β-relaxation		γ-transition		Modulus (MPa)
		Temp. (°C)	Intensity	Temp. (°C)	Intensity	
1	Poly(decene-1)	- 25	0.2887	- 118	0.04677	2.244
2	Poly(dodecene-1)	- 19	0.2362	- 117	0.04319	2.335
3	Poly(tetradecene-1)	- 11	0.1961	- 118	0.04392	1.875
4	Poly(hexadecene-1)	- 1	0.1611	- 119	0.04433	2.163
5	Poly(octadecene-1)	5	0.1300	- 120	0.04330	2.0125

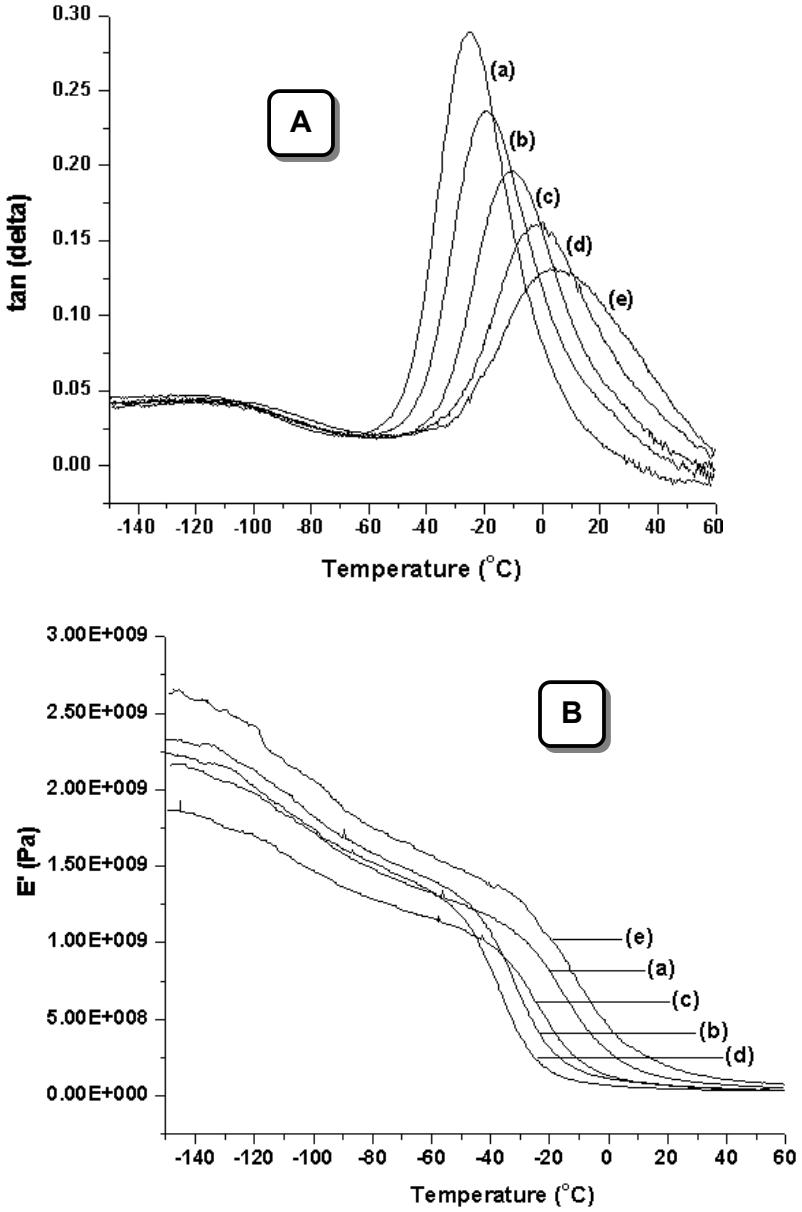

Figure 5.21. DMA of (a) poly(decene-1) (**1**), (b) poly(dodecene-1) (**1**), (c) poly(tetradecene-1) (**1**), (d) poly(hexadecene-1) (**1**) and (e) poly(octadecene-1) (**1**): [A] β-relaxation and γ-transition, [B] E' (modulus, MPa)

5.3.3.6.1. T_g vs degree of branching

The present study deals with copolymers containing isolated methyl branches of different sequence levels of methylenes with regioirregular head-to-head methyl branches and variable lengths of side chain branches on T_g. T_g is low for poly(octadecene-1) and tends to increase for polymers derived from lower α-olefins having carbon number < 18. T_g is dependent on isolated methyl branches and regio-

irregular head-to-head methyl linkages rather than on the chain length of the branch. The higher intensity of β-relaxation in the case of poly(decene-1) is due to large interfacial interaction of amorphous and crystalline regions which is due to higher content of isolated and regio-irregular methyl branches. This implies that the enhanced intensity of the β-peak is probably a consequence of an increase in amorphous volume due to branching rather than the branches themselves.

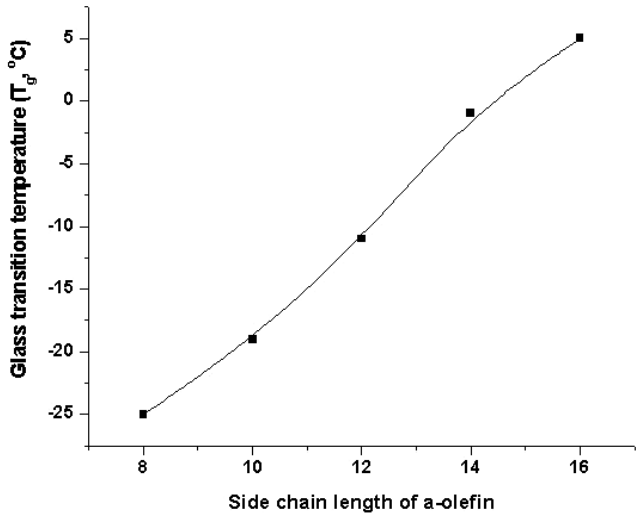

Figure 5.22. Dependence of side chain length of α-olefin on T_g

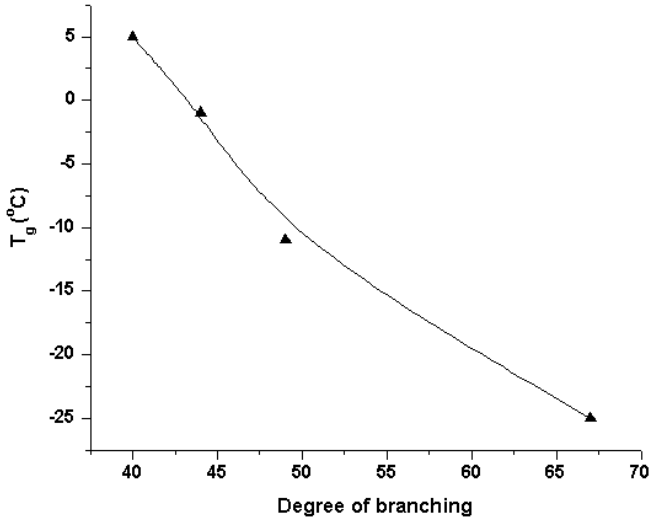

Figure 5.23. Dependence of degree of branching on T_g

SUMMARY AND CONCLUSIONS

Several conclusions cab be drawn on the effect of chain running on poly(α-olefin)s properties. These are summarized below

(1) Poly(octadecene-1)s synthesized at different temperatures have similar number of branches. However, the nature of branches is different. 1,2-insertion of monomer followed by 2,ω-enchainment is faster than the insertion of another monomer at higher polymerization temperatures. This leads to large number of methylene sequences in between methyl branches. The frequency level of these methylene sequences leads to multiple melting peaks in the case of poly(octadecene-1)s. Simultaneous crystallization of side chain as well as main chain is observed for poly(octadecene-1)s synthesized at lower polymerization temperatures, wherein, the concentration of hexadecyl branches is high. T_g's of all poly(octadecene-1)s are similar. Higher intensity of β-transition is observed when methine branch points are connected to large number of C_1 (methyl) branches.

(2) Poly(octadecene-1)s synthesized at different monomer concentrations have similar number of branches. Subsequent 2,ω- or 1,ω-enchainments are frequent at lower concentrations. This gives rise to long sequences of methylenes in the backbone. The resulting polymer, thus, has higher melting and crystallization temperature. T_g is similar for all polymers. The intensity of β-transition is high for poly(octadecene-1) synthesized at higher monomer concentrations.

(3) The extent of chain running (i.e., 2,ω-, 1,ω-enchainments) decreases with increase in the carbon number of α-olefins. Insertion of lower α-olefin into nickel cations-carbon (secondary) is much faster due to relatively less steric hinderance. The long methylene sequences in the backbone as well as in the side chain in case of poly(α-olefin)s with carbon number > 12 results in higher melting and crystallization temperatures. Presence of large number of short chain branches results in more amorphous nature of polymer in case of poly(decene-1)s, exhibiting lower T_g and a higher intensity of β-transition. The trend of T_g and intensity of β-transition of poly(α-

olefin)s is as follows: poly(decene-1) > poly(dodecene-1) > poly(tetradecene-1) > poly(hexadecene-1) > poly(octadecene-1).

5.4. REFERENCES

(1) Mohring, V. M.; Fink, G. *Angew. Chem., Int. Ed. Engl.* **1985,** *11*, 24.

(2) Killian, C. M.; Tempel, D. J.; Johnson, L. K.; Brookhart, M. *J. Am. Chem. Soc.* **1996**, *118*, 11664.

(3) McCord, E. F.; McLain, S. J.; Nelson, L. T. J.; Arthur, S. D.; Coughlin, E. B.; Ittel, S. D.; Johnson, L. K.; Tempel, D.; Killian, C. M.; Brookhart, M. *Macromolecules* **2001**, *34*, 362.

(4) Landis, C. R.; Sillars, D. R.; Batterton, J. M. *J. Am. Chem. Soc.* **2004**, *126*, 8890.

(5) Busico, V.; Cipullo, R.; Romanelli, V.; Ronca, S.; Togrou, M. *J. Am. Chem. Soc.* **2005**, *127*, 1608.

(6) Simon, L. C.; de Souza, R. F.; Soares, J. B. P.; Mauler, R. S. *Polymer* **2001,** *42,* 4885.

(7) Henschke, O.; Knorr, J.; Arnold, M. *J. Macromol. Sci., Pure Appl. Chem.* **1998,** *A35,* 473.

(8) Mader, D.; Heinemann, J.; Walter, P.; Mulhaupt, R. *Macromolecules* **2000**, *33,* 1254.

(9) Alamo, R.; Domszy, R.; Mandelkern, L. *J. Phy. Chem.* **1984**, *88,* 6587.

(10) Shirayama, K.; Kita, S.; Watabe, H. *Makromol. Chem.* **1972**, *151,* 97.

(11) Mandelkern, L. *Polymer* **1985**, *17,* 337.

(12) Bassi, I. W.; Corradini, P.; Fagherazzi, G.; Valvassori, A. *Eur. Polym. J.* **1970**, *6,* 709.

(13) Guerra, G.; Ruiz de Ballesteros, O.; Venditto, V.; Galimberti, M.; Sartori, F.; Pucciariello, R. *J. Polym. Sci., Part B: Polym. Phys.* **1997**, *37,* 1095.

(14) Ruiz de Ballesteros, O.; Auriemma, F.; Guerra, G.; Corradini, P. *Macromolecules* **1996**, *29,* 7141.

(15) Walter, P.; Trinkle, S.; Suhm, J.; Mader, D.; Friedrich, C.; Mulhaupt, R. *Macromol. Chem. Phys.* **2000,** *201,* 604.

(16) Hung, J.; Cole, A. P.; Waymouth, R. M. *Macromolecules* **2003**, *36,* 2454.

(17) Guerra, G.; Galimberti, M.; Piemontesi, F.; Ruiz de Ballesteros, O. *J. Am. Chem. Soc.* **2002**, *124*, 1566.

(18) Suhm, J.; Heinemann, J.; Thomann, Y.; Thomann, R.; Maier, R. D.; Schleis, T.; Okuda, J.; Kressler, J.; Mulhaupt, R. *J. Mater. Chem.* **1998**, *8,* 553.

(19) Johnson, L. K.; Killian, C. M.; Brookhart, M. *J. Am. Chem. Soc.* **1995**, *117,* 6414.

(20) Chien, J. C. W.; Babu, G. N.; Newmark, R. A. *Macromolecules* **1994,** *27,* 3383.

(21) Brintzinger, H. H.; Fischer, D.; Mulhaupt, R.; Rieger, B.; Waymouth, R. M. *Angew. Chem., Int. Ed. Engl*. **1995**, *34*, 1143.

(22) Asakura, T.; Demura, M.; Yamamoto, K. *Polymer* **1987**, *28*, 1037.

(23) Busico, V.; Cipullo, R.; Chadwick, J. C.; Modder, J. F.; Sudmeijer, O. *Macromolecules* **1994**, *27,* 7538.

(24) Busico, V.; Cipullo, R. *Prog. Polym. Sci.* **2001,** *26,* 443.

(25) Zambelli, A.; Locatelli, P.; Bajo, G.; Bovey, F. A. *Macromolecules* **1975,** *8,* 687.

(26) Soga, K.; Shiobo, T.; Takemura, S.; Kaminsky, W. *Makromol. Chem. Rapid Commun.* **1987**, *8,* 305.

(27) Cheng, H. N.; Ewen, J. A. *Makromol. Chem.* **1989**, *190,* 1931.

(28) Busico, V.; Cipullo, R.; Talarico, G.; Caporaso, L. *Macromolecules* **1998**, *31,* 2387.

(29) Grassi, A.; Zambelli, A.; Resconi, L.; Albizzati, E. Mazzocchi, R. *Macromolecules* **1988**, *21,* 617.

(30) Zambelli, A.; Sessa, I.; Grisi, F.; Fusco, R.; Accommazzi, P. *Macromol. Chem. Rapid Commun.* **2001**, *22,* 297.

(31) Ittel, S. D.; Johnson, L. K.; Brookhart, M. *Chem. Rev.* **1999**, *99*, 1169.

(32) Stefan, M. *Angew. Chem., Int. Ed.* **2001**, *40,* 534.

(33) Guan, Z.; Cotts, P. M.; McCord, E. F.; McLain, S. J.; *Science* **1999**, *283,* 2059.

(34) Brintzinger, H. H.; Fisher, D.; Mulhaupt, R.; Rieger, B.; Waymouth, R. M. *Angew. Chem., Int. Ed. Engl.* **1995**, *34,* 1143.

(35) Imanishi, Y.; Naga, N. *Prog. Polym. Sci.* **2001,** *26,* 1147.

(36) Schubbe, R.; Angermund, K.; Fink, G.; Goddard, R. *Macromol. Chem. Phys.* **1995,** *196,* 467.

(37) Carman, C. J.; Tarpley, A. R.; Goldstein, J. H. *Macromolecules* **1973**, *6,* 719.

(38) Asakura, T.; Nishiyama, Y.; Doi, Y. *Macromolecules* **1987**, *20,* 616.

(39) Alizadeh, A.; Richardson, L.; Xu, J.; McCartney, S.; Marand, H.; Cheung, Y. W.; Chum, S. *Macromolecules* **1999**, *32,* 6221.

(40) Alamo, R. G.; Mandelkern, L. *Thermochim. Acta.* **1994**, *238,* 155.

(41) Crist, B.; Claudio, E. S. *Macromolecules* **1999**, *32,* 8945.

(42) Almo, R. G.; Mandelkern, L. *Macromolecules* **1991**, *24,* 6480.

(43) Li, Y.; Yvonne.; Akpalu, A. *Marcomolecules* **2004**, *37,* 7265.

(44) Popli, R.; Glotin, M.; Mandelkern, L. *J. Polym. Sci., Part B: Polym. Phys. Ed.* **1984**, *22,* 407.

(45) Khannan, Y. P.; Turi, E. A.; Taylor, T. J.; Vickroy, V. V.; Abbott, R. F. *Macromolecules* **1985**, *18,*1302.

(46) Gray, R. W.; McCrum, N. G. *Polym.Sci. Part A2*. **1969**, *7,*1329.

(47) Resconi, L.; Cavallo, L.; Fait, A.; Piemontesi, F. *Chem. Rev.* **2000**, *100,*1253.

CHAPTER 6

KINETICS OF HEXENE-1 POLYMERIZATION USING [(*N*, *N'*-DIISOPROPYLBENZENE)2,3-(1,8-NAPTHYL)-1,4-DIAZABUTADIENE]DIBROMONICKEL / METHYLALUMINOXANE CATALYST SYSTEM

6.1. INTRODUCTION

Metallocene catalysts are composed of essentially single type of catalytically active center, which produces very uniform homopolymers with narrow molecular mass distributions, reflected by polydispersities of $M_w/M_n \approx 2$[1-3]. In contrast to Ziegler-Natta and metallocenes, late transition metal catalysts in combination of methylaluminoxane give poly(α-olefin)s with low molecular weight due to rapid β-hydride elimination and transfer reactions which compete with chain growth[4-11].

In 1995, Brookhart and coworkers reported synthesis of late transition metal catalysts (nickel and palladium-α-diimine) for olefin polymerization. These catalyst systems in combination with methylaluminoxane (MAO) produce high molecular weight polymer with a unique microstructure which is different from Ziegler (or) metallocene based poly(α-olefin)s. The rate of transfer (or) termination reactions are presumed to be suppressed by an increase in the axial steric bulk of these catalysts resulting in higher molecular weight poly(olefin)s[12-16].

Living polymerization methods are of great interest for the synthesis of polymers with precisely controlled molecular weight, narrow molecular weight distributions, end functionalized polymers and well defined block copolymers. Whereas tremendous advances in living/controlled polymerization have been made by using anionic, cationic, and radical based polymerization, there are relatively fewer examples of living olefin polymerization using transition metal catalysts. The following criteria have been generally recognized as necessary to characterize a polymerization as "living polymerization". (1) A linear first-order time-conversion plot, (2) linear increase of $\bar{M}_n$ with number-average degree of polymerization of the polymer increases linearly as a function of conversion, (3) faster rate of initiation compared to rates of propagation, (4) absence of termination reactions, (5) narrow molecular weight distributions, (6) polymerization should proceed to complete monomer consumption and (7) chain growth continues upon successive addition of the same monomer or a new monomer capable of propagating from the same active chain end.

Although several reports of "living" polymerization of α-olefins are available in the literature, rarely they have been subjected to rigorous scrutiny to ensure that necessary and sufficient conditions of "livingness" are met. Very often, isolated information such as narrow molecular weight distribution or linear dependence of $\bar{M}_n$

with conversion (or) yield and molecular weights determination by gel permeation chromatography with reference to poly(styrene) standards have been used as evidence of "livingness" of α-olefin polymerization[13,17-24]. There are no kinetic results reported in the literature to unequivocally establish the absence of termination and transfer reactions.

Therefore, we undertook a critical evaluation of the kinetics of hexene-1 polymerization by [(*N*,*N*′-diisopropylbenzene)-2,3-(1,8-napthly)-1,4-diazabutadiene] dibromonickel (**1**)/methylaluminoxane catalyst system. Experiments were performed at varying catalyst and monomer concentrations in the temperature range of -10 to 35 ^{o}C, with a view to characterize the kinetics parameters for propagation and transfer reactions.

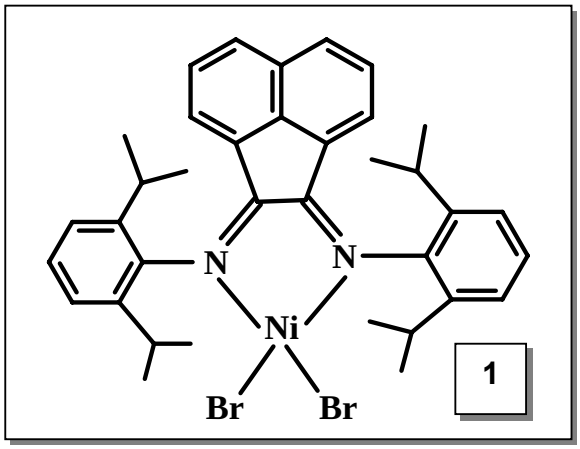

6.2. EXPERIMENTAL

6.2.1. Materials

These are discussed in Chapter 3.

6.2.2. Synthesis of catalyst

Catalyst 1 was synthesized according to reported procedure[12].

6.2.3. Synthesis of poly(α-olefin)s

Synthesis procedures are discussed in Chapter 3.

6.2.4. Gas chromatography (GC)

GC methods for analysis of unreacted monomer during polymerization are discussed in Chapter 3.

6.2.5. Gel permeation chromatography (GPC)

Procedure for determining absolute number average molecular weights are discussed in Chapter 3.

6.2.6. Kinetics of hexene-1 polymerization

Kinetics of hexene-1 polymerization was studied by estimating unreacted monomer as a function of time. Kinetic runs were performed using a bench-top single-neck glass reactor (Chapter 3, **Figure 3.2**) connected to a 3-way stop-cock with septum-adaptor and provided with a magnectic stirring bar. Required amount of catalyst (**1**, $3.4x10^{-4}$ M) was placed in the reactor. In a separate round bottom flask freshly distilled hexene-1 (3 mL, 0.5 M) + cyclohexane (internal standard) (1 mL, 0.16 M) + toluene (44 mL) was taken. 1 mL of this solution was taken out for G.C analysis from the reaction mixture at time 't_o'. This solution was transferred to the reactor containing the catalyst through a cannula. Polymerization was initiated by adding MAO solution ($3.4x10^{-2}$ M) at the specified temperature (0 ^oC). Approximately 2 mL of the sample was taken out every 30 min., diluted with 4 mL of toluene followed by addition of 3-4 mL of methanol to arrest the polymerization. The polymer separated from the reaction mixture. The supernatant liquid, which consists of unreacted monomer, internal standard and methanol, was analyzed by gas chromatography for monomer conversion. The resulting polymer was washed three times with acetone and dried under vacuum.

The conversion at different reaction times were determined using the eq 1,

$$x_p = 1- [(M_t/I_t) \div (M_o/I_o)] \quad \text{---------- (1)}$$

Where, x_p = conversion at a given time, t;

$[M_t/I_t]$ = mol ratio of monomer to internal standard (cyclohexane) at time t, which is same as their peak area ratio;

$[M_o/I_o]$ = mol ratio of monomer to internal standard at zero time determined in the same way.

The raw data obtained from experiment above is shown in **Table 6.1**. A representative plot of time vs conversion can be seen in **Figure 6.1**.

Table 6.1. Homopolymerization of hexene-1 using **catalyst 1**/MAO

Entry	Time (t, min.)	Area (using GC)		$\ln(M_o/M_t)$	Conversion (x_p)
		Hexene-1 (M_t)	Cyclohexane (I_t)		
1	0	73.8084 (M_o)	26.1916 (I_o)	NA	NA
2	30	65.7411	34.2589	0.1157	0.3191
3	60	58.9327	41.0673	0.2250	0.4908
4	80	53.7408	46.2592	0.3172	0.5878
5	100	48.6631	51.3369	0.4165	0.6637
6	120	43.5638	56.4362	0.5272	0.7261

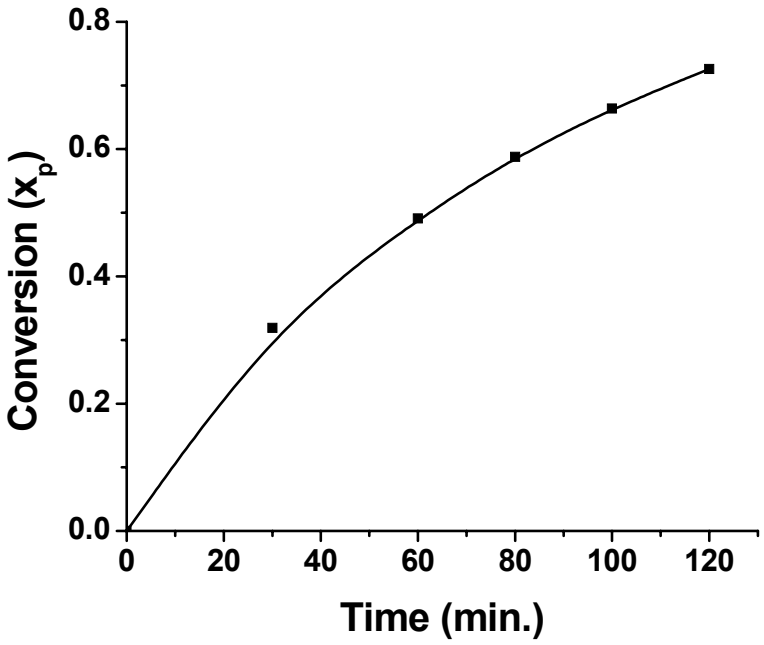

Figure 6.1. Plot of time vs conversion (x_p)

6.3. RESULTS AND DISCUSSION

Homopolymerization of hexene-1 was performed using **1**/MAO. Experiments were performed at varying catalyst and monomer concentrations in the temperature range of -10 to 35 ^{o}C.

6.3.1. Kinetics of polymerization of hexene-1

The rate constants of hexene-1 polymerization using 1/MAO are summarized in **Table 6.1** and **6.2**. The results of the kinetic experiments performed at different temperatures (T_{eff}), variable catalyst ($[I]_o$) and monomer concentrations ($[M]_o$) are discussed in the following paragraphs.

Table 6.2. Kinetics of hexene-1 polymerization by **1**/MAO (polymerization time 2 h)

Entry	T_p (^oC)	[cat.].10^4 (M)	[H-1] (M)	[H-1/ cat]	[Al/ Cat]	x_p[a], max	$P_{n,\,th}$[b] (at x_p, max)	$P_{n,\,SEC}$[c] (at x_p, max)	M_w/M_n (at x_p, max)	Cat_{eff}[d]
1	35	3.40	0.50	1470	100	93	1367	1428	1.39	0.96
2	20	3.40	0.50	1470	100	88	1302	1878	1.29	0.69
3	10	3.40	0.50	1470	100	85	1245	1621	1.23	0.77
4	0	3.40	0.50	1470	100	73	1067	1196	1.18	0.89
5	-10	3.40	0.50	1470	100	45	659	868	1.27	0.76
6	0	1.84	0.50	2720	185	32	872	996	1.43	0.88
7	0	2.26	0.50	2210	150	51	1142	1457	1.19	0.78
8	0	5.10	0.50	980	70	78	767	988	1.24	0.77
9	0	3.40	0.33	970	100	64	622	775	1.26	0.80
10	0	3.40	0.66	1940	100	69	1339	1838	1.23	0.73
11	0	3.40	0.82	2410	100	64	1554	2220	1.35	0.70

[a] conversion obtained at t_{max}, $x_{p,\,max} = 1-[(M_t/I_t)/(M_o/I_o)]$,
[b] $P_{n,\,th} = ([M]_o/[I]_o).\ x_{p,\,max}$,
[c] $P_{n,\,SEC} = (M_{n,\,SEC} - M_{ini})/M_{monomer}$,
[d] 'Cat_{eff}' is the catalyst efficiency determined from the ratio of calculated and experimental number-average degree of polymerization

The expression for the unimolecular termination is derived by integrating the rate expressions for propagation and termination. The rate equation is given by eq 1, where 'k_{app}' (= $k_p[P^*]$) is the apparent rate constant obtained by the initial slope of the first-order time-conversion plot, k_p and k_t are the rate constants of propagation and termination respectively. '$[P^*]$' (= $f.[I]_o$) is the active center concentration, and 'f' is the catalyst efficiency. The values of k_{app} and k_t were determined by a nonlinear fitting procedure using eq 2.

$$\ln \frac{[M]_0}{[M]_t} = \frac{k_{app}}{k_t}(1 - e^{-k_t t}) = \frac{k_p[P^*]}{k_t}(1 - e^{-k_t t}) \qquad \text{---------- (2)}$$

Homopolymerization of hexene-1 using **1**/MAO at different catalyst concentrations and the resulting first-order time-conversion plot is shown in **Figure 6.2**. The downward curvature of first-order time-conversion plot at lower catalyst concentrations indicates the presence of termination reaction. Conversion (i.e., $\ln(M_o/M_t)$ tends to increase with increase in catalyst concentration. However, the effect of termination is more significant at lower catalyst concentrations. The deviation from first-order linearity is also observed at higher catalyst concentrations indicating termination. The rate of propagation increases with increase in catalyst concentration. The values of k_{app}, k_t were determined by a non-linear fitting procedure using eq 2. The details of polymerization conditions and rate constants are shown in **Table 6.2** and **6.3**.

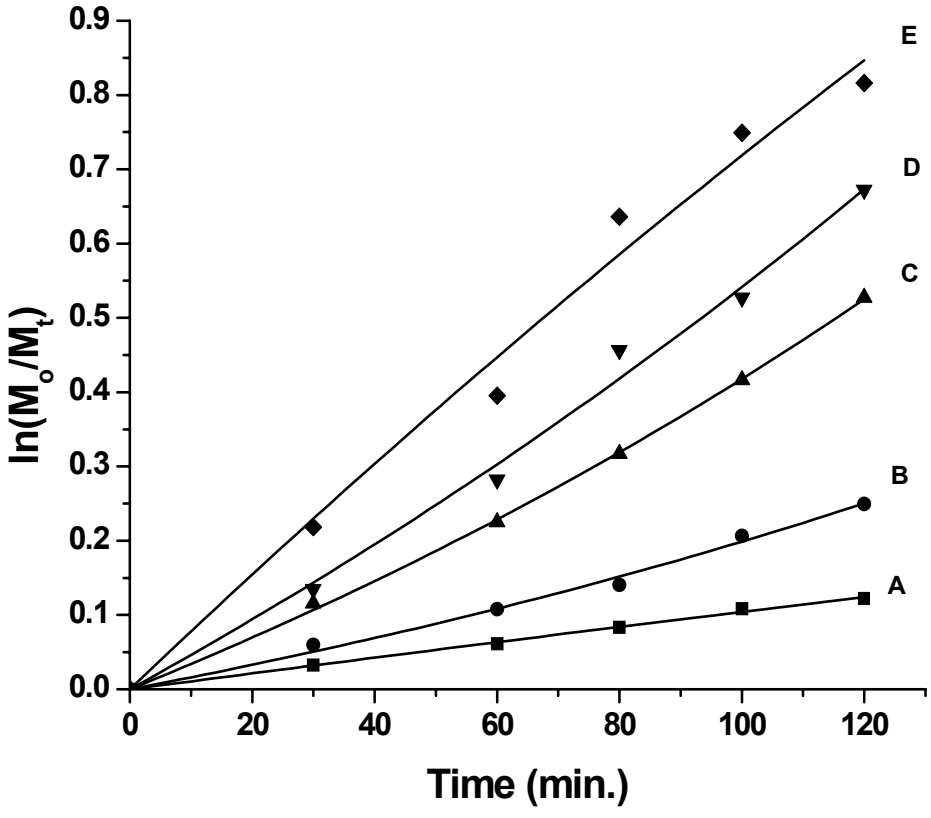

Figure 6.2. First-order time-conversion plot of hexene-1 polymerization at different catalyst concentrations: (A) 1.84×10^{-4} M; (B) 2.26×10^{-4} M; (C) 3.40×10^{-4} M (D) 5.10×10^{-4} M and (E) 6.23×10^{-4} M.

Table 6.3. Rate constants of hexene-1 polymerization using **1**/MAO

Entry	$[P^*]^a.10^4$	k_{app} x 10^5 (sec^{-1})	k_p^b x 10^2 (L mol^{-1} sec^{-1})
1	3.26	25.13	77.10
2	2.35	16.68	71.00
3	2.62	9.28	35.43
4	3.03	5.55	18.31
5	2.58	0.26	10.20
6	1.62	1.80	11.11
7	1.76	2.63	14.96
8	3.93	7.60	19.33
9	2.72	6.40	23.53
10	2.48	4.65	18.75
11	2.38	3.83	16.10

[a] active center concentration, $[P^*] = Cat_{eff}.[I]_o$, $[I]_o$ = catalyst concentration,
[b] rate of propagation, $k_p = k_{app}/[P^*]$

A non-linear plot of degree of polymerization (P_n) with respect to conversion (x_p) indicates the occurrence of transfer reactions and slow initiation (**Figure 6.3**). The

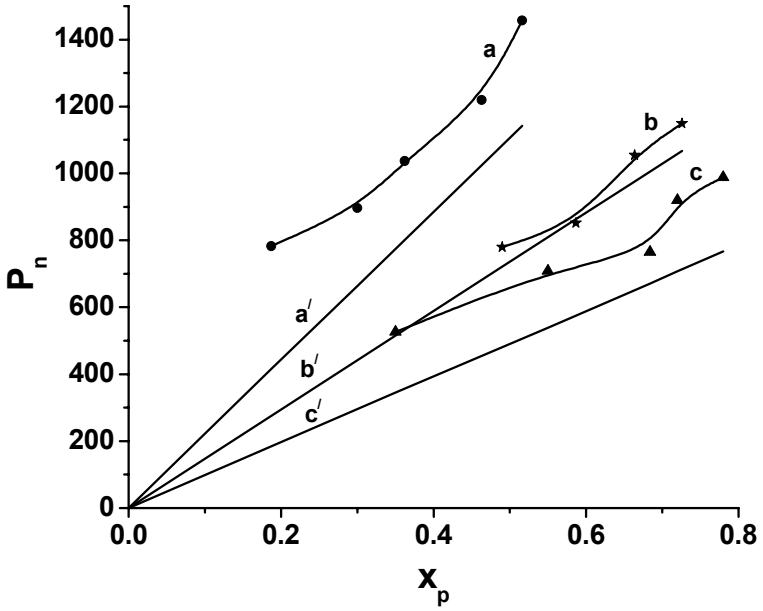

Figure 6.3. Number average degree of polymerization, P_n, vs conversion, x_p of poly(hexene-1)s synthesized using **1**/MAO at different catalyst concentrations; (a) 2.26 x 10^{-4} M, (b) 3.4 x 10^{-4} M and (c) 5.1 x 10^{-4} M. a′, b′ and c′ are corresponding theoretical values.

experimental molar masses are higher than those predicted which implies that a fraction of catalyst species was not activated or is deactivated at early stages of polymerization. The efficiency of the catalyst (Cat_{eff}) varies between 0.77 to 0.89 and under the best conditions does not exceed 90 %. The observed polydispersity of the poly(hexene-1)s is in the range of 1.18 to 1.43. The active center concentrations, [P^*], in **Table 6.2** were determined using the catalyst efficiencies (Cat_{eff}) calculated from the ratio of the theoretical and the experimental number average degrees of polymerization, P_n. Absolute molecular weight of poly(hexene-1) was determined by gel permeation chromatography (as described in Chapter 3, page 61) using refractive index (RI), viscosity and light scattering (LS) detectors.

Figure 6.4 represents a bilogarithmic plot of k_{app} vs [P*], which is linear with a slope of 1.23 ± 0.009. This corresponds to a reaction order of 1.23 with respect to catalyst. The slightly higher value of reaction order in the present case must be attributed to artifacts of experiments. Odian and coworkers reported a reaction order of 1.0 with respect to catalyst for polymerization of hexene-1 using *rac*-$Me_2Si(H_4Ind)_2ZrCl_2$/ MAO[25]. The absolute molecular weights of poly(hexene-1)s obtained using various catalyst concentrations is shown in **Figure 6.5**. The molecular weight of poly(hexene-1)s clearly level off beyond a ratio of [hexene-1/catalyst] of 1500. These results show that noticeable chain transfer reactions occur at higher [hexene-1/catalyst] ratio.

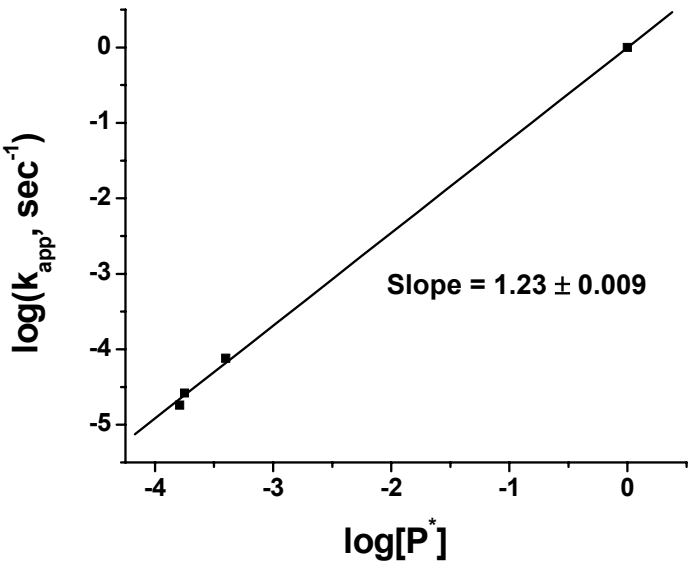

Figure 6.4. Reaction order with respect to catalyst concentration for hexene-1 polymerization at 0 ^oC.

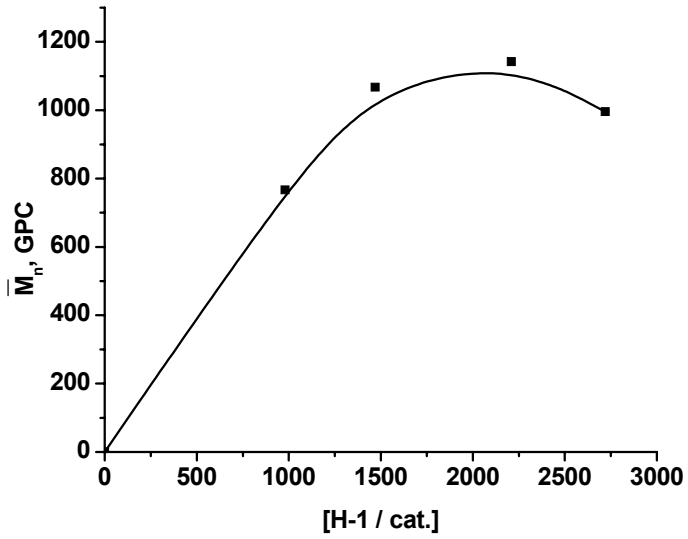

Figure 6.5. Dependence of [hexene-1/catalyst 1] on molecular weight ($\bar{M}_n$)

6.3.2. Effect of temperature

The effect of temperature on the rate of polymerization was studied in the range -10 to 35 ^{o}C. First-order time-conversion plot showed a downward curvature at temperatures of -10, 0 and +10 ^{o}C, indicating the presence of termination reaction (**Figure 6.6**). Propagation rate constant (k_p) of hexene-1 polymerization at 35, 20, 10, 0 and -10 ^{o}C are shown in **Table 6.4**. 1,2- or 2,1-insertion of hexene-1 into nickel cation-carbon following by with and without enchainment has been shown in **Scheme 6.1**. As

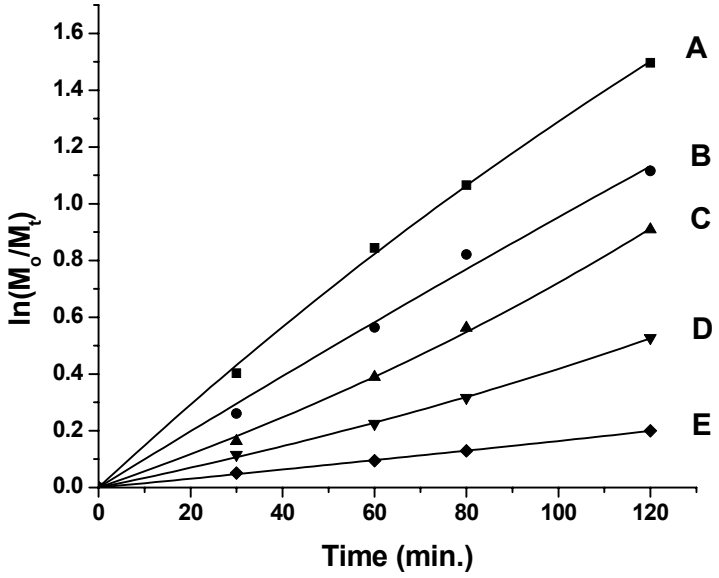

Figure 6.6. First-order time-conversion plot for the polymerization of hexene-1 at (A) 35 ^{o}C, (B) 20 ^{o}C, (C) 10 ^{o}C, (D) 0 ^{o}C and (E) -10 ^{o}C.

discussed in Chapter 4 (section 4.3.4.1.1), at higher polymerization temperatures the rate of 2,1-insertion of hexene-1 into nickel cation-carbon bond, following 1,ω-enchainment is high. This leads to nickel-primary carbon [Ni^+-CH_2-$(CH_2)_4$-CH_2-P] species (Path C). 1,2-insertion of hexene-1 into nickel cation-carbon bond gives nickel-β-substituted alkyl species [Ni^+-CH_2-$CH(CH_2)_3CH_3$-P] species (Path A). The increase in k_p with increasing polymerization temperature can be explained by the fact that the relative population of reactive species, i.e., Path B and C is higher than Path A at higher temperatures.

Table 6.4. Comparison of propagation rate constants

Entry	Polymerization temperature (^oC)	k_p x 10^2 (L mol^{-1} sec^{-1})
1	35	77.10
2	20	71.00
3	10	35.43
4	0	18.31
5	- 10	10.20

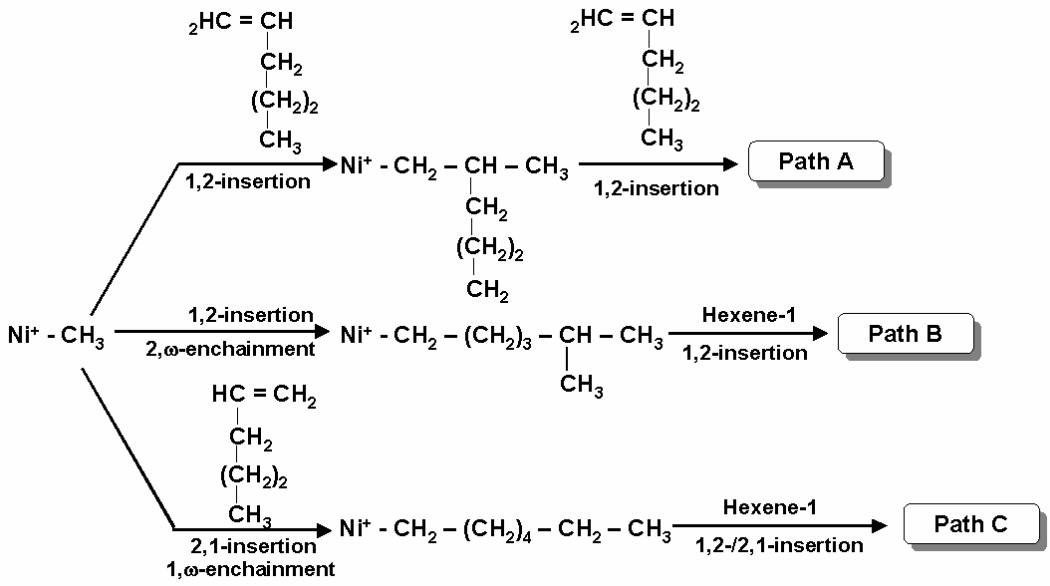

Scheme 6.1. Possible insertions and enchainments of hexene-1 using **catalyst 1**/MAO

6.3.2.1. Activation energy (E_a)

The Arrhenius plot (**Figure 6.7**) obtained using the overall propagation rate constant, k_p, at five different temperatures (-10, 0, 10, 20 and 35 ^oC) was found to be linear with an activation energy, $E_{a,app}$ = 4.3 kcal/mol. **Table 6.5** summarizes the activation energy values of polymerization using Ziegler and metallocene catalyst found in literature.

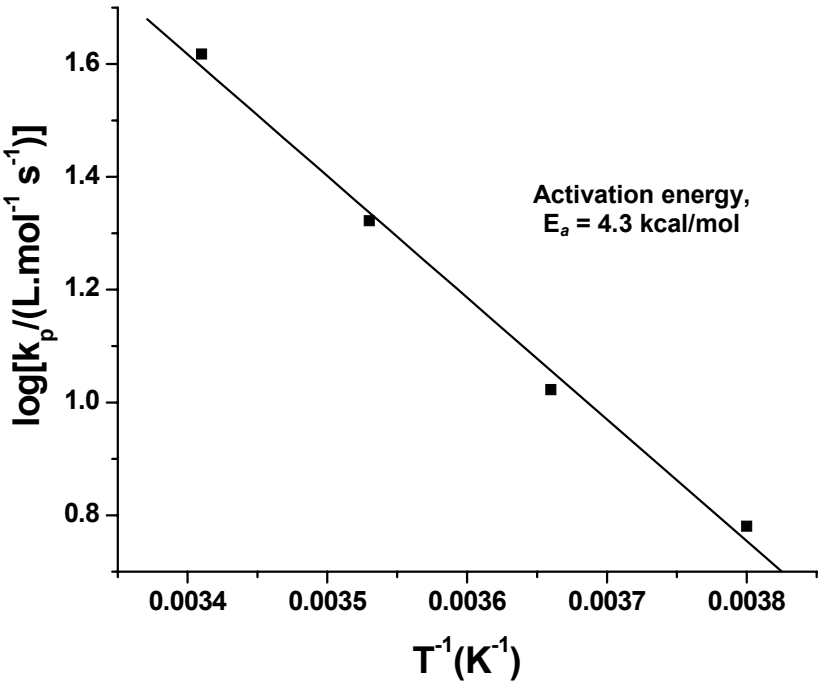

Figure 6.7. Arrhenius plot for the polymerization of hexene-1 using **catalyst 1**/MAO

Table 6.5. Summary of activation energies of poly(hexene-1)s using different catalyst systems

Entry	Catalyst system	k_p x 10^2 (L mol^{-1} sec^{-1})	Activation energy (kcal/mol)
1	**Catalyst 1**/MAO	77.10	4.3
2[26]	$TiCl_4$/TIBAL	---	9.5
3[27]	*rac*-Et$(Ind)_2ZrCl_2$/MAO	---	12.4
4[25]	*rac*-$Me_2Si(H_4Ind)_2ZrCl_2$/MAO	---	14.1
5[28]	*bis*(η-$CH_3C_5H_5$) (η^4-C_5H_8) Zr /$B(C_6F_5)_3$	6.25	20.1

The activation energy differences of hexene-1 polymerization using **catalyst 1**/MAO with Ziegler and metallocene catalyst systems can be explained as follows;

(i) Coordination of hexene-1 in 1,2-fashion with metal cation-carbon bond and followed by insertion is similar for **catalyst 1** (**Scheme 6.1**, Path A), Ziegler and metallocene catalysts.

(ii) In the case of **catalyst 1**, 1,2-insertion of hexene-1 into nickel cation-carbon bond followed by 2,ω-enchainment lead to methyl branches (**Scheme 6.1**, Path B). Possibility of further hexene-1 coordination followed by insertion is much faster in the case of Path B. This type of enchainment is not observed with Ziegler and metallocene catalyst systems. The rate of monomer insertion is much faster for Path B.

(iii) 2,1-insertion of hexene-1 followed by 1,ω-enchainment lead methylenes in the backbone (**Scheme 6.1**, Path C). This path is unique only for **catalyst 1**/MAO systems, whereas, in the case of Ziegler and metallocene catalysts, β-hydride elimination from 2,1-inserted species is observed resulting in the formation of trans-vinylene end-groups[29-31].

6.4. CONCLUSIONS

Based on the kinetics the following salient conclusions can be drawn.

1. The downward curvature of first order time-conversion plot clearly indicates the presence of termination reactions during the polymerization. Occurrence of transfer reactions is also evident by the observed non-linear plot of degree of polymerization with respect to conversion.

2. Experimentally observed absolute molar masses of poly(hexene-1)s are higher than that predicted by theory. This indicates that not all catalytically active species participate in chain initiation or some of the active species get deactivated at the very early stages of polymerization.

3. The extent of chain transfer reactions was found to be higher at higher [hexene-1/catalyst] ratio.

4. The best catalyst efficiency observed under reaction conditions explored was 90 %.

5. The reaction order was found to be 1.23 with respect to catalyst.

6. The activation energy for the polymerization of hexene-1 using **catalyst 1**/MAO is lower than similar polymerization using early transition metal catalysts. Higher insertion rates of hexene-1 into nickel cation-primary carbon bond as a consequence of chain running is presumably the reason for this observation.

In summary, hexene-1 polymerization using **catalyst 1**/MAO does not fulfill the rigorous kinetic criteria of "living" polymerization.

6.5. REFERENCES

(1) Brintzinger, H. H.; Fischer, D.; Mulhaupt, R.; Rieger, B.; Waymouth, R. M. *Angew. Chem., Int. Ed., Engl*. **1995**, *34*, 1143.

(2) Bochmann, M. *J. Chem. Soc., Dalton Trans*. **1996**, 255.

(3) Kaminsky, W. *Macromol. Chem. Phys*. **1996**, *197*, 3907.

(4) Mohring, V. M.; Fink, G. *Angew. Chem., Int. Ed. Eng*. **1985**, *24*, 1001.

(5) Peuckert, M.; Keim, W. *Organometallics* **1983**, *2*, 594.

(6) Keim, W.; Appel, R.; Storeck, A.; Kruger, C.; Goddard, R. *Angew. Chem., Int. Ed. Eng*. **1981**, *20*, 116.

(7) Klabunde, U.; Ittel, S. D. *J. Mol. Catal*. **1987**, *41*, 123.

(8) Schmidt, G. F.; Brookhart, M. *J. Am. Chem. Soc*. **1985**, *107*, 1443.

(9) Rix, F. C.; Brookhart, M. *J. Am. Chem. Soc*. **1995**, *117*, 1137.

(10) Rix, F. C.; Brookhart, M.; White, P. S. *J. Am. Chem. Soc*. **1996**, *118*, 4746.

(11) Ittel, S. D.; Johnson, L. K.; Brookhart, M. *Chem. Rev*. **2000**, *100*, 1169.

(12) Johnson, L. K., Killian, C. M.; Brookhart, M. *J. Am. Chem. Soc*. **1995**, *117*, 6414.

(13) Killian, C. M.; Tempel, D. J.; Johnson, L. K.; Brookhart, M. *J. Am. Chem. Soc*. **1996**, *118*, 11664.

(14) Mecking, S. *Angew. Chem., Int. Ed*. **2001**, *40*, 534.

(15) Suzuki, N.; Yu, J.; Masubuchi, Y.; Horiuchi, A.; Wakatsuki, Y. *J. Polym. Sci. Part. A: Polym. Chem*. **2003**, *41*, 293.

(16) Guan, Z. *J. Polym. Sci. Part. A: Polym. Chem*. **2003**, *41*, 3680.

(17) Gottfried, A. C.; Brookhart, M. *Macromolecules* **2003**, *36*, 3085.

(18) Mehrkhodavandi, P.; Schrock, R. R. *J. Am. Chem. Soc*. **2001**, *123*, 10746.

(19) Jeon, Y. M.; Park, S. J.; Heo, J.; Kim, K. *Organometallics* **1998**, *17*, 3161.

(20) Jayaratne, K. C.; Sita, L. R. *J. Am. Chem. Soc*. **2000**, *122*, 958.

(21) Scollard, J. D.; McConville, D. H. *J. Am. Chem. Soc*. **1996**, *118*, 10008.

(22) Hagihara, H.; Shiono, T.; Ikeda, T. *Macromolecules* **1998**, *31*, 3184.

(23) Reinartz, S.; Mason, A. F.; Lobkosky, E. B.; Coates, G. W. *Organometallics* **2003**, *22*, 2542.

(24) Rose, J. M.; Cherian, A. E.; Coates, G. W. *J. Am. Chem. Soc*. **2006**, *128*, 4186.

(25) Zhao, X.; Odian, G.; Rossi, A. *J. Polym. Sci. Part. A: Polym. Chem*. **2000**, *38*, 3802.

(26) Badin, E. J. *J. Am. Chem. Soc*. **1958**, 6549.

(27) Chien, J. C. W.; Gong, B. *J. Polym. Sci. Part. A: Polym. Chem*. **1993**, *31*, 1747.

(28) Karl, J.; Dahlmann, M.; Erker, G.; Bergander, K. *J. Am. Chem. Soc. **1996**, 120*, 5643.

(29) Babu, G. N.; Newmark, R. A.; Chien, J. C. W. *Macromolecules* **1994**, *27*, 3383.

(30) Rossi, A.; Odian, G.; Zhang, J. *Macromolecules* **1995**, *28*, 1739.

(31) Suzuki, N.; Yamaguchi, Y.; Fries, A.; Mise, T. *Macromolecules* **2000**, *33*, 4602.

CHAPTER 7

SUMMARY AND CONCLUSIONS

7.1. SUMMARY AND CONCLUSIONS

Single site group IV metallocene based catalyst (Ti, Zr and Hf) systems have been well studied for the polymerization of α-olefins in the last decade. Metallocene based innovations with respect to both catalyst and polymer development have been very significant and the relationship of catalyst-activity-polymer property has reached a high level of achievement, both, academically as well as from an industrial point of view. The most striking feature of group IV metallocene catalysts is their capability to control polymer microstructures. New generation of catalysts of group VIII metal-based systems, i.e., nickel- and palladium(α-diimine) for the polymerization of α-olefins, olefin containing polar groups and cyclic olefins has been of more recent interest. The concept of "chain running" (or) "chain walking" (or) "chain straightening" has made possible synthesis of polymers with various topologies. In spite of all these developments, the stereo- and regio- chemistry of poly(α-olefin)s and the process of insertion of α-olefin into M-C in the synthesis of poly(α-olefin)s by group IV and VIII is still not clearly understood in the literature.

In this thesis synthesis, structure and property of poly(α-olefin)s prepared using nickel(α-diimine)/MAO catalyst system are described.

Homopolymerization of hexene-1 with nickel(α-diimine) catalyst results in poly(hexene-1)s containing different types of branches and varying number of methylene units in the backbone. Types of branches identified by NMR spectroscopy include, butyl (C_4), longer than butyl (C_4) and methyl (isolated and *meso* and *racemic* head-to-head). Formation of ethyl (C_2) and propyl (C_3) branches were not observed. The migration of the nickel during polymerization not only causes the formation of branches other than C_4, but also the runs of methylene units in the backbone due to complete 1,6-enchainment (chain running). The observed formation of regio-irregular methyl branches requires an insertion of hexene-1 in the nickel-secondary carbon. Formation of methyl branches and 1,ω-enchainment were also been observed during the polymerization of octene-1, decene-1, tetradecene-1 using the same catalyst system. The extent formation of these subunits in the polymer depend on polymerization temperature. A plausible explanation for the formation of different branches has been proposed. *This study is the first comprehensive investigation into the origins of stereo- and regiochemistry of*

hexene-1 insertion into nickel cation-carbon (primary/secondary) bond. Influence of chain running on microstructural features of poly(hexene-1)s have been elucidated using high resolution NMR spectroscopy.

Homopolymerization of octadecene-1 under varying reaction conditions was studied. Significant chain running is observed at higher polymerization temperature. However, 1,2-insertion followed by chain running (i.e., 2,ω-enchainment) resulting in the formation of isolated methyl branches is a predominant mode of addition under these conditions. Interestingly insertion of octadecene-1 into a sterically hindered nickel cation-carbon (secondary) bond is high at higher polymerization temperatures, which gives regio-irregular (*rac*- and *meso*) head-to-head methyl branches. 2,1-insertion of octadecene-1 into a nickel-carbon bond followed by chain running (i.e., 1,ω-enchainment) results in a sequence of 18 methylenes in the backbone. 1,ω-enchainment is invariant with reaction temperatures. The microstructure of the polymer including different type of branches and chain running has been studied by Nuclear Magnetic Resonance (NMR) spectroscopy. Differential Scanning Calorimetry (DSC) of poly(octadecene-1)s showed four melting transitions (T_m) indicating the presence of four different types of crystalline regions/blocks. The origins of this T_m's are mainly due to crystallization of side chains and variable lengths of isolated methylene sequences in the main chain. T_m of poly(octadecene-1)s tends to increase with increase in methylene sequences in the backbone. T_g's of all poly(octadecene-1)s are similar. Higher intensity of β-transition is observed when methine branch points are connected to large number of C_1 (methyl) branches. Poly(octadecene-1)s synthesized at different monomer concentrations have similar number of branches. The extent of chain running (i.e. 2,ω-, 1,ω-enchainments) decreases with increase in the carbon number of α-olefins. Insertion of lower α-olefin into nickel cations-carbon (secondary) is much faster due to relatively less steric hinderance. The long methylene sequences in the backbone as well as in the side chain in case of poly(α-olefin)s with carbon number > 12 results in higher melting and crystallization temperatures. Presence of large number of short chain branches results in more amorphous nature of polymer in case of poly(decene-1)s, exhibiting lower T_g and a higher intensity of β-transition. The trend of T_g and intensity of β-transition of poly(α-olefin)s is as follows: poly(decene-1) > poly(dodecene-1) > poly(tetradecene-1) > poly(hexadecene-1) > poly(octadecene-1). *This is the first*

observation of a higher α-olefin insertion into a nickel cation-secondary carbon bond. The most important feature of chain straightened poly(ocatdecene-1)s is the observation that side chain and main chain segments crystallize simultaneously. The intensity of β-relaxation is dependent on number of C_1 (methyl) branches connected to the branching point carbon.

Kinetics of hexene-1 polymerization was investigated using [(*N,N´*-diisopropylbenzene)-2,3-(1,8-napthly)-1,4-diazabutadiene]dibromonickel / methylaluminoxane catalyst. Experiments were performed at varying catalyst and monomer concentrations in the temperature range of -10 to 35 ^{o}C. First order time-conversion plot shown a downward curvature at temperatures of -10, 0 and +10 ^{o}C, indicating the presence of termination reaction. A non-linear plot of degree of polymerization (P_n) with respect to conversion indicates occurrence of transfer reactions and slow initiation. The experimental molar masses are higher than predicted, which implies that a fraction of catalyst species could not be activated or is deactivated at the early stages of the reactions. The efficiency of the catalyst (Cat_{eff}) varies between 0.77 to 0.89. The observed polydispersity of the poly(hexene-1)s is in the range of 1.18 to 1.39. The reaction order was found to be 1.23 with respect to catalyst. The Arrhenius plot obtained using the overall propagation rate constant, k_p, at five different temperatures (-10, 0, 10, 20 and 35 ^{o}C) was found to be linear with an activation energy, $E_{a,\ app}$ = 4.3 kcal/mol. *Thus it is established using kinetic studies that hexene-1 polymerization using nickel(α-diimine)/MAO catalyst is accompanied by significant occurrence of chain termination and transfer reactions. Thus these polymerization do not satisfy the rigorous kinetic criteria for "living" polymerization.*

7.2. FUTURE PROSPECTS OF RESEARCH

The present research on synthesis, structure and property studies of polyolefins prepared using late transition metal catalysts has opened up many new avenues for investigations. These are as follows:

- Study of microstructure of chain straightened poly(α-olefin)s synthesized by late transition nickel(α-diimine) catalyst using ^{13}C NMR techniques, i.e., 2D

INADEQUATE and solid state NMR for better understanding of stereo-, regiochemistry of α-olefin insertion into nickel cation-carbon (primary/secondary).

- Study the effect of chain running on mechanical and rheology properties.

- Study of kinetics of homopolymerization of hexene-1 using $NiMe_2$(α-diimine)/$B(C_6F_5)_3$; to examine whether, the extent of transfer reaction is minimized in the presence of the boron activator.

LIST OF PUBLICATIONS

1. A study of the structure of poly(hexene-1) prepared by nickel(α-diimine)/MAO catalyst using high resolution NMR spectroscopy.

Subramanyam, U.; Rajamohanan, P. R.; Sivaram, S. *Polymer* **2004**, *45*, 4063.

2. Novel Tetrahedral Ni(II) Complex Featuring Pyrazole Derived ligand Yields Highly Branched Oligomers of Ethylene.
   Mukherjee, A.; **Subramanyam**, **U**.; Puranik, V.G.; Mohandas, T.P.; Sarkar, A.
   Eur. J. Inorg. Chem. **2005**, 1254-1263.

3. Synthesis and characterization of poly(α-olefin)s using nickel(α-diimine)/MAO catalyst: Effect of chain running on polymer properties. (Full paper)
   Subramanyam, U.; Sivaram, S. *J. Polym. Sci. Part. A: Polym. Chem.* **2006**.
   (Under preparation)

4. Kinetics of hexene-1 polymerization using [(*N*,*N*′-diisopropylbenzene)-2,3-(1,8-napthyl)-1,4-diazabutadiene] dibromonickel/methylaluminoxane catalyst system.
   Subramanyam, U.; Sivaram, S. *J. Polym. Sci. Part. A: Polym. Chem.* **2006**.
   (*Under preparation*)

5. Transition metal catalysts for polymerization of higher α-olefins. (*Review*).
   Subramanyam, U.; Sivaram, S. (*Under preparation*).

CONTRIBUTION TO NATIONAL/INTERNATIONAL SYMPOSIA/CONFERENCES

1. Studies on microstructure of poly(α-olefin)s made with Ni(α-diimine)/MAO catalyst system.
   Subramanyam, U.; Sivaram, S.; Rajamohnan, P.R.
   Fourth National Symposium in Chemistry, 1-3 February, 2002.

Organized jointly by National Chemical Laboratory and University of Pune,Pune. (*Poster Presentation*).

2. Novel formation of regio- irregular methyl branches in hexene-1 polymerization using late transition nickel (α-diimine)/MAO catalyst system: mechanistic study using high-resolution NMR spectroscopy.
   Subramanyam, U.; Sivaram, S.
   Internal Seminar on Frontiers of Polymer Science and Engineering (Macro 2002), 9-11 December, 2002.
   Organized by Indian Institute of Technology, Kharagpur. (*Oral Presentation*).

3. Synthesis and characterization of poly(α-olefin)s using nickel(α-diimine)/MAO catalyst: study of the effect of chain running on polymer properties.
   Subramanyam, U.; Sivaram, S.
   Recent Advance in Organometallics Catalysis and Olefin Polymerization, Indo-US Conference, 10-12 December, 2003.
   Organized by Department of Chemistry, Indian Institute of Technology Madras, Chennai 600 036, India. (*Poster presentation*).

4. Kinetics of hexene-1 polymerization using [(*N, N*′–diisopropyl benzene)-2,3-(1,8-napthyl)-1,4-diazabutadiene] dibromonickel/methylaluminoxane catalysts.
   Subramanyam, U.; Sivaram, S.
   IUPAC International Symposium on Ionic Polymerization, 23-28 October, 2005, Goa, India.
   Organized by National Chemical Laboratory, Pune 411 008, India. (*Poster presentation*).